

## Chapter 2

# Analysis of Glucose, Cholesterol and Uric Acid

### 2.1 Literature Review

#### 2.1.1 Importance of Glucose, Cholesterol and Uric Acid

Glucose is one of the most critical for life compounds found in nature, acting as the primary fuel for glycolysis and being present in pathways of aerobic and anaerobic respiration [1]. Clinically it is used to evaluate diabetes, a metabolic disorder considered to be a major world health problem. In diabetes pancreas does not produce sufficient amounts of insulin, or the insulin produced is not used effectively. World Health Organization estimates that 347 million people worldwide have diabetes with more than 80 % of those living in low- and middle-income countries. It was also estimated that 1.5 million deaths were directly caused by diabetes in 2012, and that it will be the 7th leading cause of death in 2030. Diabetes increases the risk of heart disease and stroke, foot ulcers that together with infection can lead to limb amputation, retinopathy resulting in blindness and kidney failure [2]. Glucose in blood is normally in the range of 3.5–5.3 mmol/L and in urine 0.1–0.8 mmol/L [3].

Uric acid is the primary end product of purine metabolism, with daily production of about 350 mg and additional daily intake of around 300 mg. In most mammals uric acid reacts with uricase degrading to allantoin, which is then excreted from body with urine. A natural antioxidant, uric acid is responsible for up to 60 % of the free radical scavenging activity in human blood. High levels of uric acid are related with diseases such as gout, Lesch-Nyan disease, obesity, diabetes, hypertension, high cholesterol and renal dysfunction. Acute causes of abnormally high levels of uric acid include large alcohol intake, chemotherapy and diet rich in proteins. Prolonged high levels of this compound result in creation of monosodium urate crystals in tissues and areas around the joints. Patients suffer from recurrent flares of severe joint inflammation and are more prone to cardiovascular dysfunctions. Crystals can be naturally dissolved by lowering the serum uric acid level below

360  $\mu\text{mol/L}$  [4]. Low concentration of uric acid was noted in cases of multiple sclerosis, Parkinson's disease and Alzheimer [5]. Uric acid in blood is normally in the range of 0.1–0.4 mmol/L and in urine 1.5–4.4 mmol/L [6].

Cholesterol is the most abundant of sterols, synthesized by animals. In vertebrates it is localized predominantly in liver. Cholesterol is almost absent in prokaryotes (e.g. bacteria) and rare in plants, where sterols with different side chains are dominant [7]. In human body, part of cholesterol is synthesized and rest comes from food of animal origin like meat, milk and eggs [8]. Cholesterol present in food can undergo autooxidation during processing and storage, forming metabolites of proved cytotoxicity, apoptotic and pro-inflammatory effects. Autooxidation is caused by contact with oxygen, exposure to sunlight, heating treatment and others. Those toxic derivatives of cholesterol can also be generated in human body through different oxidation mechanisms. Diseases that can be potentially initiated or aggravated include atherosclerosis, neurodegenerative processes and kidney failure [7]. Other diseases associated with abnormal levels of cholesterol include myocardial infarction, coronary heart disease, lipid disorders, liver failure and diabetes [9, 10].

Excess cholesterol present in blood can deposit in arteries and lead to plaque formation (atherosclerosis). A piece of thus formed plaque may break off, forming a blood clot, which in turn may block or decrease the blood flow in the heart, brain or other body part. In the case of severe blockage a heart attack or stroke can occur leading to surgery (bypass surgery, angioplasty, or stent placement), or even premature death [8].

Cholesterol travels through veins in particles called lipoproteins. The most common types are: very low density lipoproteins (VLDL), low-density lipoproteins (LDL), high density lipoproteins (HDL). Elevated levels of LDL cholesterol and reduced levels of HDL result in increased risk of developing blockages in the coronary arteries. Thus—taking men as an example—HDL less than 1.0 and LDL higher than 4.1 mmol/L are considered risk factors of cardiovascular disease (Table 2.1). The most recommended test to access serum cholesterol is the lipid panel or lipid profile in which the total, HDL, LDL cholesterol and fasting triglycerides levels are measured [8].

**Table 2.1** Serum cholesterol levels, all data in mmol/L [8]

	Total cholesterol	LDL	Triglycerides		HDL
Normal	<5.2	<2.6	<1.7	Low	1.0 (men) 1.3 (women)
Borderline high	5.2–6.2	3.4–4.1	1.7–2.2	Medium	1.3–1.5
High	$\geq 6.2$	$\geq 4.1$	$\geq 2.3$	High	$\geq 1.5$

## 2.1.2 Methods of Quantification

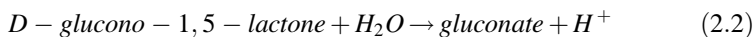
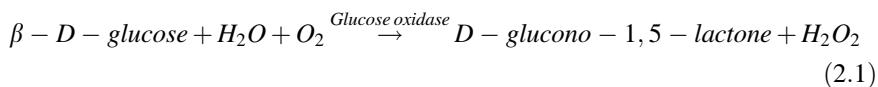
### 2.1.2.1 Common Detection Methods

#### Glucose

Assessing glucose levels is among the most important analytical tasks, with glucose tests forming about 40 % of all blood tests in 2011 [11] and approximately 85 % of the world market of biosensors in 2005 [12].

Glucose is a reducing sugar, and early methods of its quantifications were based on its ability to reduce copper that could later form stable precipitates or colorimetric end-products (Benedict's solution, the Folin–Wu method). Unfortunately those methods could not differentiate glucose from other reducing sugars [1]. Nowadays synthetic boronic acids and glucose-binding proteins such as concanavalin A are used for sensitive and selective, non-enzymatic glucose sensing.

At present most methods utilize enzymes such as glucose oxidase or glucose dehydrogenase. Glucose dehydrogenase uses  $\text{NAD}^+$  as a cofactor and produces NADH, is oxygen independent but the cofactors are relatively expensive and unstable [12]. Glucose oxidase (EC 1.1.3.4) is inexpensive and uses oxygen as a co-substrate (Eq. 2.1). Upon returning to its active state it transfers electrons to oxygen producing hydrogen peroxide that can be subsequently detected [12]. Operation range depends on the kind of microorganism from which the enzyme is extracted and most commonly falls between pH 4–7. Enzyme is highly specific to glucose but can be deactivated in solution containing  $\text{Ag}^+$  ions,  $\text{Hg}^{2+}$ ,  $\text{Cu}^{2+}$ . Glucose oxidase is the most common enzyme used in glucose biosensors, with all commercial optical sensors in 2011 relying on this enzyme [11].



In enzymatic optical glucose sensing we can distinguish measurement of the intrinsic UV fluorescence (Tryptophan in GOx and FAD coenzyme) which increases upon addition of glucose due to conformational change. Another group of methods is based on the consumption of oxygen usually utilizing luminescent complexes of ruthenium, platinum or palladium which are strongly quenched by oxygen. Glucose can be assessed also via measurement of changes in pH, with protons produced upon reaction of gluconolactone with water (Eq. 2.2), however the buffer capacity and the initial pH of the sample have to be taken into account. Another possibility is the quantification of hydrogen peroxide formed during the enzymatic reaction [11]. In this case commonly a second enzyme, namely peroxidase (e.g. from horseradish), is used to drive the oxidation of a chromophore. Commercial coupled systems include chromophores such as:

phenol/4-aminoantipyrine, amplex red (10-acetyl-3,7-dihydroxyphenoxazine) and o-dianisidine/sulfuric acid [1].

In the case of electrochemical enzymatic sensing both enzyme families, oxidases and dehydrogenases are widely used for electrooxidation of glucose. They present different redox potentials, cofactors and co-substrates, turnover rates and selectivity to glucose (oxidase is more selective and its cofactor is bound more strongly). Direct electron transfer between cofactor and enzyme is much too slow, and therefore mediators are used. Commercial electrochemical glucometers usually utilize mediators such as ferricyanide, ruthenium hexamine, Os complex, phenantroline or quinone. To prevent leaking of the electroactive components, redox hydrogels can be applied. The most used redox hydrogels directly catalyzing glucose electrooxidation are made from glucose oxidase enzyme and water-soluble polycationic polymers such as poly(4-vinylpyridine), poly(N-vinylimidazole) or poly(acrylamide)-copoly(N-vinylimidazole), with complexes of  $\text{Os}^{2+}/\text{Os}^{3+}$  [13].

Oxygen is being consumed upon the enzymatic reaction, thus it is possible to estimate the glucose concentration by the decrease of oxygen concentration. Oxygen can be monitored with a platinum or indium tin oxide (ITO) electrode [13].

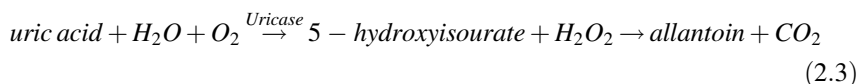
Nevertheless most assays are based on amperometric monitoring of hydrogen peroxide, where peroxide is catalytically electrooxidized (commonly at about 0.6 V vs. SCE) or electroreduced (typically  $-0.1$  V vs. SCE). Hydrogen peroxide can be also used to oxidize peroxidase which is later electroreduced directly or by means of a mediator. Electrooxidation catalysts include: platinum, palladium, nickel cyclam, ruthenium, ruthenium-platinum alloys, iridium dioxide, single-walled carbon nanotubes and polypyrrole functionalized multiwalled-carbon nanotubes. Most common electroreduction catalysts are: platinum, gold nanoparticles distributed in porous silicate;  $\text{Cu}^{2+}$ ,  $\text{Fe}^{2+}$ ,  $\text{Zn}^{2+}$  and  $\text{Ce}^{3+}$ -modified silicate xerogels [12, 13].

Other methods of glucose detection include separation by means of: high performance liquid chromatography, capillary zone electrophoresis or gas chromatography and posterior quantification by means of detectors such as: flame ionization, refractive index, nitrogen-phosphorus detector, pulsed amperometry, evaporative light scattering, UV, and fluorescence [1].

State of the art techniques tend to be non-invasive, directly measuring interstitial fluid, sweat or breath, or analyzing impedance of the skin and underlying tissue [12].

## Uric Acid

Uric acid can be detected enzymatically, by means similar to mentioned before for glucose. During reaction with uricase (EC 1.7.3.3), uric acid is converted to 5-hydroxyisourate with formation of hydrogen peroxide. 5-hydroxyisourate is later converted to allantoin and carbon dioxide (Eq. 2.3). Hydrogen peroxide can be quantified colorimetrically or electrochemically, with or without the use of peroxidase.



Optimum pH depends on the microorganism from which the enzyme was extracted, but in general is in the range of 6.5–11. The enzyme has high specificity for uric acid but the reaction can be inhibited by uric acid analogues and compounds chelating copper [14].

Uric acid can be detected also without the use of uricase. In case of optical methods, most common approaches include direct spectrophotometric detection (maximum at 293 nm) [15] and reduction of phosphotungstic acid leading to formation of tungsten blue [16].

This compound can be also quantified electrochemically, but interferences from ascorbic acid, which presents similar oxidation potential at common electrodes (platinum, gold, carbon) have to be taken into account [17]. Other common interferences include dopamine, xanthine and hypoxanthine. Successful detection in the presence of those interferences was already described with gold electrodes modified with thiols, ground electrodes from glassy carbon and pyrolytic graphite [15], carbon paste electrodes electrochemically pretreated [18], with Nafion layer [19], with sodium do-decyl benzene sulfate [20],  $\beta$ -cyclodextrin [21] or cobalt Schiff base composite [22].

Another interesting approach is based on molecularly imprinted polymers. Lakshmi et al. [5] presented this kind of polymer prepared from melamine and chloranil, which after template removal was coated directly onto the surface of a hanging mercury drop electrode, via charge-transfer interactions. Later the same molecularly imprinted polymer was mixed with graphite into a sol-gel matrix, and the resultant composite used to modify the surface of a graphite electrode.

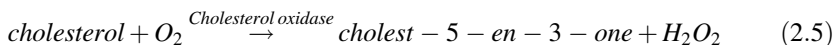
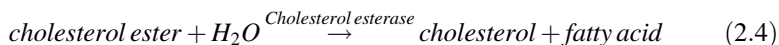
Similarly as with glucose, to avoid problems caused by interferences, uric acid can be at first separated by means of high performance liquid chromatography, gas chromatography or capillary zone electrophoresis and subsequently detected by one of the cited techniques.

## Cholesterol

Chemical analysis of cholesterol was typically based on Liebermann-Burchard and Zak reactions. Upon reaction with various strong Bronsted and Lewis acids colored products are formed. Liebermann-Burchard reaction is carried out in acetic acid-sulfuric acid-acetic anhydride medium resulting in blue-green product. Zak reaction is performed in acetic acid-sulfuric acid medium with addition of  $\text{Fe}^{3+}$  ions, leading to red product. Both methods are unfortunately prone to interference from hemoglobin and bilirubin and use corrosive reagents [23].

Nowadays, serum cholesterol analysis is commonly accomplished using a three-enzyme assay. Since around 70 % of serum cholesterol is esterified, typically serum is first incubated with cholesterol esterase (EC 3.1.1.13) to release free

cholesterol (Eq. 2.4). Cholesterol is then enzymatically oxidized by means of cholesterol oxidase (EC 1.1.3.6) leading to formation of cholest-5-en-3-one and hydrogen peroxide (Eq. 2.5). In typical assay peroxidase enzyme is used to reduce hydrogen peroxide and subsequently oxidize an indicator molecule. Common indicators are 4-aminopyrine with phenol and 2,4,6-tribromo-3-hydroxybenzoic acid but other aforementioned methods of detection of hydrogen peroxide can also be applied [7, 10].



Cholest-5-en-3-one can be also determined directly by spectrophotometric analysis at 240 nm [10].

### 2.1.2.2 Detection on Paper

#### Optical

An interesting system for the detection of glucose and uric acid is the above-mentioned platform by Dungchai et al. [6] which uses multiple indicators to achieve enhanced accuracy. With mixtures of 4-aminoantipyrine, 3,5-dichloro-2-hydroxybenzenesulfonic acid, o-dianisidinedihydrochloride, potassium iodide, acid black, and acid yellow it was possible to quantify glucose (0.5–20 mmol/L), lactate (1–25 mmol/L), and uric acid (0.1–7 mmol/L). Another worth mentioning system was constructed as a proof-of-concept device in a single sheet of paper [24]. 4-aminoantipyrine and 3,5-dichloro-2-hydroxy-benzenesulfonic acid were used as indicators. With the use of appropriate oxidase enzymes and horseradish peroxidase it was possible to quantify glucose (4–20 mmol/L), lactate (5–25 mmol/L), and uric acid (3–15 mmol/L) in artificial urine. Recently Fung et al. [25] described an equipment free, ladder-bar, glucose sensor. Three lines of goat anti-mouse IgG–horseradish peroxidase conjugate were deposited along a nitrocellulose strip. Sensing principle was based on different reaction times of successive lines due to the delay in the release of 3,3'',5,5'-tetramethylbenzidine from the reagent pad. Glucose concentration smaller than 5 μmol/L results in one line, 5–100 μmol/L in two lines and higher than 100 μmol/L in three lines.

Also equipment-free but this time distance-based measurement of cholesterol was proposed by Allen et al. [26] already a quarter-century ago. Proposed assay is based on cholesterol esterase, cholesterol oxidase and horseradish peroxidase and a reaction of hydrogen peroxide with dyes (3-methyl-2-benzothiazolinone hydrazine, N,N-dimethylaniline). Buffered solution of peroxidase is used as the wicking solution, which is transported by the wicking pad to sample region where a blood sample is spotted. Cholesterol from the sample reacts with cholesterol esterase and

oxidase from the subsequent pad, and later hydrogen peroxide formed upon this reaction passes to the measurement pad. The measurement pad is uniformly modified with aforementioned dyes. Length of the pad that changes color upon reaction is proportional to the cholesterol concentration in the sample. The same author deposited a patent [27] describing a laminated paper device for cholesterol detection based on similar sensing principle. Additionally authors indicated possible use of detergents such as polyoxyalkylenes, ethoxylatedalkylphenols, octylphenoethylene oxide condensates and polyoxyethylene lauryl ethers, or anionic detergents, such as bile acids. Other examples of uric acid, cholesterol and glucose sensors are resumed in Table 2.2.

### Electrochemical

First multianalyte electrochemical system based on paper was presented by Dungchai et al. [3] in 2009. Hydrophilic channels were delimited by means of photolithography and electrodes screen printed in the test zones. Three electrode system was used, including carbon with Prussian blue working and auxiliary electrodes and Ag/AgCl reference. Each of the three detection zones was modified with one of the following enzymes: glucose oxidase, lactate oxidase or uricase. Analytes in the control serum samples were detected by means of chronoamperometry, with the optimal detection potential for hydrogen peroxide (0 V). Device was capable of quantifying glucose (up to 100 mmol/L), lactate (up to 50 mmol/L), and uric acid (up to 35 mmol/L).

In 2010 Carvalhal et al. [38] described separation and quantification of ascorbic and uric acids. Gold electrodes were deposited on paper or polyester (two systems presented), and the linear range was between 0.05–0.2 mmol/L for uric acid and 0.05–0.4 mmol/L for ascorbic acid.

An interesting system for the detection of glucose was proposed by Liu and Crooks [39]. An integrated metal/air battery supplies power for the electrochemical sensor and electrochromic readout (visual quantification of Prussian blue spot). Prussian blue is reduced to its colorless counterpart prior to the assay. When a glucose sample in artificial urine is injected, urine activates the internal battery, which provides energy for the sensing assay. Paper forms two reservoirs one used by the sensor and other by the Al/air battery and is stacked between two ITO electrodes. Battery consists of an activated carbon cathode, paper reservoir forming a separator and metal foil anode.

Recently several systems applying graphene were also proposed including a wax printed platform comprising of a sample area and four channels leading to four test zones presented by Labroo et al. [40]. In each test zone two silver paste electrodes were interconnected with graphene-ink modified with appropriate enzyme. Device was used for multiplex detection of glucose, lactate, xanthine and cholesterol. Detailed assay procedures such as sample and stock solution preparation methods are not described, thus it is hard to analyze the system in detail. Another electrochemical detection system for cholesterol based on graphene was presented by

**Table 2.2** Literature review on colorimetric detection of glucose, uric acid and cholesterol on paper

Analyte	Architecture	Indicator	Enzymes	Linear range	References
Glucose, uric acid	Spot-test	4-amino antipyrine + N-ethyl-N (3-sulfopropyl)-3-methyl-aniline sodium salt (for glucose) and +3,5-dichloro-2-hydroxy acid sodium (for uric acid)	Glucose oxidase, urate oxidase, horseradish peroxidase	0.3–1 mmol/L for both compounds	[28]
Uric acid	Lateral flow assay	3,5,3',5'-tetramethyl benzidine and positively charged gold nanoparticles	Non mentioned, but detection is based on H <sub>2</sub> O <sub>2</sub>	0–0.7 mmol/L	[29]
Glucose, lactate, uric acid and cholesterol	Spot test	Graphene oxide@SiO <sub>2</sub> @CeO <sub>2</sub> hybrid nanosheets having peroxidase activity and O-phenylenediamine, 2,2'-azinobis(3-ethylbenzothiazoline)-6-sulfonic acid, 3,3',5,5'-tetramethyl/benzidine	Respective oxidase enzymes	At least 0–30 mmol/L for all analytes	[30]
Glucose	Lateral flow assay with self-calibration	4-aminoantipyrine, 2,4,6-tribromo-3-hydroxy benzoic acid	Glucose oxidase, horseradish peroxidase	2.4–11.4 mmol/L	[31]
Glucose	3D wax patterned paper, double sided adhesive tape device with fluidic timer	Diethyl phenylenediamine and 1-chloro-4-naphthol	Glucose oxidase, horseradish peroxidase	0–5 mmol/L	[32]
Glucose, protein, alkaline phosphatase, alanine aminotransferase, and uric acid	Multiple lateral flow assay for demonstration of a new vapor-phase polymer deposition fabrication method	For glucose and uric acid: glucose test based on oxidation of potassium iodide, uric acid on commercially available kit	For glucose and uric acid: glucose oxidase, uricase and horseradish peroxidase	Glucose 0–2.8 mmol/L, uric acid 0–0.8 mmol/L	[33]

(continued)



Table 2.2 (continued)

Analyte	Architecture	Indicator	Enzymes	Linear range	References
Nitrite, albumin, glucose and uric acid	Multiple lateral flow assay for demonstration of a new paraffin stamping fabrication method	For glucose and uric acid:glucose test based on oxidation of potassium iodide and uric acid on the described earlier reagents used by Dungchai et al. [6]	For glucose and uric acid: glucose oxidase, uricase and horseradish peroxidase	Glucose 0–12 mmol/L and uric acid 0–5 mmol/L	[34]
Protein, cholesterol, glucose	Multiple wax printed lateral flow assay, qualitative	Glucose and cholesterol assays based on oxidation of potassium iodide	Glucose oxidase, cholesterol oxidase, horseradish peroxidase	Yes/no response for PBS buffer or 40 mmol/L cholesterol, and 5 mmol/L glucose	[35]
Glucose, nickel, glutathione	Lateral flow assay with barriers delimited with wax, with distance-based, equipment-free detection	3,3' diaminobenzidine in peroxidase substrate kit	Glucose oxidase, horseradish peroxidase	7–200 nmol/L	[36]
Glucose	Spot-test, reusable	Ceria nanoparticles	Glucose oxidase	0–100 mmol/L	[37]

Ruecha et al. [41]. System was based on three electrodes: an Ag/AgCl reference, carbon auxiliary electrode and graphene, polyvinylpyrrolidone and polyaniline modified carbon working electrode. After further modification of the working electrode with cholesterol oxidase it was possible to detect cholesterol by means of cyclic voltammetry in the range of 50  $\mu\text{mol/L}$ –10 mmol/L.

Several worth mentioning systems coupled with readers were also described. For example use of a custom-made handheld electrochemical reader that enabled multiple simultaneous measurements [42]. Paper-based device comprises of eight modules, each of them includes a paper channel delimited with wax and three screen printed carbon electrodes. Test zones were modified with one of the following enzymes: glucose oxidase, lactate oxidase or uricase and an electron-transfer mediator ( $\text{K}_3[\text{Fe}(\text{CN})_6]$ ). It was possible to quantify glucose (up to 20 mmol/L), lactate (up to 25 mmol/L), and uric acid (up to 10 mmol/L) by means of chronoamperometry. In another approach paper-based devices were adapted to work with commercially available glucometers [43]. Test strips were printed: with wax to obtain hydrophilic channel, with silver ink for wires and contact pads and with carbon ink to acquire four electrodes. Test were carried out for glucose (detection up to 2.8 mmol/L), cholesterol (0.5–5.2 mmol/L), lactate (1–11 mmol/L), and ethanol (up to 3 mmol/L).

Other systems include chemiluminescent detection of glucose and uric acid [44], and fluorescent detection of sodium, potassium, calcium, chloride, pH, glucose, bicarbonate, urea and creatinine using a smart phone-based fluorescence meter [45].

### 2.1.3 *Quantification of Proteins*

Enzyme immobilization studies, which will be described later in the text, indirectly led to investigation of protein quantification methods. As some enzyme immobilization methods include washing steps it was necessary to confirm the amount of enzyme present on paper. Without this information it would not be possible to compare the results between different immobilization methods tested. Proteins and the most abundant of them in human body albumin are also important clinical indicators.

#### 2.1.3.1 **Clinical Significance of Determination of Protein Levels**

Measurement of total protein and albumin content in urine are one the most useful clinical markers for early stages of kidney disease (albumin > 30 mg/L). Increased levels of both total protein and albumin in urine are associated with increased risk of myocardial infarction, stroke, bladder cancer, diabetes, urinary tract infections [46, 47].

Tests for total urinary protein and albumin can be performed in three ways: a semi-quantitative estimation with a dipstick, determination of the protein to

creatinine ratio in a spot of urine and protein excretion using 24-h urine collection. Albumin is a single chain molecule and one of the most abundant proteins in urine, daily excretion is around 10 mg, comparing with daily protein excretion of around 100 mg. Concentration of albumin in urine is about 5000 times lower than in plasma [48].

Standard urine dipsticks (bis (3',3''-diiodo-4'4''-dihydroxy-5'5''-dinitrophenyl)-3,4,5,6-tetrabromosulfonphthalein dye) usually quantify protein concentrations above 200–300 mg/L. Methods conventionally used in a laboratory to measure urinary albumin include nephelometry, immunoturbidimetry, enzyme-linked immunosorbent assays, radioimmunoassay and high-performance liquid chromatography [47, 48].

Serum total protein and albumin levels decrease in the case of depressed synthesis (end-stage liver disease, intestinal malabsorption syndromes, and protein-calorie malnutrition) or increased losses (nephrotic syndrome and severe burns). The only clinical cause of elevated serum albumin is acute dehydration [48].

Biuret reaction is the most widely applied method of measuring total serum protein. Serum proteins react with copper sulfate in sodium hydroxide forming violet complex. Albumin is usually measured by a dye-binding technique (e.g. bromocresol green, bromophenol blue, 2-(4'-hydroxyazobenzene) benzoic acid, tetrabromophenol blue), later globulin can be evaluated by subtraction of albumin content from the total amount of protein [47, 49]. Other popular tests include Bradford [50] and Lowry methods [51].

### 2.1.3.2 Detection of Proteins in Paper-Based Devices

Simple, qualitative spot tests for amino acids and proteins have been known for decades, as for example the Ninhydrin test. As already mentioned a range of dipsticks using dye binding techniques is commercially available. Literature review of recent paper-based protein detection platforms includes examples such as the use of tetrabromophenol blue. By means of this device with walls delimited with photoresist, it was possible to quantify albumin in the range of 25 mg/L–5 g/L [52]. The same methodology but with bromophenol blue was applied in another device, this time cut manually. Tree shaped design included seven channels, which were used to perform simultaneous calibration during the assay. Device was tested in artificial urine and allowed to quantify albumin in the range of 0.08–5 mg/mL [53]. It is worth mentioning that both systems use citric buffer outside its working range (pH 1.8). A commercial assay kit for protein was used to prepare an origami paper-based device, with wax barriers. This platform allowed detection of albumin in human urine in the range 5–20 mg/mL and presented good correlation of the result with a commercial dipstick test [54]. Paper-based system was also constructed to perform electrophoresis, and was successfully applied to separate main proteins (IgG and albumin) in calf serum. Detection was based on direct

measurement of protein fluorescence [55]. Other recently presented systems are designed for IgG detection, and include: use of a chemiresistor [56] as well as potentiometric [57] and electrochemiluminescent [58] detection.

### ***2.1.4 Enzyme Immobilization on Paper***

Enzymes are biocatalysts performing and regulating processes in living matter. They are very effective, often display regio- and chemoselectivity, high activity and specificity and operate under mild conditions (physiological pH and temperature) [59].

Researchers often emphasize how properties of paper make it an ideal substrate for sensors for the developing world. It has to be remembered that those resource limited settings often lack proper refrigeration during storage and transport, can suffer from energy loss, lack of supplies etc. Even with so many reports describing new paper-based platforms being published, few of them explore their storage stability.

A large number of paper-based sensors is based, at least to some extent, on enzymatic reactions. Protein immobilization methods are known to increase shelf life of such sensors. In fact properly designed immobilization can be beneficial to almost all enzyme properties, such as activity, specificity, selectivity, reduction of inhibition and aforementioned stability. Stability is dictated by the nature and number of bonds between the enzyme and the support, degree of confinement, immobilization conditions and microenvironment created. Immobilized enzymes can gain new interesting properties, as higher volumetric activity or optimized performance under specific conditions (e.g. organic solvents, alkaline, acidic conditions, elevated temperatures). Other example is the possible reusability: enzyme can be recycled and used again reducing the overall cost. Enzyme attached to a support can form a selective sorbent for protein purification or can be used in systems for controlled release of drugs. On the other hand, poorly designed, immobilization can in some cases lead to decreased stability [60–62].

Immobilization methods can be classified as requiring support and support-free, or according to the nature of linkage, based on adsorption, covalent binding and cross-linking, entrapment and encapsulation.

When supports are necessary they should present high density of reactive groups and good compatibility with the surface of the enzyme. Popular supports include synthetic resins, biopolymers and inorganic polymers (silica, zeolites). Use of porous supports is an interesting approach, which permits good dispersion of enzyme molecules, and reduces possible interactions with the external environment, thus preventing aggregation, autolysis or proteolysis etc. Dry filter paper is able to absorb more than its weight when immersed in a solution. Non-volatile components will be retained in the paper structure after drying. Unmodified cellulose possesses a slightly anionic, hydrophilic surface, which can to some extent interact with tyrosine groups and offers few functional (carboxyl) groups. Fortunately paper usually

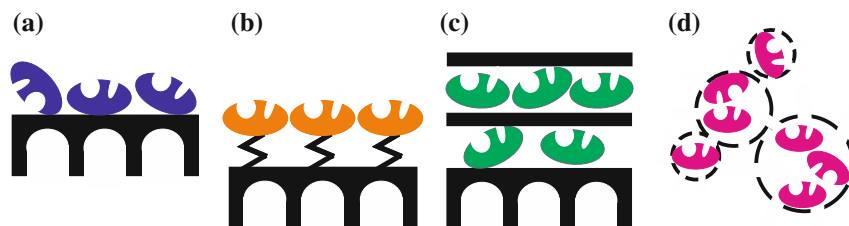


**Fig. 2.1** Schematic representation of **a** adsorption, **b** covalent linkage, **c** entrapment, **d** encapsulation

incorporates also hemicellulose, lignin and other additives, therefore providing a wider range of possible reactive centers. Paper can be also chemically treated (i.e. oxidized) or coated with polymers in order to obtain functional groups of interest [60, 63].

Adsorption (Fig. 2.1a) is simple, inexpensive and does not modify the enzyme chemically. Interaction between the support and enzyme will depend on their character. Thereby hydrophobic supports will be more adequate for enzymes with lipophilic surface resulting in van der Waals interactions. Glycosylated enzymes and the ones with hydrophilic amino acid residues on the surface can interact via hydrogen bonds. Unfortunately this type of immobilization can result in subsequent leaching and the distribution of the enzyme in paper matrix is difficult to control. This method is also highly influenced by the reaction/deposition conditions, like pH that will impact the surface charge [61, 64].

Covalent binding (Fig. 2.1b) rigidifies structure of the enzyme. Usually short spacer arms are used between the enzyme and the support. Distorting agents such as heat, extreme pH or organic solvents will not be able to induce a conformational change of the enzyme that could lead to inactivation. As enzyme is tightly fixed problem with leaching is minimal. Covalent immobilization can also induce a favorable orientation of enzyme molecules. Nevertheless chemical modification can lead to denaturation during the immobilization process, and reaction residue can influence subsequent applications. If the enzyme is deactivated, the support, sometimes costly is also rendered useless. Bifunctional cross-linkers, such as glutaraldehyde can be used to produce carrier-free agglomerates of enzyme molecules or to bind enzymes to a support [60, 62, 65].

In the case of entrapment (Fig. 2.1c) enzymes are typically enclosed in a polymer matrix (organic polymer, sol-gel). This type of immobilization prevents direct contact with the environment, diminishing effects of gas bubbles, solvents and mechanical shear, but can obstruct mass transfer. Sometimes additional covalent attachment is applied to prevent leakage. Layer-by-layer (LbL) assembly, can also be used. In this case support is consecutively exposed to polymer solutions of opposite charge. Adsorption of subsequent layers is achieved by electrostatic interactions and in some cases hydrogen bonds [63, 64].

Encapsulation (Fig. 2.1d) results in similar characteristics to entrapment. It is also possible to immobilize enzymes on colloidal particles that could be later used as a bioactive ink or added to the pulp during the papermaking process. In this case immobilization can be carried independently in an optimized environment [63].

Nowadays, genetically modified enzymes incorporating appropriate binding domains, which adhere spontaneously to cellulose and/or hemicellulose can be used for biochemical coupling with the support. In the case of paper many engineered enzymes with cellulose binding domains are already commercially available, but their price is usually higher [63].

This work will be focused on enzymes from oxidoreductase family, namely glucose oxidase, uricase and cholesterol oxidase. They are all multimeric, and were shown to dissociate under hydrostatic and osmotic pressure, increased temperature and extreme pH. However stabilization was accomplished by means of immobilization (entrapment, covalent linkage, adsorption) [66].

### **2.1.5 Flow in Paper Matrix**

#### **2.1.5.1 Fluid Mechanics in Micro and Nano-Scale**

Microfluidic systems manipulate fluids in the amounts of  $10^{-9}$ – $10^{-18}$  L, inside channels with dimensions of few to hundreds of micrometres. In traditional fluid dynamics, the scale of flow greatly exceeds molecular levels, therefore flow is usually considered as continuous and molecular interactions can be neglected or represented just in physical constants such as viscosity. Scaling down of the fluid path leads to a transition regime between continuum and molecule dominated conditions. The basic hypothesis of continuum is no longer applicable. In a molecular size channel, molecules form discrete number of organized layers, resulting in apparent viscosity even  $10^5$  higher than macro scale values. Viscosity dominates over the forces of inertia resulting in fluid flow characteristic for low Reynolds numbers. Flow in microscale is laminar, thus fluids do not mix convectively. Surface forces like surface tension, van der Waals interaction etc. gain more significance. Heat transport has also a much greater impact and fluid can be driven not only by applied pressure difference but also with the use of electric fields, capillary force and gradients in interfacial tensions. Because of so many differences as compared with the macro scale, the design of a device equipped with channels of micrometer dimensions should be preceded by a thorough analysis of the behavior of the fluid in the system [67–70].

#### **2.1.5.2 Flow in Paper Channel**

Standard sheets used in paper-based sensing have thickness between 100–360  $\mu\text{m}$  (Whatman n° 1 Chromatography paper 180  $\mu\text{m}$ , standard copy paper 80  $\text{g/m}^2$

106  $\mu\text{m}$ , Whatman n° 3 Chromatography paper 360  $\mu\text{m}$ ). Therefore, microfluidics dictates the laws governing flow in paper networks. Paper is also porous, which means that liquid will be driven inside the matrix by capillary forces. In general, two kinds of flow can be distinguished, one being the wet-out process and the other the fully wetted flow.

In the first case, the fluid front is wicking along a dry, porous matrix, and the flow can be described by the Washburn equation [71]:

$$L^2 = \frac{\gamma D t}{4\mu} \quad (2.6)$$

where,  $L$  is the distance moved by the fluid front,  $D$ —the average pore diameter,  $t$ —time,  $\gamma$ —the effective surface tension and  $\mu$  equals viscosity. According to the equation the fluid front velocity decreases with time. Movement of the liquid into the paper caused by surface tension is counteracted by the viscous resistance which grows with the increase of the fluid column.

The second kind of flow is the fully wetted case, usually only observed in the electrochemical flow-through sensors. In this type of devices samples travel along a wetted channel towards the wicking pad at the time when flow is already well established. Wicking of this nature can be described by the Darcy's law:

$$Q = -\frac{\kappa WH}{\mu} * \frac{\Delta P}{L} \quad (2.7)$$

where,  $Q$ —is the volumetric flow rate,  $\kappa$ —the fluid permeability of paper,  $WH$ —area of the channel perpendicular to flow and  $\Delta P/L$ —the pressure difference along the channel. To analyze flux in a channel of varying width, device can be divided in segments. An analogy can be drawn to Ohm's law for computing current through a circuit of  $N$  resistors.  $\Delta P$  will stand for voltage change,  $Q$  act as the fluidic counterpart of current, and  $\frac{\mu L_i}{\kappa W_i H_i}$  as the resistance for each segment  $i$ . The same analogy can be used for fluidic elements in parallel, but in this case reciprocals of resistances add. Based on abovementioned equation, one can predict that all strips of constant width will have the same transport time if their length is equal. In contrast to the wetting process, velocity is constant in a constant-width fully wetted strip [72]. Even small changes in the architecture of the channel can significantly enhance performance of the sensors. Well planned device architecture can allow sequential delivery of reagents, achievement of desired reaction or incubation time and many others.

### 2.1.5.3 Computer Modeling

Numerical simulations of microfluidic devices could reduce the time from concept to prototype, helping to optimize the device. Task of architecture optimization is becoming increasing complex, and difficult to achieve experimentally especially

when counterintuitive effects have to be taken into account. Well-designed simulation could estimate performance of the system or help to explain and visualize experimental phenomena. Numerical techniques can be applied to study fundamental microfluidic problems as mixing, dispersion, controlled reagent delivery but also magnetic, magneto-rheological or acoustic phenomena. Transport of species including manipulation, sorting and storing, even chemical reactions and thermal analysis can all be simulated computationally.

Computer modeling is often based on discretization of differential equations, and can be classified by the method used for discretization as finite difference, finite element, finite volume, and boundary element methods. Some of the commercially available codes include Coventor, CFD ACE+, FLUENT and COMSOL Multiphysics. COMSOL provides a library of predefined models, including a Microelectromechanical Systems package, models for flow in porous media and many others. One model can incorporate different physical phenomena, for example fluid dynamics and mass transfer. Basically after problem formulation and choosing of the desired model, user has to define geometry, specify boundary conditions, apply material properties and select the desired mesh type. Incomplete mathematical description, too simplified model and numerical errors can lead to inaccurate results [73–77].

## 2.2 Materials and Methods

### 2.2.1 *Reagents and Materials*

Glucose Oxidase from *Aspergillusniger* 18.5 U/mg (Sigma Aldrich), Uricase 0880 4.6 U/mg (Sigma Aldrich), Cholesterol Oxidase from *Streptomyces sp.* 20 U/mg (Sigma Aldrich), soluble starch from companies Merck, Altair, Vetec, potassium iodide from Merck and Fisher, bovine serum albumin (Sigma Aldrich), Bradford reagent (Sigma Aldrich B6916-500ML), Folin-Ciocalteu (Sigma Aldrich F9252), Alginic acid Sodium salt from brown algae (Fluka 71238), Carboxymethyl cellulose 40 000, Whatman™ 3 Chr Paper, Whatman™ 1 Chr Paper, Whatman™ 20 Chr Paper, greaseproof Paper (Schoellershammer);

### 2.2.2 *Equipment*

CO<sub>2</sub> Laser cutter Gravograph LS 100, Ultraspec 2000 UV/VIS spectrophotometer, Pharmacia Biotech, Agilent Cary 500 spectrophotometer, MetrohmAutolab Potentiostat;



### 2.2.3 Substrate

As it was already mentioned different types of paper can substantially differ in chemical composition, structure etc. Therefore the following chapter will shortly describe the main types of substrate used in this work.

#### 2.2.3.1 Types of Paper

*Whatman™ Grade 1 Chr Cellulose Chromatography Paper*-made from pure cellulose with no additives of any kind, 0.18 mm thick, with smooth finish. Linear flow rate for water equal 13 cm/30 min. High wet strength [78]. Relatively high absorbency 11  $\mu\text{L}/\text{cm}^2$  [79].

*Whatman™ 3 Chr Chromatography Paper*-made from pure cellulose with no additives of any kind, 0.36 mm thick, with smooth surface. Linear flow rate for water equal 13 cm/30 min. One of the most resistant chromatography papers, considering wet strength [78].

*Standard copy paper*-grammage of 80  $\text{g}/\text{m}^2$ . Usually obtained after mechanical pulping. Made from bleached cellulose, with noticeable amount of alkyl ketene dimer ( $\sim 10\%$ ) and fillers such as  $\text{CaCO}_3$  (few%). Untreated paper is slightly hydrophobic with contact angle of  $115^\circ$  [80, 81]. Thickness around 0.10 mm, with large fibers (diameter  $\sim 20\ \mu\text{m}$ ) and low surface roughness (peak to valley  $\sim 10\ \mu\text{m}$ ). Lacks micro-sized holes and presents sufficient wet strength to pass through a wet process [82].

*Tracing paper-greaseproof Paper Schoellershammer*-grammage of 90/95  $\text{g}/\text{m}^2$ . Homogeneous surface with constant medium grammage, highly transparent, with long fibers and very low porosity. Chemically treated, usually by immersion in sulfuric acid which attacks the surface of fibers, forming an amyloid similar to starch. This amyloid fills areas between fibers resulting in enhanced impermeability to fats and water, higher tear strength and transparency [83, 84].

#### 2.2.3.2 Analysis of Paper Surface

Paper surface was observed through an optical microscope (AmScope company) connected to a computer. Photographs of the surface at various magnifications ( $\times 4$ ,  $\times 10$ ,  $\times 40$ ) were taken by means of AmScope software.

## 2.2.4 Analysis of Glucose, Cholesterol and Uric Acid

### 2.2.4.1 Optical Detection

#### Fabrication of Prototype Devices

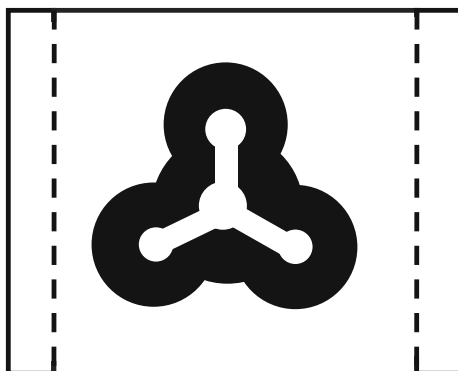
Prototype devices were produced by wax printing described earlier by Carrilho et al. [85]. Basically, Whatman™ Grade 1 Chr was cut in A4 (210 mm × 297 mm) sheets and the desired pattern printed with a XEROX Phaser printer with a solid ink containing wax. Printed paper was later placed on a hot plate set at 110 °C for around 2 min. After cooling, and cutting out of the individual systems, devices were ready to use.

All devices prepared for preliminary tests were composed of a round sampling area with three channels leading to three detection zones situated around the sampling zone (Fig. 2.2). Size of each unit varied, sampling and detection zones: 4–6 mm, channels: 5–10 mm length, 3–4 mm width. Size of the base was equal 4 × 4 cm with 0.5 cm wings, which after bending act as supports. Real size of a finished internal wax pattern is slightly smaller due to lateral spreading of wax upon heating.

#### Choice of Colorimetric Method

Colorimetric assays proposed in this study are based on enzymatic reaction of an oxidase enzyme with its substrate (glucose, uric acid or cholesterol) to produce hydrogen peroxide. Hydrogen peroxide is later detected directly without the use of a peroxidase enzyme, in order to simplify the system and reduce the cost of the assay. Chosen method should provide rapid results, function in the pH range optimal for the enzyme, not inhibit the enzymatic reaction and allow storage for considerable amount of time.

**Fig. 2.2** Design of a sample device used during preliminary experiments



All subsequent tests were carried out first with hydrogen peroxide and later with glucose oxidase and glucose. Glucose oxidase is the least expensive, and least demanding in terms of pH, temperature and storage conditions of the three proposed enzymes.

*Ferric Thiocyanate Assay*-hydrogen peroxide generated upon enzymatic reaction reacts with  $\text{Fe}^{2+}$  to form  $\text{Fe}^{3+}$  ions. Ferric ion can be then monitored as a red thiocyanate complex ( $\lambda_{\text{max}} = 500 \text{ nm}$ ) [86]. Assay conditions: 5 mmol/L  $\text{FeSO}_4$ , 100 mmol/L KSCN in HEPES buffer (pH = 6.5);

*Copper(II) ion and 2,9-dimethyl-1,10-phenanthroline method (DMP)*-after reduction of  $\text{Cu}^{2+}$  by hydrogen peroxide,  $\text{Cu}^+$  forms a yellow colored complex ( $\lambda_{\text{max}} = 454 \text{ nm}$ ) with 2,9-dimethyl-1,10-phenanthroline. Method is not affected by reaction time and complex is stable under light. pH working range 5–9 [87]. Assay conditions:  $\text{CuSO}_4 \cdot 5\text{H}_2\text{O}$  10 mmol/L in 0.2 mmol/L PBS buffer, 2,9-dimethyl-1,10-phenanthroline 50 mmol/L in ethanol;

*Iron(II) ion and 2,6-Bis(hydroxymethyl)-4-methylphenol method*-hydrogen peroxide oxidizes  $\text{Fe}^{2+}$  to form  $\text{Fe}^{3+}$  ions. Ferric ion can be then monitored with 2,6-Bis(hydroxymethyl)-4-methylphenol. Assay conditions: 2,6-Bis(hydroxymethyl)-4-methylphenol 150 mmol/L in ethanol,  $\text{FeSO}_4$  10 mmol/L; pH working range of the assay is around 2, therefore it was not possible to detect hydrogen peroxide formed after enzymatic reaction of glucose. Paper-based devices in which enzymatic and colorimetric reactions are carried out in separate zones were prepared. Glucose first undergoes enzymatic reaction and later hydrogen peroxide is transported to a detection zone modified with the colorimetric reagent. Channel separating both areas was modified with small amounts of diluted acid ( $\text{H}_2\text{SO}_4$  or  $\text{H}_3\text{PO}_4$ ) to lower the pH to a range necessary for the colorimetric assay. In order to optimize the amount of acid, devices were impregnated with indicators that change color in the desired range (thymol blue: transition in pH 1.2–2.8, malachite green: transition in pH 0.2–1.8) or cut from pH indicator paper.

*Starch-iodide method*-hydrogen peroxide generated upon enzymatic reaction reacts with iodide ions to form iodine. In the next step iodine reacts reversibly with iodide ion yielding triiodide which can further react with iodine to form pentaiodide. Triiodide and pentaiodide are linear and can enter inside the amylose helix of starch. Charge transfer between starch and iodide, results in a change in coloration from colorless to blue-black ( $\lambda_{\text{max}} = 660 \text{ nm}$ ). Molybdenum ions were shown to enhance the reaction rate in the absence of peroxidase [88]. Assay conditions: KI 3 mmol/L,  $\text{Na}_2\text{MoO}_4$  2.5 mmol/L, starch 10 mg/ml dissolved by gentle heating

*Methylene blue*-first methylene blue is reduced to colorless leucomethylene blue, for example by means of sodium thiosulfate. Later hydrogen peroxide can be used to oxidize it back to color methylene blue ( $\lambda_{\text{max}} = 660 \text{ nm}$ ). Different catalysts can be used, i.e. alumina supported metals [89, 90]. Different reaction conditions tested, varying concentrations of reagents, pH, with use of  $\text{KAl}(\text{SO}_4)_2$  or in 1 mol/L  $\text{NaOH}/\text{NaCl}$ .

### Differences in Hue and Repeatability of Digitalization

Preliminary tests were digitalized by means of a scanner and image analyzed in Corel Photo-paint  $\times 5$  using a histogram tool. Color was analyzed in RGB, CMYK and gray scale considering total signal for all the channels and each channel separately. In each case intensity of a blank area of the same size (number of pixels) and from the same device was subtracted from the mean intensity for the detection area. Maximum intensity was obtained for channels Magenta, Cyan and CMYK.

Differences in hue were observed during the preliminary experiments. It was also noted that the time during which scanner illuminates the samples is different for each digitalization.

To evaluate repeatability of quantification using a scanner, devices on which a glucose assay was carried out were scanned repeatedly 8 times and image analyzed in Corel Photo-paint  $\times 5$ .

To address the hue issue different formulations of the starch-iodide reagent were prepared using combinations of potassium iodide (Merck, Fisher) and starch (Merck—two different batches, Altair, Vetec) from different brands. Those reagents were used to prepare spot-tests for preliminary assays with cholesterol and cholesterol oxidase. Two samples for each concentration (0–10 mmol/L) of cholesterol were prepared for each of the 8 formulations of reagents.

### Solving the Autoxidation Problem

The starch-iodide method was chosen as the colorimetric assay, therefore attempts were made to solve the autoxidation problem. After around 30 min from spotting on paper, test zones changed color from colorless to brown (iodine ions). Subsequent approaches were tested:

- Optimization of pH  
Tests in PBS buffer of different pH (range 5–8, 3 replicates) were carried out, with 0.3 % hydrogen peroxide. Hydrogen peroxide was used as model analyte to avoid contributions related to different activity of glucose oxidase caused by pH change.
- Layer of liquid polymer (ethylene glycol, poly(vinyl alcohol)) on top of the detection zone modified with starch-iodide reagent;
- Protective cover cut from
  - adhesive tape (different brands and types used: Koretech, Adere–Tape Fix, Scotch);
  - transparent film with and without adhesive (Parafilm, food wrap, Tilibra book cover foil, Contact Vulcan adhesive foil);
  - lamination;

protective layer covered both sides of paper leaving only sampling area bare.

## New Fabrication Methods for Analysis of Cholesterol

Cholesterol is insoluble in water, thus stock solutions was prepared with the use of a surfactant, Triton X-100 [91]. Stock solutions with even minimal amounts of surfactant were not contained in paper channels delimited with wax, and would spread freely in the paper matrix regardless the wax pattern. It was also not possible to observe a color change for the enzymatic spot tests which can indicate enzyme inactivation or most probably disturbed interaction between tri- and pentaide ions and starch. In subsequent tests ethanol was used to prepare stock solutions of cholesterol. Other methods used to dissolve cholesterol found in the literature include use of ether [92], hexane, chloroform [93], isopropanol [94] and liposomes [95].

Even without the use of a surfactant, cholesterol solution would pass through wax barriers, spreading evenly through paper, thus it became necessary to develop a new fabrication method, compatible with this kind of sample. New device could be cut from paper, or use a polymer that would physically shut paper pores.

In the case of polymers, solutions of different concentrations were prepared and used to draw simple structures on paper. Polymers tested include: polydimethylsiloxane (PDMS), chitosan, polystyrene, polyvinyl chloride (PVC) and commercial waterproofing agents (NP Nanopool®, Germany and Waterproof spray by Sistem, Brazil). Details of polymer preparation are resumed in Table 2.3. Polymers were applied manually but in the future could be dispensed by an inkjet printer or used to fill simple gel or fountain pens. Test solutions included water, vegetable oil, as well as stock solutions of cholesterol in ethanol or Triton X-100.

Tests were performed also with paper without any delimitation, paper cut manually with scissors or paper punch, as well as a laser cutter. Depending on the type of paper and feature type (straight or curved lines) power of the laser cutter was adjusted to 5–12 % and velocity to 85–100 %. Pieces of paper could be suspended, or glued on top of a transparent film with adhesive.

## Immobilization of the Colorimetric Reagent for Enhanced Uniformity of Color Development of Uric Acid Assay

Uric acid is poorly soluble in water, methods of dissolution found in the literature include use of buffers such as PBS [96], acetate, Tris-HCl [97], borate [98], additives of  $\text{LiCO}_3$  or  $\text{Na}_2\text{CO}_3$  [99], or dissolution in concentrated NaOH [100] with subsequent dilution with buffer. It was possible to prepare stock solution of desired concentration (10 mmol/L) only in NaOH or by addition of carbonates. During experiments uric acid was solubilized with addition of small amounts of  $\text{K}_2\text{CO}_3$ .

Using simple wax printed devices presented for glucose tests (Fig. 2.2) it was possible to distinguish only light coloration around the detection area, which could indicate that the starch-iodide reagent is being carried with the uric acid sample. After the experiment 3.0 % hydrogen peroxide was spotted on the detection zone

**Table 2.3** Review of polymers applied to form barriers impermeable to cholesterol-methodology

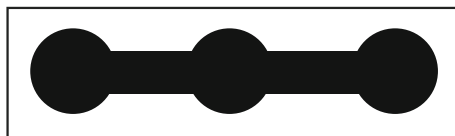
Polymer	Preparation
Chitosan	Fibers: Chitosan fibers were pressed on top of paper channel delimited with wax. Acetate buffer (pH = 2.3) was passed through the channel for 15–20 min Powder: different quantities of chitosan powder were dissolved in acetate buffer. Several layers of polymer were deposited in case of more diluted solutions
PDMS	PDMS solution 5:1 (elastomer base: curing agent) was prepared and diluted with different solvents (toluene, isopropanol, hexane) to obtain a range of concentrations. After patterning with polymer, paper was dried in ambient temperature or in an oven set at 120 °C
PVC	PVC was dissolved in tetrahydrofuran obtaining a set of concentrations. Several layers of polymer were deposited in case of more diluted solutions.
Polystyrene	Polystyrene was dissolved in toluene and heated. Concentrated stock solution was dissolved to obtain set of concentrations
Commercial waterproofing agents	NP Nanopool®: Whatman n° 1 sheet was sent to NP Nanopool® (Germany) for modification. Channels were designed with nanostructured waterproofing product and sent back to Brazil. Unfortunately due to several issues with Brazilian post service sample was delivered completely soaked with rainwater. After drying channels were filled with the test solutions Waterproof spray by Sistem: First parts of a paper slip were covered with masking tape and sprayed with the waterproofing agent to create channels. Promising results led to fabrication of more advanced structures cut by means of laser cutter with supporting channels filled with the waterproofing spray

and strong black-blue coloration was only visible in the vicinity of the border. This effect was not seen during experiments with glucose and cholesterol. Usually mean intensity of pixels of a given area is used for quantification in a graphic program. If a great part of the detection area remains discolored it will influence the results, lowering sensitivity. Because of this reason different pretreatments were applied to immobilize the indicator in the detection zone. Some attempts to provide more uniform coloration were already described in the literature and include use of polyvinyl amine [101], gelatin [102], poly(acrylic acid) and polyethylene glycol [103].

During this work tests were carried out with gelatin, poly(acrylic acid) and poly [di(ethylene glycol)]. First paper strips were modified with one of the aforementioned reagents at different concentrations. After drying, the starch-iodide solution was deposited, and in sequence glucose oxidase (1 mg/mL) and glucose (10 mmol/L). More systematic tests were performed with gelatin.

Gelatin was dissolved by heating in PBS buffer pH = 6.5 to obtain a set of concentrations: 5, 10, 15, 20, 25 mg/mL. Two types of tests were performed a lateral flow assay and a spot test, both with gelatin deposited with one of the following manners:

**Fig. 2.3** Laser cut assay for layer-by-layer tests



- a. starch-iodide reagent deposited and left to dry, subsequently modified with gelatin solution, test stored for 24 h in 4 °C;
- b. starch-iodide reagent mixed with gelatin, test stored for 24 h in 4 °C
- c. gelatin layer deposited and stored for 24 h in 4 °C, subsequently test area modified with starch-iodide reagent;

Test were stored for 24 h in 4 °C after deposition of gelatin to ensure uniform modification and drying of the polymer. Three samples of each test type were prepared (6 types) for all 5 concentrations, plus a test without gelatin. In the case of the lateral flow assay enzyme was deposited before the modified zone, and glucose sample was spotted in the beginning of the channel. After drying bottom of the paper slip was submersed in PBS buffer that would carry glucose to the enzymatic zone and later hydrogen peroxide to the detection area. In the spot test all the reagents were added on top of the starch-iodide modified area. To document the results photos were taken after 0, 2, 5, 10 and 20 min from starting of the test.

In the next step tests were carried out with uric acid and uricase. Tests included optimized assay with gelatin (10 mg/mL for lateral flow assay, gelatin on top of starch-iodide reagent) and a layer-by-layer approach. Test were performed in laser cut suspended devices shown in Fig. 2.3. Three types of assay were proposed, with zone A always serving as sampling area:

- i. area B: LbL alginate/UOx-chitosan, 2 bilayers alginate 1 mg/mL, pH = 8.5, chitosan 0.5 mg/mL, pH = 7.5; area C: starch-iodide reagent under gelatin 10 mg/mL;
- ii. area B: LbL alginate-UOx, 2 bilayers alginate 1 mg/mL, UOx in borate buffer pH = 8.0; area C: starch-iodide reagent under gelatin 10 mg/mL;
- iii. area B: starch-iodide reagent under LbL alginate-UOx, 2 bilayers alginate 1 mg/mL, UOx in borate buffer pH = 8.0; area C: without modification;

4 tests of each type were prepared and 10 mmol/L uric acid was used in all cases.

### Calibration Curves

Several attempts were made to perform lateral flow assays for uric acid and cholesterol. Some of the approaches are resumed in Fig. 2.4. Device visible in Fig. 2.4a was cut with laser leaving small uncut areas on the sides of channels (marked with arrows). Vicinity of the uncut area was modified with waterproofing

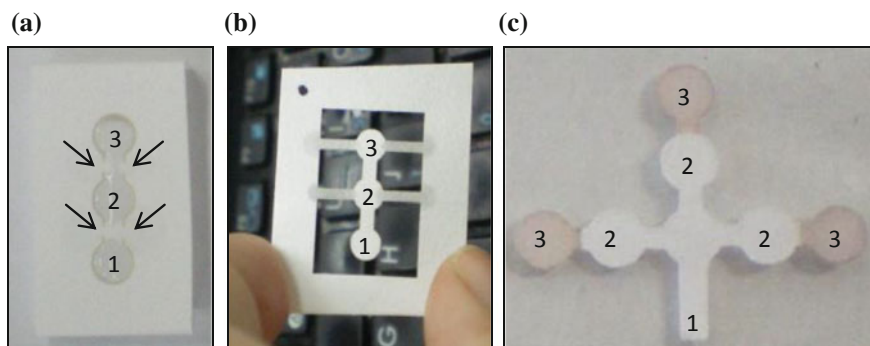


**Fig. 2.4** Some devices used for uric acid and cholesterol assays. **a** Laser cut suspended. **b** Laser cut, suspended with long supporting channels. **c** Laser cut, on a layer of adhesive foil. 1. sampling area, 2. enzymatic area, 3. detection area

agent. Due to small space dividing the assay area from the support, in some cases leaks would appear. Therefore another device was proposed (Fig. 2.4b) in which longer supporting channels filled with waterproofing agent would hold the device.

Third example shown on Fig. 2.4c is a laser cut assay, this time in physical contact with a support. Flux, observed in this case will be slightly different because of the interface formed between paper and an adhesive foil. Unfortunately it was not possible to obtain color change for lateral flow cholesterol assay. This compound could be only detected in spot tests. Probably cholesterol is too strongly retained in the paper matrix. All tests for uric acid resulted in uneven coloration around the detection zone. Because of this also uric acid was quantified in a spot test. In order to perform the tests, circles (diameter 5 mm) were cut by means of a laser cutter from Whatman n° 1 chromatographic paper and glued on top of a transparent foil with an adhesive. For the lateral flow glucose assay device shown Fig. 2.4b was used, with 4 mm diameter sample, enzymatic and detection zones, and 2 mm × 2.2 mm channels.

#### Uric acid assay:

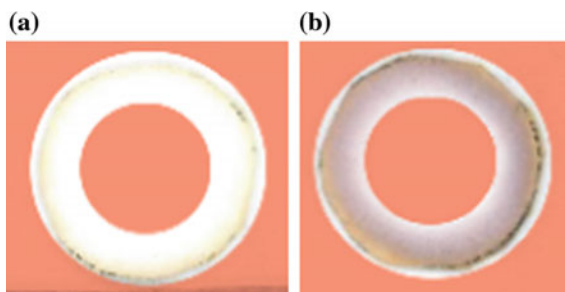
Spot test modified with 2  $\mu$ L of starch-iodide reagent,  
after drying, with 2  $\mu$ L of 15 mg/mL gelatin solution,  
after 24 h, with 2  $\mu$ L uricase solution 18.4 U/mL,  
all solutions prepared in 0.2 mmol/L PBS buffer pH = 8.0;  
2  $\mu$ L of sample solution was used to run the assay.

#### Cholesterol assay:

Spot test modified with 2  $\mu$ L of starch-iodide reagent,  
after drying, with 2  $\mu$ L cholesterol oxidase solution 20 U/mL,  
all solutions prepared in 0.2 mmol/L PBS buffer pH = 7.0;  
2  $\mu$ L of sample solution was used to run the assay.



**Fig. 2.5** Masking method used, for quantification of uric acid, **a** 0 mmol/L, **b** 5 mmol/L, masked area marked in *pink*



Glucose assay:

Enzymatic zone modified with 2  $\mu$ L of glucose oxidase solution 18 U/mL,  
 Detection zone modified with 2  $\mu$ L of starch-iodide reagent,  
 all solutions prepared in 0.2 mmol/L PBS buffer pH = 6.5.  
 8  $\mu$ L of sample solution was used to run the assay.

Corel Photopaint  $\times 5$  was used for quantification. In the case of uric acid double mask was used (Fig. 2.5) to overcome the impact of discolored middle area.

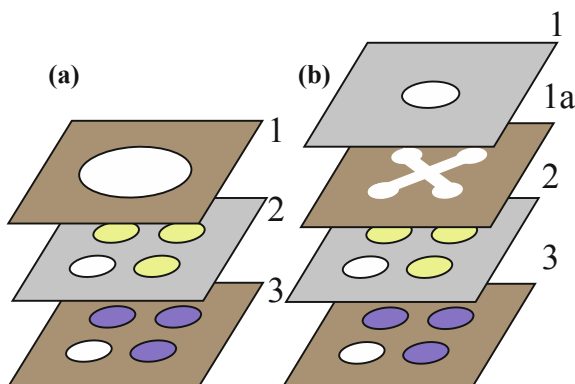
### Tangential Flow Devices

As an attempt to integrate all three assays in one device, a tangential flow system was proposed. Devices of this type, known also as 3D pads (three dimensional paper-based analytical devices), or opads (origami paper-based analytical devices) are usually assembled from several layers of paper. In this case to allow quantification of cholesterol, each paper layer was enclosed in a transparent adhesive foil. Layers were stacked together and clamped with a large paper clip. Both, paper and plastic foil were cut by means of a laser cutter. Each layer included a paper frame to stiffen the construction, and to obtain more constant thickness along the layer. Several variations of this device (Fig. 2.6) were proposed including:

- a. 1st sampling layer (varying size and format),  
 2nd four compartment enzymatic layer (with or without immobilization),  
 3rd four compartment detection layer (with or without gelatin layer) (Fig. 2.6a);
- b. as above but with an intermediate distributing layer between layers 1 and 2 (Fig. 2.6b);
- c. as above but with an acrylate holder;

Device comprised of 4 detection zones, 1 for each analyte and 1 serving as a control. Sampling area could be in the future modified with agglutination antibodies, or cut from a plasma separation membrane (e.g. Vivid™ Plasma Separation Membrane, thickness 330  $\mu$ m, material: asymmetric polysulfone). Layers are only stacked, thus it is possible to dismantle the device for quantification. Concentration of the reagents was equal as in the previous experiments destined to construct the

**Fig. 2.6** Tangential flow device. **a** Without distribution layer, **b** with distribution layer. 1. sampling area, 1a. distribution layer, 2. enzymatic zone, 3. detection zone



calibration curves. To perform the test, 2–8  $\mu\text{L}$  of the sample were spotted on the sampling area and subsequently 5–20  $\mu\text{L}$  of water or buffer was added.

#### 2.2.4.2 Methods of Enzyme Immobilization on Paper

##### Protein Quantification Methods

Next chapter will resume enzyme immobilization studies performed to prolong shelf life of proposed paper-based devices. In the case of some immobilization methods (encapsulation and methods that require washing steps) the final concentration of enzyme in the sample is not known. Therefore in order to compare activity of those samples it is necessary to quantify the amount of protein present. Several methods were tested, including the Bradford method [50], the Lowry method [51] with and without the use of surfactant, use of dyes such as bromocresol green [104] and bromophenol blue [47] as well as direct quantification (measurement of absorbance in the range of 200, 260–280 nm) [105].

Tests were performed:

- in solution—to ensure correctness of execution;
- on slips of unmodified paper—to guarantee that the lack of result is not caused by the absorption of reagents in the wax barrier;
- on  $1 \times 1$  cm devices with wax barriers—to guarantee that the lack of result is not caused by flow of reagents with subsequent additions. Two devices were used, one with a circular area of 3 mm and another in form of a square  $1 \times 1$  cm (Fig. 2.7). Square device was used for the subsequent immobilization studies. Results obtained for those two tests did not present any significant differences, thus only protocols for the  $1 \times 1$  device will be described in detail. To guarantee correctness of execution, samples of the enzyme immobilization study were encoded, and analyzed in random order. Serial number can be seen on the photograph presented in Fig. 2.7.

**Fig. 2.7** Sample devices used for immobilization tests, to guarantee correctness of execution, all samples were encoded (*number seen on the border*)



Some of the methods of protein quantification are based on interaction with specific amino acids, thus they can be applicable only to certain proteins. For this reason BSA (bovine serum albumin) was used as a model protein, and GOx (glucose oxidase) as model enzyme, both in concentration between 10 and 40 mg/mL. Distilled water was used as control. In the case of spectrophotometric analysis Ultraspec 2000 UV/VIS spectrophotometer, Pharmacia Biotech, was used for all tests in solution (water or buffer solution used as blank) and Agilent Cary 500 spectrophotometer for tests on paper (Teflon used as blank).

#### *Bromocresol green (BCG)*

Based on the interaction between the indicator and proteins accompanied by a change in coloration to blue-green. In the case of this method several different protocols were found in the literature, thus preliminary tests were carried out using succinic acid buffer pH = 4.3, with or without the addition of sodium azide 4 mmol/L and with different dye concentrations (0.5–5.5 mmol/L). For the paper-based tests maximum concentration of the dye without the use of sodium azide was used.

Test in solution 100  $\mu$ L succinic acid buffer pH 4.3 + 100  $\mu$ L of BCG 5.5 mmol/L + 50  $\mu$ L of sample or control;

Test on paper 10  $\mu$ L succinic acid buffer pH 4.3 + 10  $\mu$ L of BCG 5.5 mmol/L + 10  $\mu$ L of sample or control;

#### *Bromophenol blue (BPB)*

Based on interaction between the indicator and proteins accompanied by a change in coloration to blue. Preliminary tests for the bromophenol blue method included samples of the dye dissolved only in ethanol, and ethanol with subsequent dilution 1:1 with buffer solutions (acetate buffer pH = 2.3; citrate buffer pH = 3.2;

succinic acid buffer pH = 4.3). Citrate buffer was chosen for the subsequent analysis.

Test in solution 100  $\mu$ L citrate buffer pH 3.2 + 100  $\mu$ L of BPB + 50  $\mu$ L of sample or control;

Test on paper 10  $\mu$ L citrate buffer pH 3.2 + 10  $\mu$ L of BPB + 10  $\mu$ L of sample or control;

Subsequently calibrations curves for tests in solution were constructed for both compounds (0.3–20 mg/mL), 3 replicates were prepared for each concentration. During tests on paper it was noted that the time between application of the indicator solution and the sample has a significant impact on the observed result. Also the order in which reagents were applied on paper had a major impact. In the case when the protein is spotted first (Fig. 2.8a) resulting coloration is uneven, with more intense color appearing in the place of spotting. When BPB was spotted first, color was even on the whole modified area (Fig. 2.8b). To obtain the same result with paper already containing protein, several deposition methods were tested with best results obtained with spraying (Fig. 2.8c).

#### *Lowry method*

Copper(II) forms a complex with peptide bonds under alkaline conditions, and in result is reduced to Copper(I). Monovalent copper in turn reacts with Folin-Ciocalteu reagent. Color changes from colorless (Lowry reagent) and yellow (Folin-Ciocalteu reagent) to blue (dark blue in the case of the modified assay).

Two versions of this assay were tested:

#### *Lowry method*

Reagent A 40 mg  $\text{CuSO}_4$ , 2 g  $\text{K}_2\text{CO}_3$ , 20 mg sodium potassium tartrate, 20 mL  $\text{H}_2\text{O}$

Reagent B 80 mg NaOH, 2 mL  $\text{H}_2\text{O}$

Lowry reagent 3 parts of A + 1 part of B

Test in solution 100  $\mu$ L of sample or control + 100  $\mu$ L of the Lowry reagent (10 min) + 25  $\mu$ L of Folin-Ciocalteu reagent;

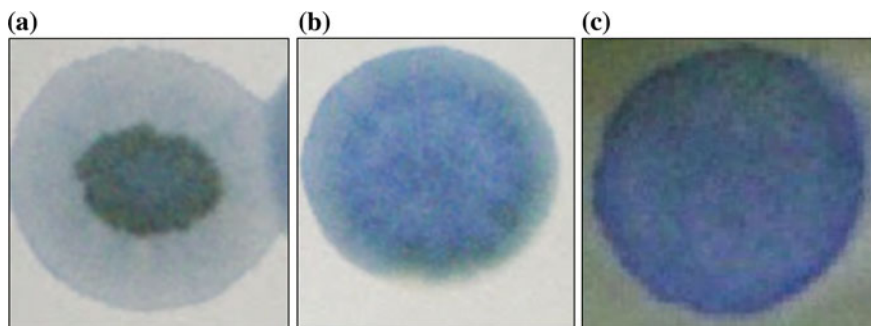


**Fig. 2.8** BPB assays depending on the order of deposition **a** BSA + BPB, **b** BPB + BSA, **c** BSA + BPB Spray

Test on paper 10  $\mu\text{L}$  of sample or control + 10  $\mu\text{L}$  of the Lowry reagent (10 min) + 10  $\mu\text{L}$  of Folin-Ciocalteu reagent;

**Modified Lowry method (with surfactant)**

Reagent A 40 mg  $\text{CuSO}_4$ , 2 g  $\text{K}_2\text{CO}_3$ , 20 mg sodium potassium tartrate, 20 mL  $\text{H}_2\text{O}$

Reagent B 20 mg sodium dodecyl sulfate, 2 mL  $\text{H}_2\text{O}$

Reagent C 80 mg  $\text{NaOH}$ , 2 mL  $\text{H}_2\text{O}$

Lowry reagent 3 parts of A + 1 part of B + 1 part of C

Test in solution 100  $\mu\text{L}$  of sample or control + 100  $\mu\text{L}$  of the Lowry reagent (10 min.) + 25  $\mu\text{L}$  of Folin-Ciocalteu reagent;

Test on paper 10  $\mu\text{L}$  of sample or control + 10  $\mu\text{L}$  of the Lowry reagent (10 min) + 10  $\mu\text{L}$  of Folin-Ciocalteu reagent;

*Bradford method*

Method listed in Brazilian Pharmacopeia. It is based on the fact that proteins upon binding displace the absorption maximum of acidic solution of Coomassie Brilliant Blue G-250 from 465 to 595 nm (color change from brown to blue).

Test in solution: 100  $\mu\text{L}$  of sample or control + 400  $\mu\text{L}$  of Bradford reagent;

Test on paper: 10  $\mu\text{L}$  of sample or control + 10  $\mu\text{L}$  of Bradford reagent;

Paper pretreatment protocol: methanol 5 min, methanol/ $\text{NH}_4\text{OH}$  5 mol/L(1:1) 10 min, methanol 2 min, methanol/ $\text{CH}_3\text{COOH}$  glacial (1:1) 10 min, rinsed several times in water;

*Direct quantification*

Aromatic rings of amino acids cause an absorbance peak at 280 nm and peptide bonds are responsible for peak around 200 nm. Secondary, tertiary and quaternary structure, and therefore factors such as pH, ionic strength affect absorbance. This method requires more sophisticated equipment than the colorimetric analysis (spectrophotometer instead of a scanner or camera) but it is nondestructive and does not require any additional reagents. First tests were carried out with a conventional spectrophotometer (Ultraspec 2000 UV/VIS, Pharmacia Biotech) by placing slips of modified paper directly on the optic path. Paper slips were immersed in water or oil. Arrangement of fibers in paper is not uniform throughout the paper therefore resulting repeatability of such tests was very low (light beam of small diameter). Next a spectrophotometer, with varian integrating sphere designed for solid samples was used (Agilent Cary 500) with Teflon serving as blank.

For tests in solution calibration curves (0.3–20 mg/mL) were prepared for both compounds, three replicates were made for each concentration.

For test on paper,  $1 \times 1$  cm devices shown in Fig. 2.7 were modified with 10  $\mu\text{L}$  of sample.

## Enzymatic Activity, Optimization of Assay Conditions

Three methods have been proposed for the assessment of enzymatic activity. The most widely used in the literature is the measurement with an oxygen probe in

which the evaluation is based on oxygen consumption during the enzymatic reaction. Several cleaning and maintenance procedures have been conducted, but unfortunately the oxygen electrode found in the laboratory proved non-functioning. Other methods are based on indirect measurement and include reaction of hydrogen peroxide with luminol or potassium iodide. The number of variations of the luminol method in the literature is considerable, and the reaction conditions have to be optimized and adapted for use on paper. Since the first tests did not provide satisfactory results, the subsequent analysis was abandoned and starch-iodide method, already optimized for detection of hydrogen peroxide on paper was used.

First, pH was optimized for the glucose oxidase reaction with starch-iodide reagent. Tests were performed in solution, using Ultraspec 2000 UV/VIS spectrophotometer.

pH optimization assay: 0.8 mL of starch-iodide reagent of appropriate pH, 1.0 mL of PBS 0.2 buffer, 0.2 mL of 5 mmol/L glucose solution, quantification performed after 10 min from addition of the enzyme. Three samples were prepared for each pH tested.

Subsequently a calibration curve for enzymatic assay in solution was prepared (enzyme concentration 0.1–10 mg/mL) in pH 5.5.

## Enzyme Immobilization Methods

Immobilization procedures are resumed in Table 2.4. Methods are divided in 5 groups: physical adsorption, entrapment in gel, layer-by-layer, covalent binding and encapsulation. Study includes using blockers (glycine, BSA), surface treatment (adsorption on a layer of polymer), use of protectants (mannitol, trehalose). Immobilization methods based on cellulose binding domains are not included, because they require use of modified enzymes that are more expensive and less available. Each sample was a square piece of Whatman n° 1 paper with a  $1 \times 1$  cm sample area defined with wax (XEROX Phaser printer). 10  $\mu$ L of solution was needed to wet the paper completely, if not stated otherwise this volume was used for all modifications. All solutions, if not stated differently were prepared in PBS pH = 5.5. In the case of layer-by-layer methods paper was covered with 3 bilayers starting with anionic polymer. In the second and third bilayer cationic polymer was mixed with glucose oxidase to obtain final concentration of 2.5 mg/mL (92.5 U/mL) of enzyme. In the case of subsequent methods: EDC, EDC/NHS, entrapment in ammonium alginate and all encapsulation methods several batches with different concentration of reagents and reaction times were prepared. Table 2.4 lists only the optimized conditions of aforementioned methods. In the case of encapsulation methods, smaller capsules were dispersed on sample papers with a pipette, larger capsules were transported manually on paper and left to dry.

**Table 2.4** Immobilization methods reviewed during this study, with their preparation procedure. Reprinted with permission from [129]

No.	Group	Method	Preparation procedure	References
1	Physical adsorption	Simple adsorption	10 $\mu$ L of GOx 5 mg/mL (92.5 U/mL)	–
2		Bovine serum albumin (BSA) blocking	10 $\mu$ L of GOx 5 mg/mL, after dry 10 $\mu$ L of BSA 5 mg/mL	[106]
3		On a layer of collagen	10 $\mu$ L of confectionary gelatin 10 mg/mL, after dry 10 $\mu$ L of GOx 5 mg/mL	[102]
4		On a layer of stearic acid	10 $\mu$ L of stearic acid 4.75 mg/mL, after dry 10 $\mu$ L of GOx 5 mg/mL	[107]
5		On a layer of polyvinyl alcohol (PVA)	10 $\mu$ L of PVA 11.5 mg/mL, after dry 10 $\mu$ L de GOx 5 mg/mL	[65, 108, 109]
6		With mannitol	10 $\mu$ L of GOx 5 mg/mL—mannitol 8 mg/mL	[6]
7		With trehalose	10 $\mu$ L of GOx 5 mg/mL—trehalose 2.75 mg/mL	[110]
8	Entrapment in gel	In starch	10 $\mu$ L of GOx 5 mg/mL—starch 10 mg/mL	[111]
9		In chitosan	10 $\mu$ L of GOx 5 mg/mL—chitosan 1.5 mg/mL; Chitosan solution was first prepared in water with acetic acid and later diluted with PBS and Na <sub>2</sub> HPO <sub>4</sub> to obtain the desired pH.	[65]
10		In polyvinyl alcohol (PVA)	10 $\mu$ L of GOx 5 mg/mL—PVA 5 mg/mL	[65, 108, 109]
11		In dextran	10 $\mu$ L of GOx 5 mg/mL—dextran 2 mg/mL	[64]
12		In ammonium alginate	10 $\mu$ L of GOx 5 mg/mL – ammonium alginate 15 mg/mL	[112, 113]
13		In carboxymethyl cellulose (CMC)	10 $\mu$ L of GOx 5 mg/mL—CMC 7 mg/mL	[64, 114]
14	Layer-by-layer	Sodium alginate-chitosan	Sodium alginate 4 mg/mL, chitosan 2 mg/mL	[115]
15		Sodium alginate-polylysine	Sodium alginate 4 mg/mL, polylysine 2 mg/mL	[115, 116]
16		Sodium alginate-polyethylenimine (PEI)	Sodium alginate 4 mg/mL, PEI 10 mg/mL	[117, 118]
17		Hyaluronic acid-chitosan	Hyaluronic acid 2 mg/mL, chitosan 2 mg/mL	[116, 119]
18		Hyaluronic acid-PEI	Hyaluronic acid 2 mg/mL, PEI 10 mg/mL	[116, 117]
19		Poly(vinyl sulfate)-chitosan	Poly(vinyl sulfate) 2 mg/mL, chitosan 2 mg/mL	[118, 120]
20		Poly(acrylic acid)-chitosan	Poly(acrylic acid) 5.6 mg/mL, chitosan 2 mg/mL	[118, 121]

(continued)

**Table 2.4** (continued)

No.	Group	Method	Preparation procedure	References
21	Covalent linkage	Glutaraldehyde crosslinking	10 $\mu$ L of GOx 5 mg/mL, when dry 10 $\mu$ L of glutaraldehyde 2.5 %	[122]
22		Glutaraldehyde crosslinking with glycine blocking	10 $\mu$ L of GOx 5 mg/mL, when dry 10 $\mu$ L of glutaraldehyde 2.5 %, after 1:30 h, samples sprayed with 1 mol/L glycine	Modified method 21
23		Schiff base	Samples of paper were submerged in 100 g/L KIO <sub>4</sub> for 12 h, washed with water and dried with a paper towel. 10 $\mu$ L GOx 10 mg/mL was spotted two times on each sample within an interval of 1 h. After 1 h 10 $\mu$ L of 6 mg/mL of NaBH <sub>3</sub> CN was spotted on each device, which were, after 2 h washed several times with water	[123]
24		EDC <sup>a</sup> with glycine blocking	10 $\mu$ L of EDC 20 mg/mL, GOx 10 mg/mL was spotted on each sample and left to react for 1 h in 4 °C. Subsequently more 10 $\mu$ L EDC/GOx mixture was spotted and left for 2 h in 4 °C. After that time 10 $\mu$ L of glycine was spotted on each sample	[124]
25		EDC <sup>a</sup> /NHS <sup>b</sup>	10 $\mu$ L of 150 mg/mL EDC, 24 mg/mL NHS was spotted and left to react for 1 h in 4 °C. After that time more 10 $\mu$ L was spotted and left to react for 3 h, also in 4 °C. Subsequently 10 $\mu$ L of GOx 10 mg/mL was spotted and after 2 h more 10 $\mu$ L GOx	[125]
26		Potassium periodate, ethylenediamine, and glutaraldehyde activation	Paper substrate immersed in hot 0.1 M KIO <sub>4</sub> for 1:30 h. Washed with water to remove excess periodate and immersed in a solution of 12.5 mg/mL of ethylenediamine for 2:30 h and in 2.5 % solution of glutaraldehyde for 1:30 h, washed 5 times with distilled water. 10 $\mu$ L of GOx 10 mg/mL was deposited on each sample	[122]

(continued)



**Table 2.4** (continued)

No.	Group	Method	Preparation procedure	References
27	Encapsulation	Sodium alginate	Solution of 30 mg/mL of sodium alginate and 20 mg/mL of GOx was added dropwise to 55 g/L of $\text{CaCl}_2$ under constant stirring	[126]
28		Sodium alginate—carboxymethyl cellulose (CMC)	Solution of 15 mg/mL of sodium alginate, 30 mg/mL of CMC and 20 mg/mL of GOx was added dropwise to 55 g/L of $\text{CaCl}_2$ under constant stirring	[126]
29		Sodium alginate—chitosan	Solution of 15 mg/mL of sodium alginate, 30 mg/mL of chitosan and 20 mg/mL of GOx was added dropwise to 55 g/L of $\text{CaCl}_2$ under constant stirring	[112]
30		PEI	5 mL of a solution of 120 mg/mL PEI with 5 mg/mL GOx was added to 25 mL of cyclohexane with 0.1 % of Triton X 100 under constant stirring. 5 min after the emulsion was formed 1.2 mg of sebacoyl chloride in 1.2 mL of cyclohexane was added to the mixture. After 10 min of reaction, another 1.5 mL of sebacoyl chloride 1 mg/mL was added and left to react for 10 min. Reaction was stopped with 25 mL of cyclohexane and the capsules washed with water several times	[127]
31		Covalent attachment to PEI capsules	As the capsules from method 30 did not show any enzymatic activity they were used as a base to covalently attach GOx by means of glutaraldehyde crosslinking. For this purpose 10 mL of a suspension of PEI capsules from the previous study was mixed with 1 mL GOD 10 mg/mL and 4 mL of glutaraldehyde 2.5 % and left to react for 1 h under constant stirring. Capsules were washed with distilled water	Modified method 30
32		Covalent attachment to silica beads	1.5 g of chromatography silica beads was mixed with 5 mL of 10 mg/mL GOx and glutaraldehyde 2.5 % and left to react for 1 h. Afterwards washed with water	[109]

(continued)

**Table 2.4** (continued)

No.	Group	Method	Preparation procedure	References
33		Chitosan	10 mL of 40 mg/mL chitosan, 20 mg/mL GOx mixture was added to 50 mL of cooking oil with 0.5 % of Tween surfactant and emulsified. After 5 min 0.8 mL of glutaraldehyde 25 % was added and left to react for 15 min 100 mL of distilled water was used to stop the reaction	[127]

<sup>a</sup>1-ethyl-3-(dimethylaminopropyl)carbodiimide

<sup>b</sup>N-hydroxysuccinimide

### Impact of Enzyme Immobilization on Stability During Storage

In all cases 3 samples with enzyme and 1 control without glucose oxidase were prepared for storage in ambient temperature and the same set for storage in 4 °C for each day of measurement. Samples were measured after 1, 3 days and 1, 2, 3, 4, 5, 6, 7, 8, 10, 12, 14, 16, 20, 24 weeks of storage. In the case of complete loss of activity observed for a given method tests were terminated prematurely. Potassium iodide-starch method was used for the evaluation of enzymatic activity. Potassium iodide-starch reagent was prepared daily, as follows: 100 mg of starch was heated in 10 mL of PBS buffer (pH = 5.5; 0.1 mol/L) for several minutes, after cooling 50 mg of potassium iodide and 5 mg Na<sub>2</sub>MoO<sub>4</sub> were added. Each time 1 mL of PBS buffer and 0.8 mL of potassium iodide-starch reagent were placed in the cuvette, after that the enzyme modified paper was submerged in a way as to not obstruct the light path, and 0.2 mL of glucose solution 5 mmol/L was added. After 15 min the solution was mixed and the spectrum was taken.

### Impact of Enzyme Immobilization on Flow in Paper Channel

Simple paper-based device was prepared with borders printed with wax (Fig. 2.9) comprising of buffer filled sponge providing the wicking solution, a 2.5 × 30 mm channel where the enzyme was immobilized and a wicking pad that guaranteed constant movement of the fluid.

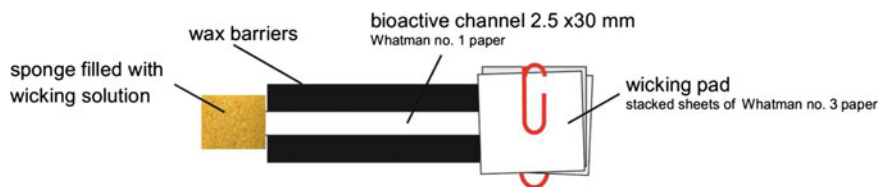


**Fig. 2.9** Paper-based device for the analysis of flow in paper matrix. Reprinted with permission from [128]

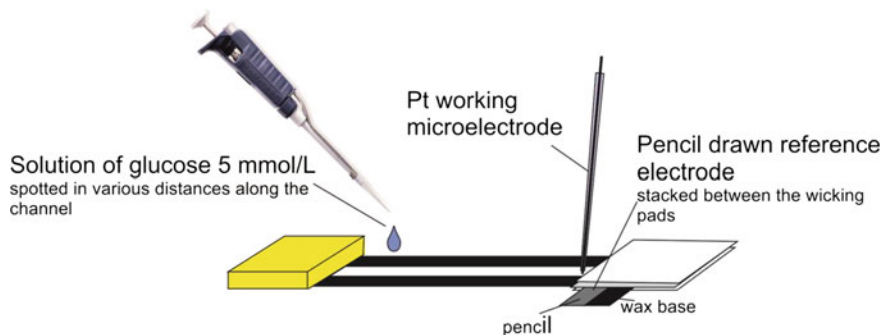


**Fig. 2.10** Electrochemical analysis of flow in paper matrix. Reprinted with permission from [128]

Two distinct flow measurements were used to guarantee the correctness of the results. In the colorimetric attempt 1  $\mu\text{L}$  of a blue food dye was spotted in the entrance and in the middle of the wetted channel. Objective of this study was to find out how immobilization influences already established flow in paper matrix. Movement of the colored solution was monitored with a series of photos made with a digital camera (Canon EOS 60D). Three devices for each immobilization method were prepared.

In the case of electrochemical measurement of flux, a pencil drawn reference electrode was placed between the device and wicking pads, a Pt working electrode was positioned in the end of the channel (Fig. 2.10). 1  $\mu\text{L}$  of 5 mmol/L glucose in water was spotted in various distances along the channel and the time necessary to obtain the maximal response of the hydrogen peroxide on the electrode was measured. The applied voltage was equal 1 V. Three devices were prepared for each immobilization method.

### Michaelis-Menten Kinetics

To analyze the metabolic activity of selected immobilization methods Lineweaver-Burk curve described by Michaelis-Menten kinetics was constructed. For this experiment only the most promising immobilization methods were selected. Therefore the tests were performed only with subsequent methods: in solution, adsorption, BSA blocking, entrapment in PVA, entrapment in starch, LbL sodium alginate-chitosan, LbL Hyaluronic acid—PEI, covalent linkage EDC/NHS. Enzymatic activity was evaluated accordingly to the previous tests (1 mL PBS; 0.8 mL of potassium iodide-starch; 0.2 mL glucose) for glucose concentrations equal 0, 0.5, 1, 5, 10, 50, 100, 200 mmol/L. Three samples were measured for each concentration. Measurements were conducted with the potassium iodide-starch reagent and different concentrations of hydrogen peroxide (0.025; 0.05; 0.1 mmol/L) to evaluate the extinction coefficient.

### 2.2.4.3 Electrochemical Detection

#### Optimization of Device's Architecture

Based on the literature data [72] and flow velocity obtained from previous experiments (Fig. 2.45) computation model of the paper network was constructed in COMSOL Mutliphysics v 4.3. "Darcy's Law" module was used to set the flux, and "Species transport in Porous Media" to describe the movement of the solution in the channel. The base fluid was water, which was later substituted with a fluid of concentration equal 1 mol/L. Permeability of paper  $\kappa = 10^{-12} \text{ m}^2$ , porosity 0.8, pressure in the entry of the channel equal 0 Pa and in the exit 130 Pa (adjusted according to experiments carried out in the bioactive channel), paper density equal  $850 \text{ kg/m}^3$ . Mesh type: "finer".

Several channel architectures were tested (Fig. 2.46), including:

- Straight channel—3 cm  $\times$  0.25 cm;
- Wide-narrow—2 cm  $\times$  0.4, 1 cm  $\times$  0.25 cm;
- Square—3 cm  $\times$  0.25 cm with a  $0.5 \text{ cm}^2$  in the middle;
- Arrow—3 cm long, entrance 0.25, after 1.5 cm widening to 0.5, exit 0.25;
- Narrowing—3 cm long, entrance 0.4 cm, exit 0.2 cm;

After computer modeling all types of devices were fabricated and their analytical performance assessed by means of chronoamperometry. For those tests 1  $\mu\text{L}$  of mixture of uric acid (1 mmol/L) and glucose (5 mmol/L) was spotted 5 mm from the entrance of the channel.

#### Analysis of Glucose and Uric Acid

##### *Preliminary Tests*

Previously described device, depicted in Fig. 2.10 was used for simultaneous detection of uric acid (direct) and glucose (indirect, after enzymatic reaction). For those tests enzyme was immobilized using Layer-by-layer method. It was possible to separate glucose and uric acid using PBS buffer pH = 5.5. After assembly, device was conditioned for 10 min counting from the complete wetting of the channel.

First tests were carried out with hydrogen peroxide, to verify if the separation is associated with modification by layer-by-layer, and enzyme present or with the cellulose matrix. It was possible to separate both compounds (hydrogen peroxide and uric acid), thus the separation ability was attributed to the cellulose matrix. It was also noted that the optimum pH for separation is 5.5.

Next, glucose solution (5 mmol/L) was passed through the bioactive channel and repeated cyclic voltammetry scans were registered. Signal started to deteriorate after 40 min. 0.7 V potential was chosen for future tests based on the CV curve format (not shown).

**Table 2.5** Concentrations of glucose and uric acid in mixed samples

	I	II	III	IV	V	VI
Glucose (mmol/L)	10	7.5	5	4	3	2
Uric acid (mmol/L)	0.1	0.3	0.5	0.7	0.9	1.2

### *Preliminary Test Destined to Construct a Calibration Curve*

Promising results led to preliminary experiments destined to construct a calibration curve. Mixed samples of glucose and uric acid were prepared with final concentrations of both compounds as stated in Table 2.5.

Three devices with narrowing channels were tested for each of the 6 samples. Experiments were carried out in random order, during two consecutive days.

### *Uniformity of Enzyme Immobilization*

When a drop is placed on top of paper, each time it wicks slightly differently, depending on the arrangement of fibers. Because of this it was proposed that low repeatability of the results is related to the different time necessary for the solution to pass through the enzymatic zone. Center of the channel was cut and layer-by-layer immobilization was carried out by dipping. Problem arose to connect back all parts of the channel. Several attempts were proposed, including:

- use of adhesive tape (Fig. 2.11a, e);
- paper clips (Fig. 2.11b);
- a device holder cut from a sponge, which provides support for while leaving the channel suspended (Fig. 2.11b–d);
- use of a plastic cover and pressure (Fig. 2.11c, d);
- interweaving of paper parts (Fig. 2.11e);

### *Electrode Positioning*

Lack of repeatability could be also related to electrode positioning. As each device serves only for one measurement, electrode needs to be positioned anew each time. Therefore 10 mmol/L solution of uric acid was injected along the channel, later electrode was lifted, positioned again, and another three injections were made in the same way as before.

In the next step different manners of electrode positioning were tested, including:

- a sponge holder, with an electrode positioned on top—weight of the electrode provides always the same pressure over paper. Different sponge holders were prepared, providing or not providing support in the electrode area;
- a sponge holder, with an electrode positioned on the bottom (Fig. 2.12a)—weight of paper provides always the same pressure;

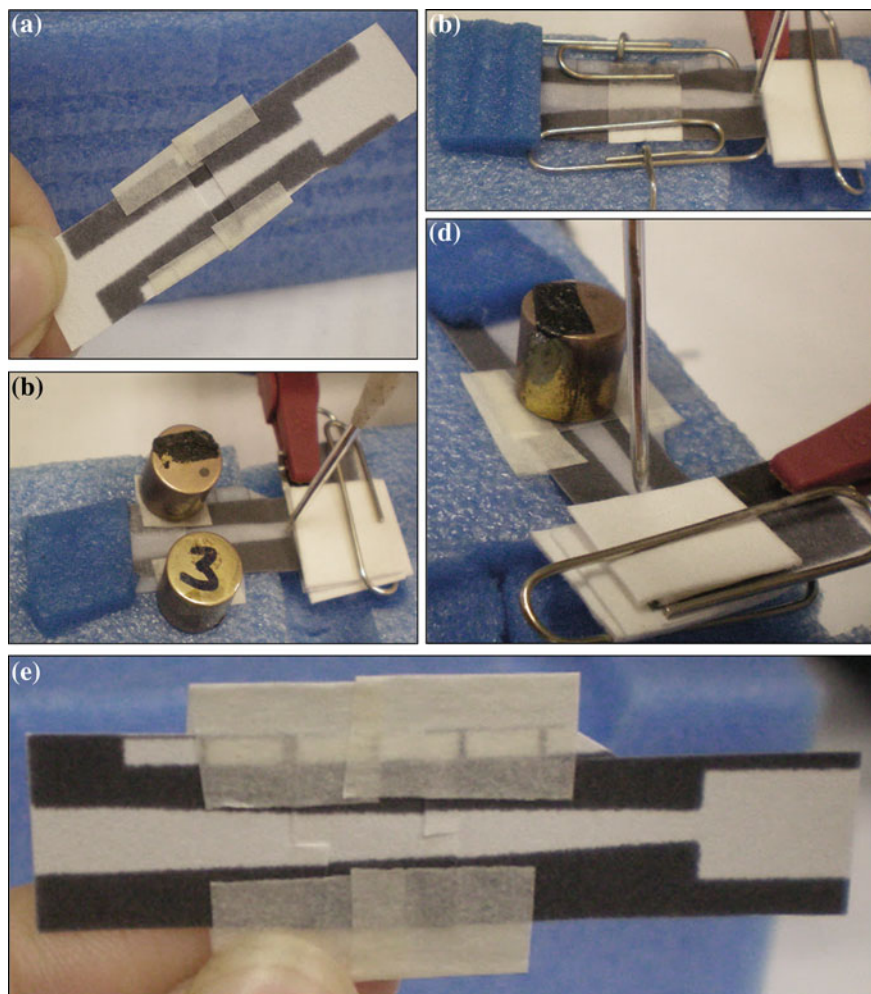


**Fig. 2.11** Some of the approaches used to connect the enzymatic zone modified by dipping with the rest of the channel. **a** cut-out part secured with an adhesive tape, **b** placed on a sponge holder and hold with paper clips, **c** covered with plastic layer and pressed with weight on both sides of the channel, **d** covered with plastic layer and pressed with weight on *top* of the channel, **e** cut-out part interwoven and secured with an adhesive tape. Figure E reprinted with permission from [128]

- a Pt wire stacked across the width of the channel (Fig. 2.12b)—enclosed between layers of plastic, or bare;
- a Pt wire passing through paper in the middle of the channel (Fig. 2.12c);

In some of the tests a Pt wire was used instead of a microelectrode enclosed in a glass capillary.



**Fig. 2.12** Some of the approaches used for electrode positioning. **a** with a sponge support, **b** with a Pt wire stacked across the width of the channel, **c** with a Pt wire passing through paper

### *Calibration Curve*

After optimization calibration curves for both compounds were constructed. Mixed samples of glucose and uric acid were prepared with the final concentrations of both compounds as stated before in Table 2.5. 1  $\mu\text{L}$  of the sample was spotted 5 mm from the entrance of the channel, where flow was already well established. Obtained signal consisted of two partially overlapping peaks. After computational resolution of peaks it was possible to construct calibration curves for both compounds based on the peak area (retention times and peak width would vary between the columns).



## (Tutaj)Analysis of Glucose, Cholesterol and Uric Acid

*Architecture*

In the case of analysis of cholesterol, wax could not be applied for device's fabrication, thus subsequent systems were cut with a laser cutter. Two architectures were proposed, with one or two working electrodes. Two electrode system (Fig. 2.13a), takes advantage of the conservation of laminar flow in paper-based devices. Sample is spotted on a sample pad and travels through two channels of identical architecture, one channel is modified with glucose oxidase, other with cholesterol oxidase. Next, hydrogen peroxide formed upon enzymatic reaction flows together with rest of the sample (i.e. uric acid) to the detection zone. Due to conservation of laminar flow one electrode will detect hydrogen peroxide, which originated from cholesterol, and the other electrode from glucose. Uric acid will be detected on both electrodes.

In case of one electrode system (Fig. 2.13b), bioactive channels have different architecture. One of the channels is longer therefore longer time will be needed for part of the sample to pass. Again one channel is modified with glucose oxidase and the other with cholesterol oxidase, but this time reaction products and the remaining sample from the straight, shorter channel will arrive on the electrode first. Uric acid will be detected two times on the same electrode.

First devices for the two electrode measurements were cut from a single sheet of paper (Fig. 2.14). Longitudinal incision was made in the middle part of the channel which divided the channel into two enzymatic zones (glucose oxidase and cholesterol oxidase). Channel was too long and too thin to support its own weight when wetted and would bend down touching the surface beneath. In principle this

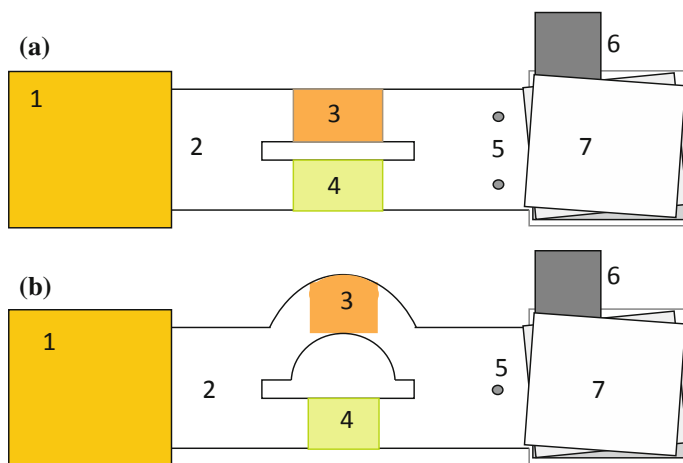


**Fig. 2.13** Devices proposed for the analysis of glucose, uric acid and cholesterol. **a** two electrode system, **b** one electrode system. 1. buffer filled sponge, 2. sampling area, 3. ChOx enzymatic zone, 4. GOx enzymatic zone, 5. working electrode(s), 6. reference electrode, 7. stack of wicking pads





**Fig. 2.14** Prototype device for two electrode measurement

kind of device could be used after optimization, also as a one electrode system, if one of the channel parts would use some flow retardant. Based on the results of enzyme immobilization uniformity from other study (electrochemical system for glucose and uric acid) subsequent test used devices assembled from separate parts.

Different thicknesses of paper (Whatman n° 1, 20, 3) were tested. Device was assembled by threading (Fig. 2.15a1, c) or interweaving of separate parts (Fig. 2.15a2, b). All types of devices (both type of linkage, different paper types) were after assembly tested with water samples to verify contact between separate parts.

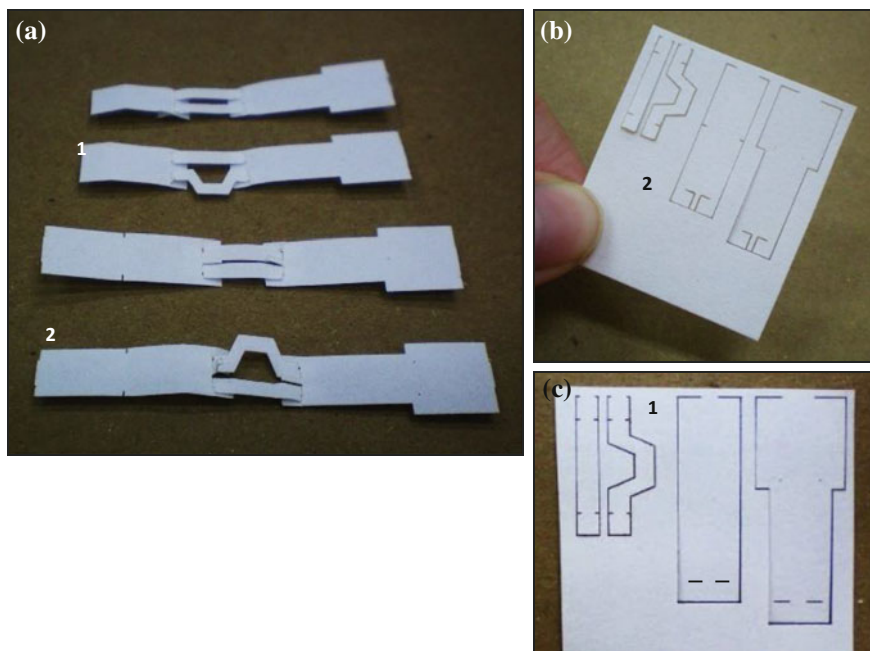


**Fig. 2.15** Devices for the electrochemical analysis of glucose, cholesterol and uric acid 1. bioactive channels passing through sample and detection pads. 2. bioactive channels interwoven with sample and detection pads. **a** assembled systems. **b, c** laser cut systems prior to assembly

### Dimensions:

- Sampling pad: 6 mm wide, composed of three areas
  - wicking area (to place a buffer filled sponge, or immerse in buffer solution) 1 cm long;
  - sampling area—1 cm long;
  - connection area—part of the channel with incisions or orifices 3 mm;
- Channels:
  - Straight— $2.5 \times 10$  mm,
  - Curved— $2.5 \times 12$  mm,
  - both with 3 mm connections on both sides;
- Detection pad:
  - connection area—part of the channel with incisions or orifices  $3 \times 6$  mm;
  - detection area— $13 \times 6$  mm with orifice(s) for electrode positioning;
  - wicking pad and reference electrode area— $10 \times 10$ ;

### *Conservation of Laminar Flow*

To guarantee the conservation of laminar flow necessary for functioning of the two electrode system one of the channels of the assembled device was placed in water and other in solution of a food dye (sponges filled with appropriate solutions placed on top of channels). Movement of solution was observed in all configurations of the device, with both types of linkage and with paper of different thicknesses.

### *Preliminary Tests and Optimization of the Architecture*

Both two and one electrode systems were tested with mixtures of glucose, cholesterol and uric acid (10 mmol/L). Paper becomes more delicate upon wetting and would tear or deflect from the electrode in the two electrode system. In this case two platinum wires are exerting force upon small piece of paper (distance between electrodes 3 mm). One electrode system, did not provide repeatable results during the first tests. Therefore architecture was modified, including two constrictions of the channel, one in the sampling area (Fig. 2.16a), and another in the electrode area (Fig. 2.16b).

Sampling constriction facilitates deposition of the sample, and helps to guarantee equal distribution into both bioactive channels. Electrode constriction not only accelerates the flow, which should result in less broadened peaks, but also guides the streams originating from each channel to the electrode.



**Fig. 2.16** Device with partially constricted channels. **a** sampling constriction, **b** electrode constriction

## 2.3 Results and Discussion

### 2.3.1 Substrate

As it can be seen on microscope pictures resumed in Fig. 2.17 all analyzed papers present homogenous structure. Both chromatography papers are to a large extent porous, with similar distribution, structure and size of fibers. Structure of copy and tracing papers is more compact, with no apparent micro-sized holes. In the case of copy paper fibers can be distinguished only at the highest magnification ( $\times 40$ ) and their diameter is considerably smaller than in the case of chromatographic paper. Other, rounded structures of different light transmission properties can be also observed in the vicinity of the fibers, they can be associated with additives such as starch,  $\text{CaCO}_3$  etc. Tracing paper forms a continuous structure with few, compact fibers of small diameter seen on the surface. This kind of structure could be expected after chemical treatment with sulfuric acid.

### 2.3.2 Optical Detection

#### 2.3.2.1 Choice of Colorimetric Method

*Ferric thiocyanate assay*—highly reproducible assay in solution and on paper for hydrogen peroxide sample, depends on pH ( $< 7$ ). No change of coloration observed when glucose and glucose oxidase were used.

*Copper(II) ion and 2,9-dimethyl-1,10-phenanthroline method (DMP)*—method was successfully applied for tests in solution and on paper, for both hydrogen peroxide and glucose, with change of color from bright yellow to dark orange-yellow (Fig. 2.18a). Unfortunately after just 15 min the control zone of paper-based device also changed color. It was possible to quantify glucose on paper in the range 0.1–10 mmol/L. Promising method for paper-based detection of

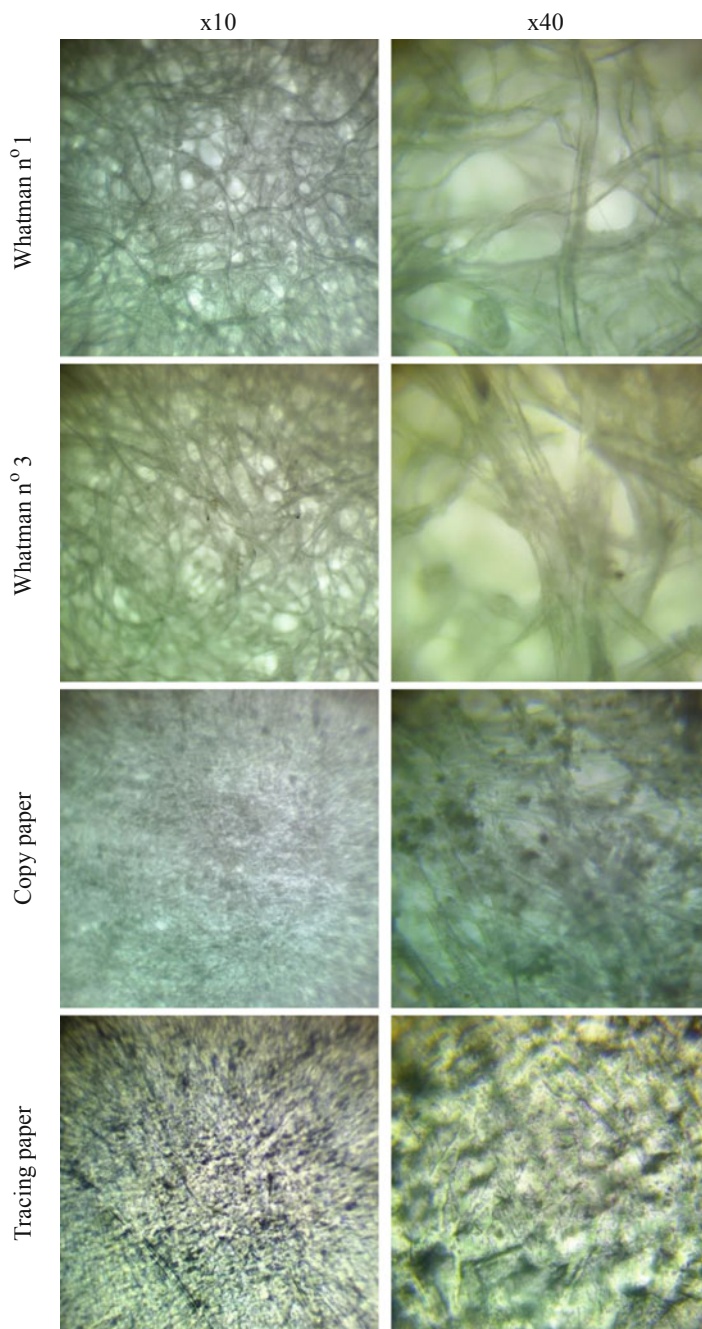


**Fig. 2.17** Surface of different paper substrates seen through an optical microscope

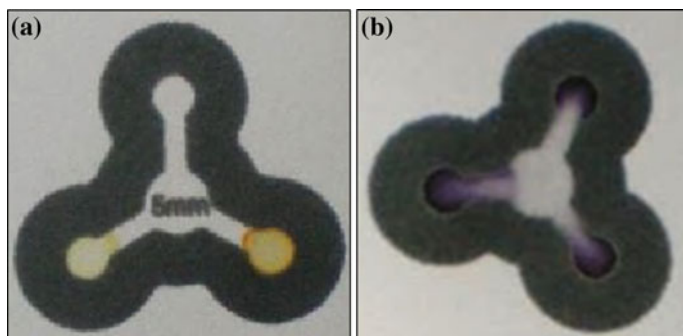


**Fig. 2.18** Paper-based colorimetric reactions for the analysis of hydrogen peroxide. **a** Copper-DMP method (*left down* without GOx, *right down*—modified with enzyme), **b** Potassium iodide-starch method

glucose, nevertheless because of delicate changes in coloration, quantification should be made by means of a scanner or camera, and not by visual comparison with standards.

*Iron(II) ion and 2,6-Bis(hydroxymethyl)-4-methylphenol method*—reproducible results obtained in solution and on paper for hydrogen peroxide sample. pH working range  $\sim 2$ , therefore was not possible to detect hydrogen peroxide formed after enzymatic reaction of glucose. Tests on paper where enzymatic and colorimetric reactions were carried out in separate zones were not reproducible.

*Starch-iodide method*—drastic change in coloration from colorless to black blue (Fig. 2.18b), for reaction in solution and on paper, for both hydrogen peroxide and glucose. Method uses easily accessible, non-toxic reagents and has a wide pH working range. After around 30 min due to autoxidation of iodide-starch reagent control zone changes coloration to some extent. It was possible to quantify glucose on paper in the range 0.1–10 mmol/L. Based on described results starch-iodide method was chosen for subsequent tests.

*Methylene blue*—assay carried out successfully only for hydrogen peroxide and only in solution. Leucomethylene blue solution is unstable and oxidizes spontaneously.

### 2.3.2.2 Differences in Hue and Repeatability of Digitalization

Repeatability of digitalization: The standard deviation of intensity of a given area for 8 subsequent scans was equal 3.9 units (total value for CMYK), which contributes to  $\sim 1.5\%$  of maximum signal (histogram range: 0–255). Repeatability is associated not only with digitalization but also manual positioning of the masking tool in the computer program.

Differences in hue: Least reproducible and least intensive results were obtained when corn starch from Altair company was used to prepare the starch-iodide

reagent. Potassium iodide from Fisher resulted in weaker signal than Merck, both reagents were still before their expiration date. Observed differences were associated with inappropriate storage (i.e. humidity). The lowest standard deviation between two assays and highest linearity of the calibration curve for cholesterol were obtained for combination of potassium iodide from Merck and starch from Vetec. Different concentrations of amylose, amylopectin and proteins in starches of different suppliers can cause variations in hue and intensity.

### 2.3.2.3 Solving the Autoxidation Problem

Single Factor Anova was performed to test if pH has any impact on color intensity (pH range 5–8, 3 replicates). When intensity was expressed in CMYK, data divided into two groups, with no difference between results ( $F < F_{crit}$ ) for pH 5, 5.5, 7 and 6, 8. Higher intensities were observed for the first group. In the case of Cyan channel no significant difference was observed between results for all pH values. Therefore single channel should be used for subsequent data analysis.

After dissolving starch-iodide reagent in 0.1 mmol/L PBS buffer (pH = 6.5 used) autoxidation would not occur for 1–2 weeks depending on storage conditions. This time could be prolonged further with use of covers. Use of liquid polymers was discarded due to inhibition of colorimetric reaction and hydrophobization of the modified region. All adhesive tapes used during study contained glucose present in glue. Sugars are often used in glue formulations as a non-toxic and inexpensive modulator of viscosity. Covers without adhesive only stacked against paper by means of paper clips did not exert any effect on shelf life. Lamination had positive effects on storage stability but heat applied during the process led to deactivation of enzymes and adhesive also contained glucose. Finally transparent, adhesive book cover foil from Con-tact Vulcan was used to fabricate the cover as it was the only material tested which did not cause false positive reaction with glucose oxidase. Device was tested during a period of 4 weeks in ambient conditions and brown colorations from iodine ions did not appear.

### 2.3.2.4 New Fabrication Methods for Analysis of Cholesterol

Table 2.6 resumes results of tests carried out with different polymers. PDMS, polystyrene and commercial waterproofing spray by Sistem were able to retain all test solutions.

In the case of paper slips without any boundary the size of the detection area depends on the precision of deposition, temperature and homogeneity of paper. The greatest problem in this case is the delimitation of the area in the graphic program. Manual cutting or use of paper punch results in low resolution and reproducibility.

In the case of manual application of polymers resolution and reproducibility are also very low, thus a device presented in Fig. 2.19e was proposed. In this case parts of the device which are important to the assay, as the reaction or the detection zone



**Table 2.6** Review of polymers applied to form barriers impermeable to cholesterol

Polymer	Preparation	Example
Wax	Test solutions spread freely through wax barriers (Fig. 2.19a)	Fig. 2.19a
Chitosan	Fiber: chitosan fiber partially dissolved clogging paper pores (Fig. 2.19b). Unfortunately using fiber is not practical and does not allow good resolution Powder: it was not possible to replicate results obtained with chitosan fiber using powder, independently of the concentration	Fig. 2.19b
PDMS	Polymer spread over the paper independently of the drying method and concentration used. All devices regardless the solvent used were able to retain water, vegetable oil and both cholesterol stock solutions (with Triton X-100 and ethanol). Simple devices were drawn on top of a laser printed design (Fig. 2.19c)	Fig. 2.19c
PVC	Independently of the concentration simple devices were not able to retain any of the test solutions	
Polystyrene	Simple devices prepared with diluted polystyrene solution were able to retain all test solutions (Fig. 2.19d)	Fig. 2.19d
Commercial waterproofing agents	NP Nanopool®: Some parts of the channel designed along the whole paper sheet did not retain the test solutions, except water which was retained perfectly each time. Results were inconsistent probably due to prolonged contact with water during shipment Waterproof spray by Sistem: Prepared devices were able to retain all test solutions. Figure 2.19e shows a device cut with laser cutter with 4 supporting channels (uncut parts of the structure, marked with arrows) filled with waterproofing spray	Fig. 2.19e

are precisely cut by means of a laser cutter. Device is suspended on paper structure by means of channels filled with a waterproofing polymer.

### 2.3.2.5 Immobilization of the Colorimetric Reagent for Enhanced Uniformity of Color Development of Uric Acid Assay

Paper modified with poly[di(ethylene glycol)] appeared oily, and black-blue coloration was only visible in the area unmodified with the polymer. Poly(acrylic acid) also resulted in oily appearance of the paper, and paper strips modified with higher concentrations became twisted upon drying. Color resulting from the enzymatic and colorimetric reactions was clearly visible but reproducibility of the assay was very low. Uniformity of color development was highly dependent on the method used for polymer application.

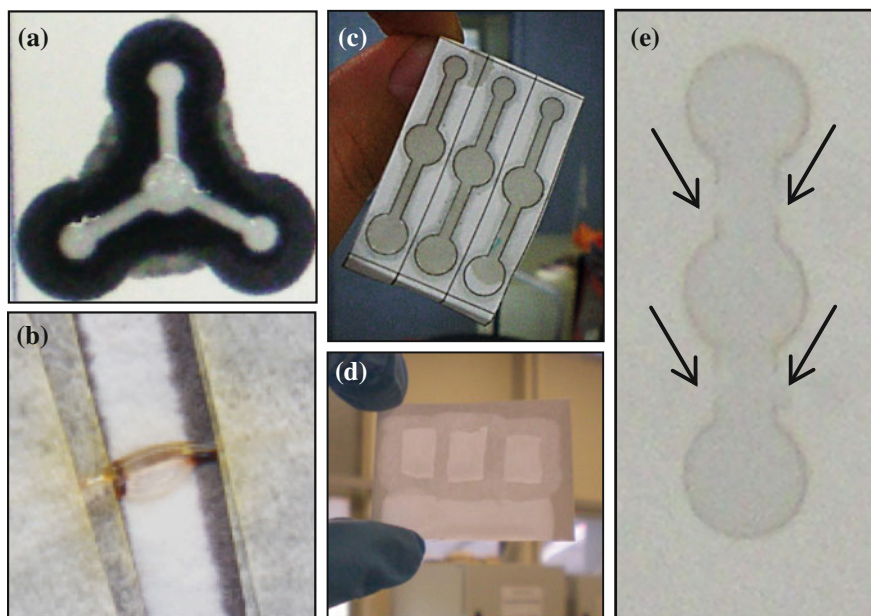


**Fig. 2.19** **a** Device with wax barriers filled with Triton X-100, **b** Partially dissolved chitosan fiber. **c** Simple device with borders delimited with PDMS retaining solution of Triton X-100, **d** Simple polystyrene device retaining solution of Triton X-100 (*center*) and vegetable oil (lower external part of paper), **e** laser cut device with supporting channels marked with *arrows*

Gelatin proved to be more promising, thus more detailed study was performed. In cases where gelatin was on top or mixed with the starch-iodide reagent it should additionally protect it from oxidation, not only enhancing the uniformity of color development but also the shelf life of the final device. Results are resumed in Fig. 2.20.

All the tests with gelatin resulted in more uniform color development than tests without the polymer. In case of lateral flow assay without gelatin, indicator is carried with the flux resulting in uneven coloration spread on larger area. All spot tests showed some level of uniformity in color development, with lighter middle area where solutions were added and darker edges. In both lateral flow assay and spot test best result was obtained with gelatin deposited on top of the starch-iodide reagent. Optimum concentrations were 10 mg/mL for lateral flow assay and 15 mg/mL for the spot test.

Lateral flow assays for uric acid prepared with LbL technique were designed to separate enzymatic and colorimetric reactions. Glucose assay did not present problems with uneven coloration. Thus if only hydrogen peroxide would pass to the detection zone in the uric acid assay color should develop evenly. Unfortunately in all cases color developed forming a ring around the detection zone (Fig. 2.21). Most reproducible results were obtained for the first assay (LbL alginate/UOx-chitosan in



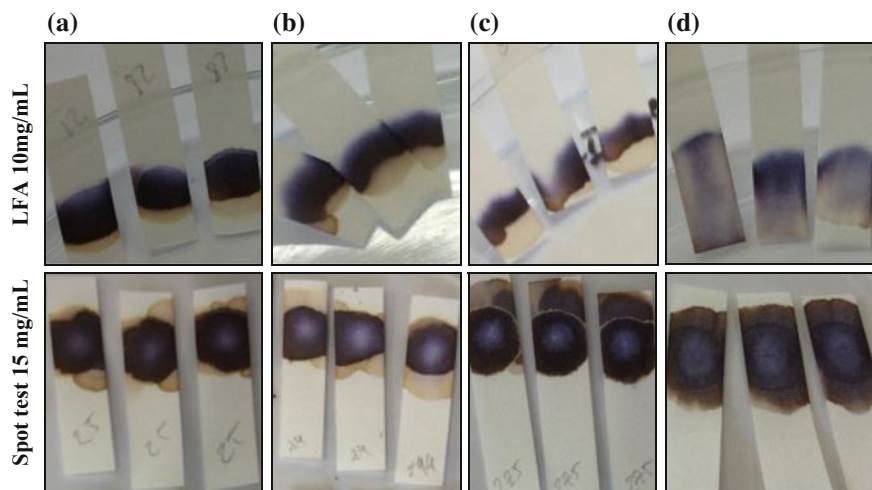
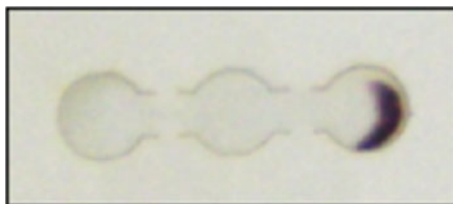


**Fig. 2.20** Photographs of lateral flow assays and spot tests taken after 20 min. Only the concentrations of gelatin which gave the best results are shown. **a** Starch-iodide under gelatin layer. **b** Starch-iodide mixed with gelatin. **c** Starch-iodide on top of gelatin layer. **d** Starch-iodide without gelatin

**Fig. 2.21** Uric acid test



the middle zone, starch-iodide reagent under gelatin in detection zone). Similar results were obtained for the third type of assay (starch-iodide under LbL in the middle zone) but interestingly color did not appear in the middle zone where the starch-iodide reagent was deposited, but in the third area, in the same ring format as in the previous assay. Starch-iodide was therefore carried with the fluid. Second assay, without chitosan in LbL formulation was the least reproducible.

### 2.3.2.6 Calibration Curves

Uric acid: With the results obtained by means of a spot test it was possible to construct a calibration curve presenting good linearity  $R^2 = 0.993$  in the range of interest 0.1–2.5 mmol/L. Calibration curve (Fig. 2.22) is described by equation  $y = 12.7 \pm 0.44x + 4.4 \pm 0.30$ ,  $N = 3$ . Limit of detection, estimated according to IUPAC Gold Book as the concentration of the analyte giving a signal equal to the blank plus  $3 \times$  the standard deviation of the blank is equal 0.10 mmol/L.

**Fig. 2.22** Calibration curve for uric acid–colorimetric method, spot test with starch-iodide indicator immobilized in gelatin

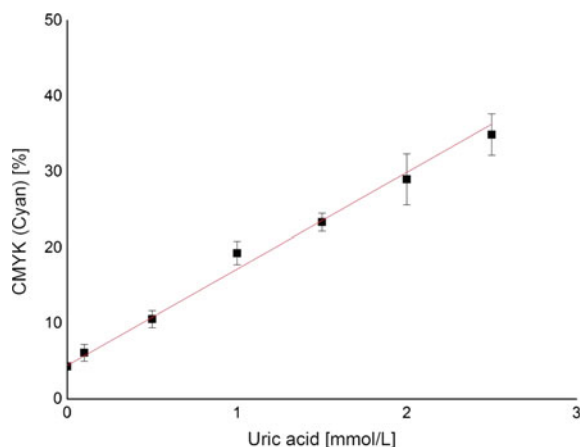
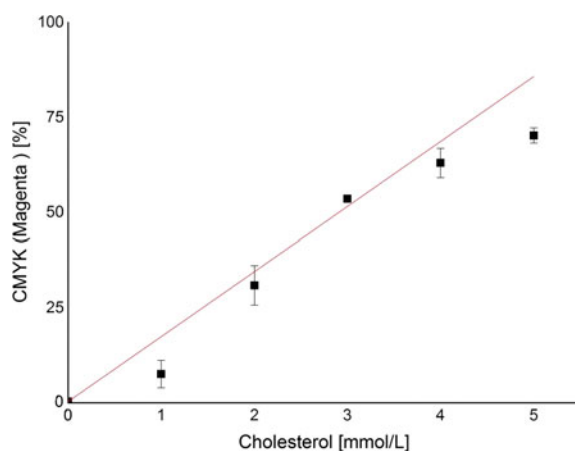


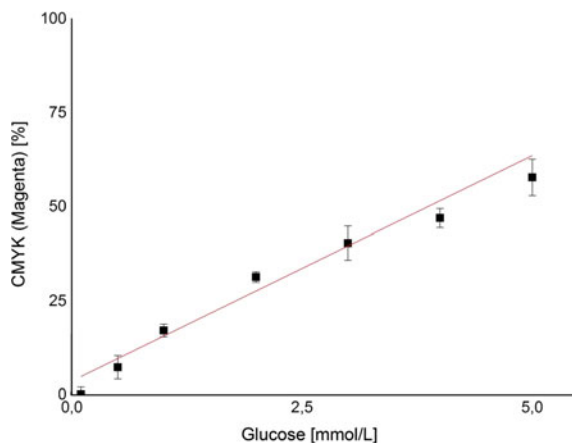
**Fig. 2.23** Calibration curve for cholesterol–colorimetric method, spot test



**Cholesterol:** With the results obtained by means of a spot test it was possible to construct a calibration curve presenting good linearity  $R^2 = 0.991$  in the range of interest 1.0–5.0 mmol/L. Calibration curve (Fig. 2.23) is described by equation  $y = 17.08 \pm 0.74x + 0.33 \pm 0.49$ ,  $N = 3$ , with limit of detection equal 0.02 mmol/L.

**Glucose:** With the results obtained by means of a lateral flow assay it was possible to construct a calibration curve presenting good linearity  $R^2 = 0.938$  in the range of interest 0.2–5 mmol/L. Calibration curve (Fig. 2.24) is described by equation  $y = 11.97 \pm 1.25x + 3.7 \pm 2.6$ ,  $N = 3$ . Limit of detection, is equal 0.2 mmol/L.

**Fig. 2.24** Calibration curve for glucose–colorimetric method, lateral flow assay



### 2.3.2.7 Tangential Flow Devices

Devices without the intermediate distribution layer, resulted in an uneven coloration (Fig. 2.25c). Inclusion of a distribution layer allowed to obtain uniform coloration for the glucose assay, and similar ring type result as observed in the spot test for uric acid.

Figure 2.25b shows two type of acrylate covers with different sizes of the sampling orifice. Without the acrylate holder it was difficult to reproducibly clamp

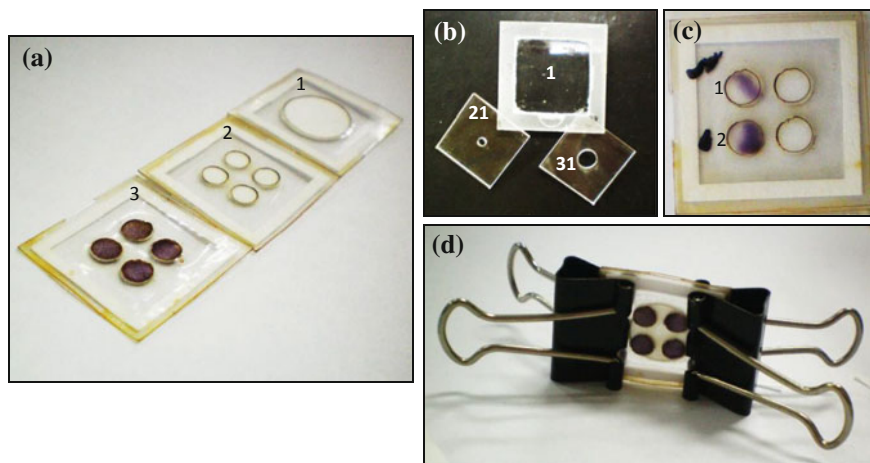


**Fig. 2.25** Photographs of a sample tangential flow device. **a** individual layers: 1. sampling layer, 2. enzymatic layer, 3. detection layer (test with  $\text{H}_2\text{O}_2$ ); **b** acrylate holder: 1. base, 2. cover with a small sampling orifice, 3. cover with a large sampling orifice; **c** Results obtained for a device without distribution area 1. uric acid, 2. glucose; **d** assembled device, clamped between two paper clips

the device. Paper clips exerted more pressure in certain points of the assay, and their positioning had great influence on uniformity of color development. When device was enclosed in a holder with a cover tightly fitting the bottom piece, color development seemed slower and did not reach the same intensity as with open device. It was proposed that lack of readily available oxygen can be the cause of such results, therefore a slightly smaller cover with a larger sampling orifice was proposed (Fig. 2.25b3).

It was not possible to detect cholesterol in any of the devices. To overcome this problem, in order to move cholesterol from the sampling layer, an organic solvent should be used or surfactant added to the running buffer. Cholesterol oxidase modified paper could be also in direct contact with the sampling pad, in this way enzyme could react with cholesterol in the sampling area and later only hydrogen peroxide would flow to the detection zone. It was possible to quantify glucose and uric acid with results similar to obtained in previous tests (the same linear working range but lower repeatability).

### 2.3.3 *Methods of Enzyme Immobilization on Paper*

#### 2.3.3.1 Protein Quantification Methods

All tested methods were successfully applied for measurements in solution.

*Bromocresol green*—in the case of bromocresol green method positive results of the preliminary tests on paper (Fig. 2.32) for BSA samples, and weak results for GOx led to formation of calibration curves (tests in solution) in the range of 0.3–20 mg/mL for both compounds. Linear dependence was observed for BSA samples (Fig. 2.26) and no trend for the GOx (Fig. 2.27), therefore method was discarded from subsequent tests on paper. Differences observed for those two compounds can be related to smaller number of amino acid residues participating in reaction in the case of GOx.

*Bromophenol blue*—after promising results of the preliminary bromophenol blue tests (Fig. 2.32) for both BSA and GOx, calibration curves were constructed for both compounds (tests in solution). Higher sensitivity was observed for BSA (Fig. 2.28) as compared with GOx (Fig. 2.29). Curve for GOx was described by equation  $y = 0.42x + 1.96$ ,  $SD = 0.04$  for  $N = 3$ . It was noted that the order of deposition of reagents is crucial for the reproducibility of the results (tests on paper). If the protein was deposited first (which would be the case of the immobilization studies) the dye would spread only on a small area forming regions of uneven coloration. To overcome this problem dye could be deposited first or sprayed (Fig. 2.30) on top of the protein instead of spotted (Fig. 2.31). Even with those two modifications it was not possible to obtain sufficient reproducibility to construct a calibration curve for GOx for tests on paper and only for BSA.

*Lowry method*—for both variations of the Lowry method no changes in coloration was observed for any of the paper samples (Fig. 2.32). Both variations of the test

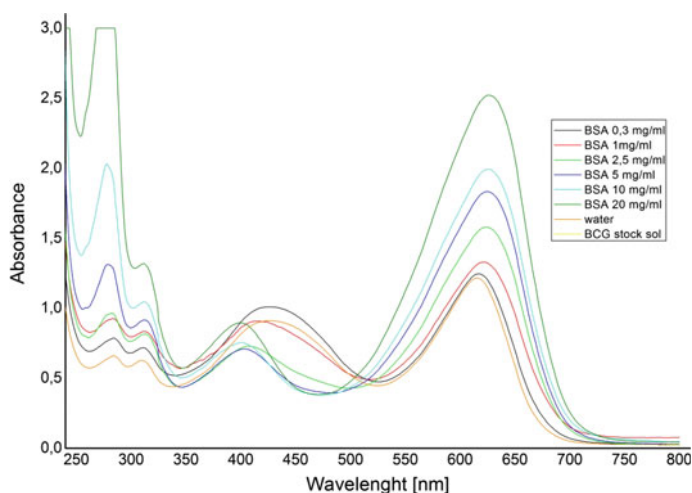


**Fig. 2.26** Absorption spectrum for different concentrations of BSA, bromocresol green method, tests in solution

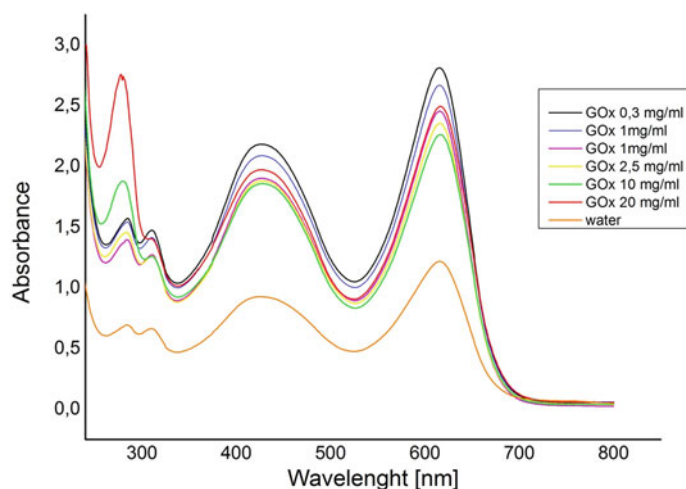


**Fig. 2.27** Absorption spectrum for different concentrations of GOx, bromocresol green method, tests in solution

(with or without the surfactant) were correctly executed, as was confirmed in the experiments carried out in solution.

*Bradford method*—in the case of Bradford method all samples (water, BSA and GOx) resulted in change of coloration of the modified paper (Fig. 2.32). It was presumed that false positive result obtained for the water sample can be caused by

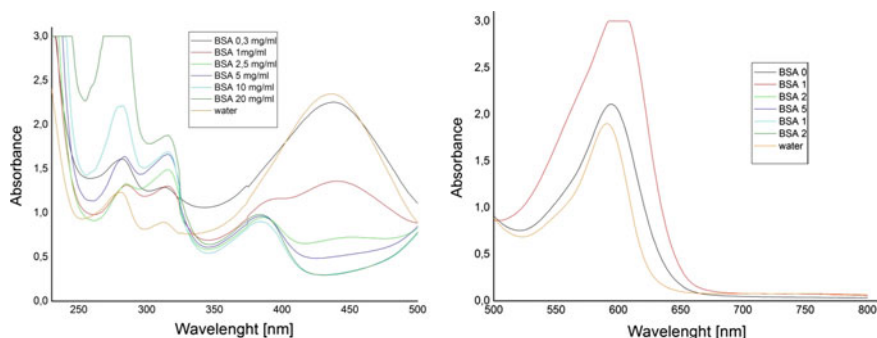


**Fig. 2.28** Absorption spectrum for different concentrations of BSA, bromophenol blue method, tests in solution. Due to high intensity observed for concentrations above 1 mg/mL of BSA spectrum was divided in two ranges with higher concentrations masked for wavelengths above 500 nm

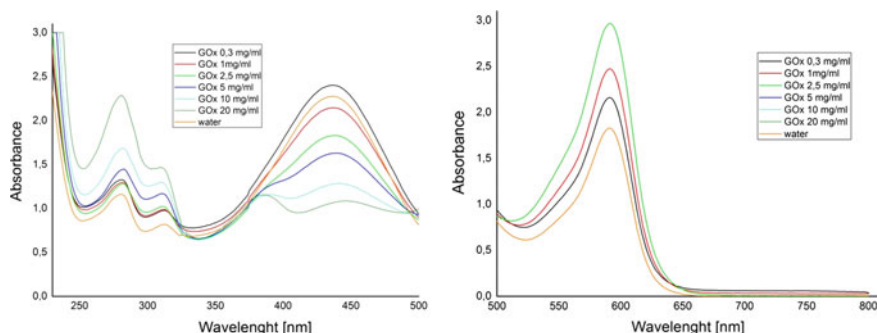


**Fig. 2.29** Absorption spectrum for different concentrations of GOx, bromophenol blue method, tests in solution. Due to high intensity observed for concentrations above 2.5 mg/mL of GOx spectrum was divided in two ranges with higher concentrations masked for wavelengths above 500 nm

contamination of paper. Therefore a cleaning procedure was applied, including washing in methanol, methanol with ammonium hydroxide, methanol with acetic acid and distilled water, but even with such prepared paper the results remained unchanged. Tests in solution confirmed correct execution of the test.

*Direct quantification*-absorption spectra for BSA and GOx are shown in Figs. 2.33 and 2.34. Sensitivity is lower for GOx but clear dependence of absorbance at 280 nm with concentration can be seen for both compounds.

For tests on paper intensity around 280 nm is too low, but proteins can be quantified by the absorption peak at 200 nm (Figs. 2.35 and 2.36).

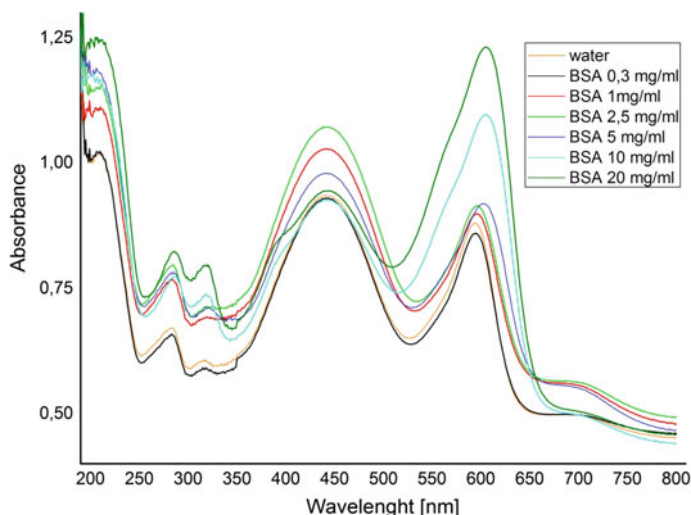


**Fig. 2.30** Absorption spectrum for different concentrations of BSA, bromophenol blue method, tests on paper, BPB deposited with spray

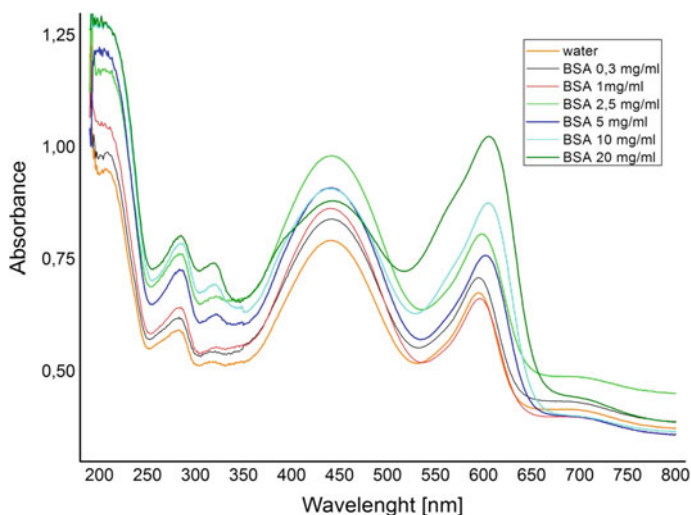


**Fig. 2.31** Absorption spectrum for different concentrations of BSA, bromophenol blue method, tests on paper, BPB deposited with a pipette

Calibration curves were constructed for both BSA and GOx on paper using inclination of the spectrum in the region of 204–220 nm ( $N = 3$ ). Data show linear dependence for concentrations between 0.3 and 5 mg/mL for BSA  $y = -0.0031x + 0.0008$ ,  $R^2 = 0.9961$ , and for 1–20 mg/mL GOx  $y = -0.0021x + 0.0004$ ,  $R^2 = 0.9999$ .



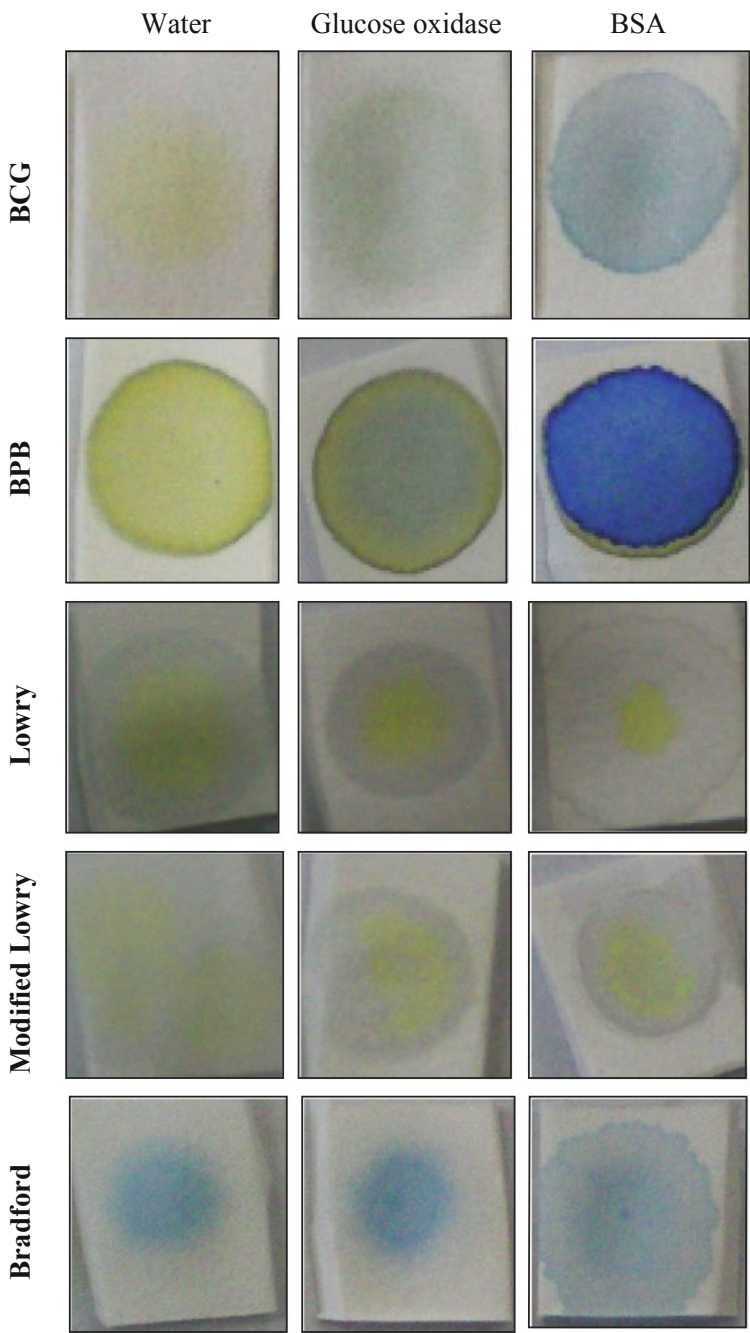
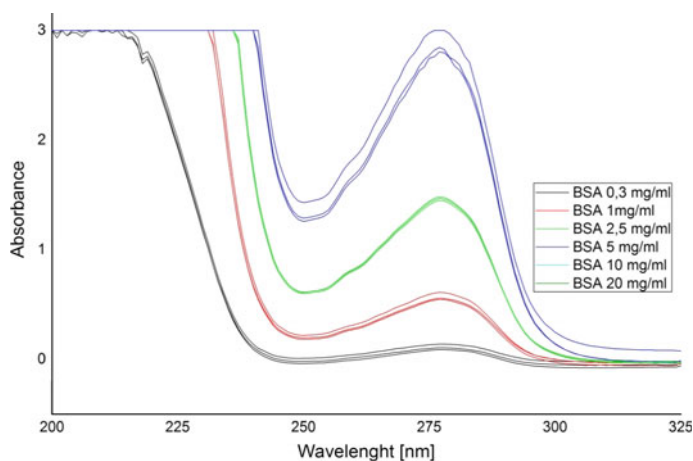
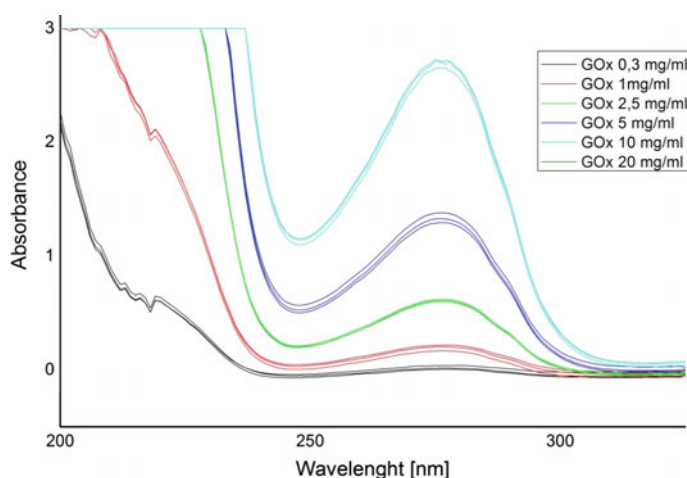


Fig. 2.32 Comparison of all methods for quantification of proteins, tests on paper





**Fig. 2.33** Absorption spectrum for different concentrations of BSA, direct quantification, tests in solution



**Fig. 2.34** Absorption spectrum for different concentrations of GOx, direct quantification, tests in solution

### 2.3.3.2 Enzymatic Activity, Optimization of Assay Conditions

Based on data presented in Fig. 2.37 subsequent tests were performed in pH 5.5. Highest activity and low standard deviation was observed for assay performed in this condition. Calibration curve for the amount of enzyme used for reaction, showed linearity in the region between 0.5 and 5 mg/mL,  $y = 0.5x - 0.4$ ,  $R^2 = 0.982$ ,  $N = 3$ . For immobilization studies 5 mg/mL enzyme concentration was chosen.

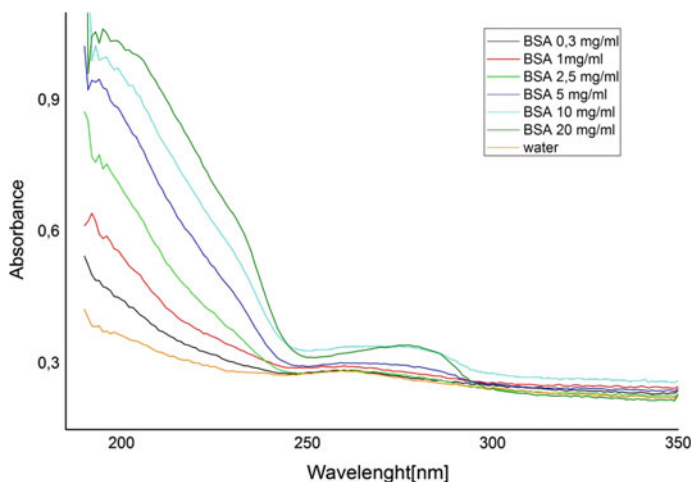


**Fig. 2.35** Absorption spectrum for different concentrations of BSA, direct quantification, tests on paper

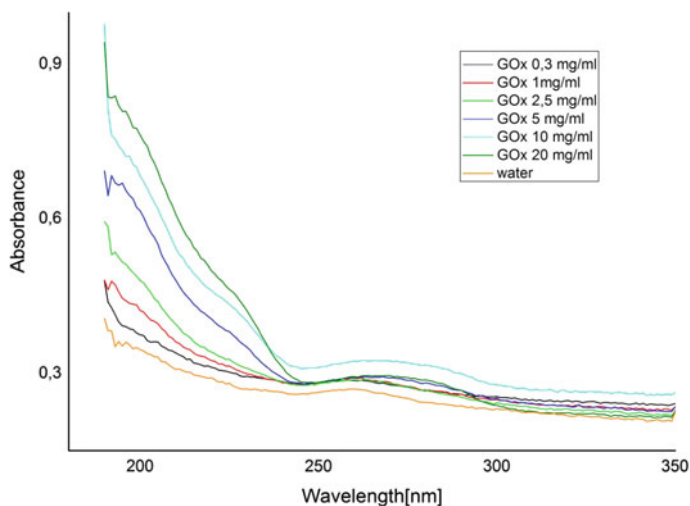
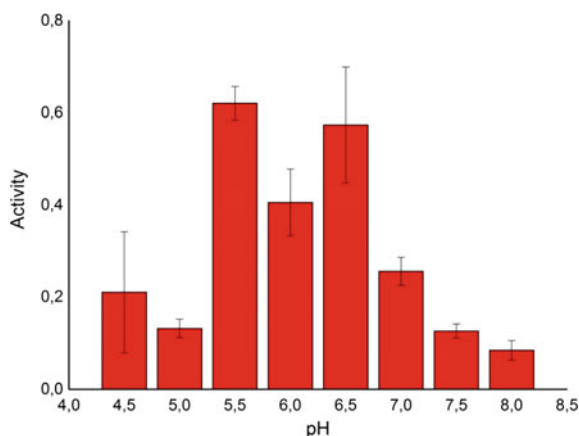


**Fig. 2.36** Absorption spectrum for different concentrations of GOx, direct quantification, tests on paper

### 2.3.3.3 Enzyme Immobilization on Paper-Quantification of Proteins

Direct quantification was applied to confirm amount of protein present after immobilization. Each time before assessment of enzymatic activity paper devices were analyzed for the amount of protein present. Table 2.7 summarizes the results of quantification of protein for all the immobilization methods tested. After

**Fig. 2.37** Activity of enzymatic reaction depending on pH. Activity expressed as absorbance maximum in the range 570–580 nm. Standard deviation for N = 3



analyzing the standard deviation and comparing measured and theoretical protein content it can be clearly seen this method is only capable to quantify protein in case of: simple adsorption, adsorption on stearic acid, on PVA, with mannitol, entrapment in starch, chitosan, PVA, dextran, alginate, CMC and LbL sodium alginate-PEI technique (Table 2.7 blue marked methods). In case of encapsulation methods, and covalent linkage with washing steps higher standard deviation between the samples would be acceptable, but analysis of spectra (not shown) confirms that this method is not applicable. In the case of glutaraldehyde linkage it was noted that after just 3 days for samples stored in room temperature and 1 week for storage in 4 °C a new band appeared around 240 nm, which was accompanied by complete loss of activity. It clearly shows that the crosslinking reaction continues slowly deactivating the enzyme. High background signal was noted for: BSA blocking, adsorption on collagen, LbL alginate-chitosan, LbL alginate-polylysine, LbL Hyaluronic acid–chitosan, LbL hyaluronic acid–PEI, LbL poly(vinyl sulfate)–chitosan, LbL poly(acrylic acid)–chitosan, glutaraldehyde crosslinking with glycine blocking, EDC and EDC/NHS (Table 2.7 brown marked methods). Activation with potassium periodate, ethylenediamine and glutaraldehyde colored the paper and it was not possible to obtain spectra in the region of interest.

### 2.3.3.4 Impact of Enzyme Immobilization on Stability During Storage

Results of enzymatic activity will be analyzed using the theoretical quantity of protein used for preparation of samples. This fact should not have any impact on most of methods, apart from encapsulation, activation with potassium periodate, ethylenediamine and glutaraldehyde, as well as Schiff base method.

Figures 2.38, 2.39, 2.40, 2.41 and 2.42 resume the initial (24 h) activity of immobilization samples (N = 3) with normalized absorbance. Range of the results for the initial enzymatic activity was very large, two methods (LbL alginate-chitosan

**Table 2.7** Theoretical and experimental protein content in samples prepared with different immobilization methods

			Theoretical protein concentration (mg/cm <sup>2</sup> )	Average protein concentration measured (mg/cm <sup>2</sup> )	St. dev. (N = 18)
Physical adsorption	1	Simple adsorption	0.05	0.05	0.002
	2	BSA blocking	0.05	0.03	0.009
	3	On collagen	0.05	0.02	0.002
	4	On stearic acid	0.05	0.05	0.002
	5	On PVA	0.05	0.05	0.004
	6	With mannitol	0.05	0.06	0.002
	7	With trehalose	0.05	0.06	0.008
Entrapment in gel	Simple	8 In starch	0.05	0.05	0.002
		9 In chitosan	0.05	0.05	0.003
		10 In PVA	0.05	0.05	0.003
		11 In dextran	0.05	0.06	0.002
		12 In ammonium alginate	0.05	0.05	0.002
		13 In CMC	0.05	0.05	0.003
		14 Sodium alginate—chitosan	0.05	0.04	0.019
	Layer-by-layer	15 Sodium alginate—polylysine	0.05	0.02	0.007
		16 Sodium alginate—PEI	0.05	0.05	0.006
		17 Hyaluronic acid—chitosan	0.05	0.01	0.030
		18 Hyaluronic acid—PEI	0.05	0.04	0.003
		19 Poly(vinyl sulfate)—chitosan	0.05	0.00	0.025
		20 Poly(acrylic acid)—chitosan	0.05	0.02	0.033
Covalent linkage	21	Glutaraldehyde crosslinking	0.05	0.02	0.025
	22	Glutaraldehyde crosslinking with glycine blocking	0.05	0.02	0.005
	23	Schiff base I	0.20	0.04	0.006
	24	EDC with glycine blocking	0.20	-0.02	0.029
	25	EDC/NHS II	0.20	0.01	0.020
	26	KIO <sub>4</sub> , ethylenediamine, and glutaraldehyde activation	0.10	—	—
Encapsulation	27	Sodium alginate II	unknown	0.04	0.007
	28	Sodium alginate—CMC	unknown	0.02	0.025
	29	Sodium alginate—chitosan	unknown	0.05	0.012
	30	PEI	unknown	—	—
	31	Covalent attachment to PEI capsules	unknown	—	—
	32	Covalent attachment to silica beads	unknown	0.05	0.007
	33	Chitosan	unknown	0.03	0.022
		Possible protein quantification			
		High background signal prevents reliable quantification			

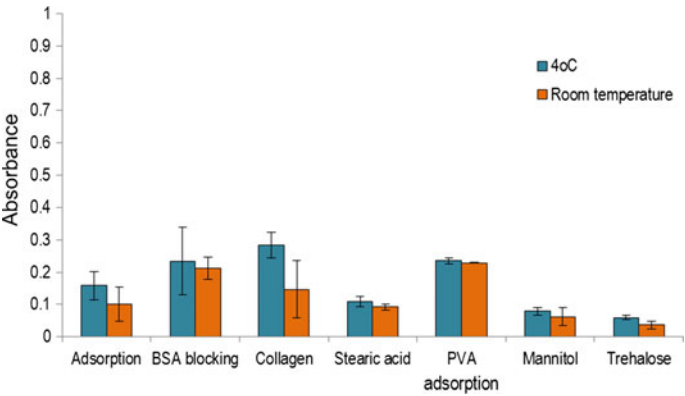


**Fig. 2.38** Initial enzymatic activity of adsorption methods. Reprinted with permission from [129]

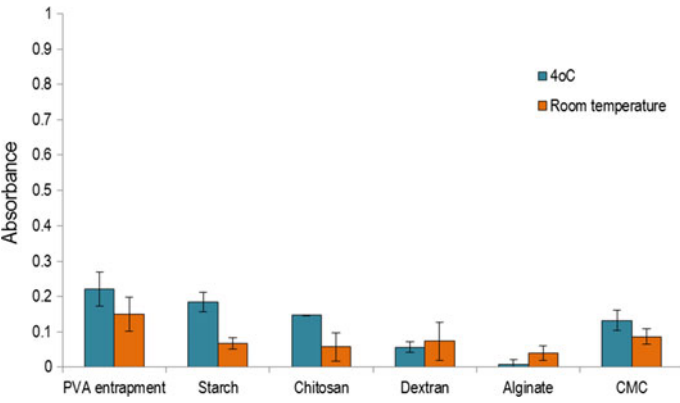


**Fig. 2.39** Initial enzymatic activity of simple entrapment methods. Reprinted with permission from [129]

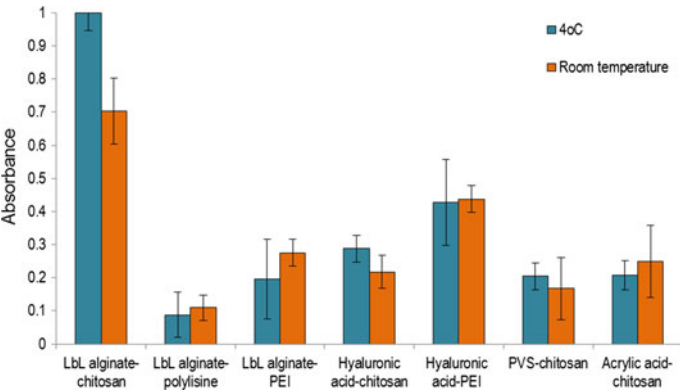


**Fig. 2.40** Initial enzymatic activity of LbL entrapment methods. Reprinted with permission from [129]

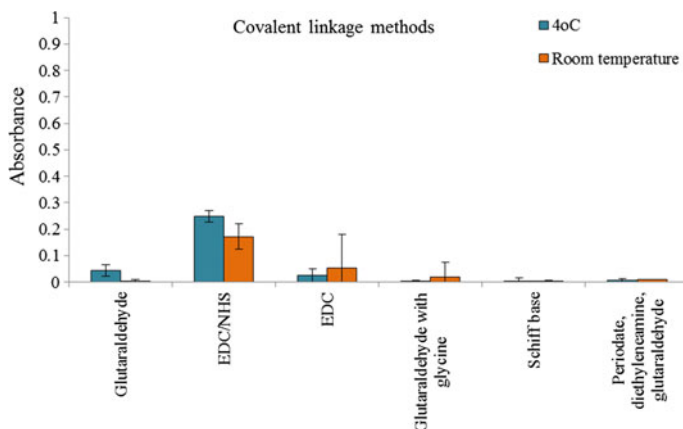


**Fig. 2.41** Initial enzymatic activity of covalent linkage methods. Reprinted with permission from [129]

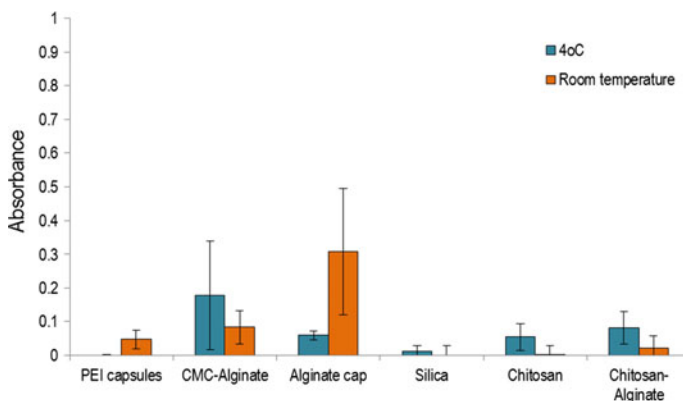


**Fig. 2.42** Initial enzymatic activity of encapsulation methods. Reprinted with permission from [129]

and EDC/NHS) presented absorbance higher than the working range of the spectrophotometer ( $>3$ ) in those two cases presented results are after 48 h.

Table 2.8 resumes the impact of storage temperature and time on enzymatic activity; results are shown as percentage of the initial activity observed for each method after 24 h. Methods in which activity dropped to 0 % after just 1 day of storage were not included in the summary.

Choice of enzyme immobilization method will depend mostly on the application, and the characteristic in question: long term stability, stability in room temperature, work in flow conditions, ease of preparation etc. Selected method should meet both catalytic (selectivity, stability, productivity) and non-catalytic (ease of separation, minimum leakage etc.) requirements. There is no general universally applicable

**Table 2.8** Impact of time and temperature of storage on enzymatic activity. Reprinted with permission from [129]

			Day 1	Day 3	Week 1	Week 2	Week 3	Week 4	Week 5	Week 6	Week 7	Week 8	W 10	W 12	W14	W16	W 20	W 24	
Physical adsorption	1	Simple adsorption	4°C	>75 %			>50 %							>25 %			>10 %		<10 %
			RT	>75 %		>50 %	>25 %										>10 %		<10 %
	2	BSA blocking	4°C	>75 %										>50 %			>25 %	>10 %	
			RT	>75 %					>50 %					>25 %			<10 %		
	3	On collagen	4°C	>75 %			>50 %									>25 %			>10 %
			RT	>75 %				>50 %			>25 %			>10 %			<10 %		
	4	On stearic acid	4°C	>75 %		>50 %					>25 %							<10 %	
			RT	>75 %			>25 %			<10 %									
	5	On PVA	4°C	>75 %			>50 %							>25 %			<10 %		
			RT	>75 %	>50 %	>25 %							>10 %			<10 %			
	6	With mannitol	4°C	>75 %				>50 %				>25 %				>10 %	<10 %		
			RT	>75 %	>50 %			>25 %				<10 %							
	7	With trehalose	4°C	>75 %				>50 %				>25 %			<10 %				
			RT	>75 %					>50 %		>25 %			17 %		<10 %			
Entrapment in gel Simple	8	In starch	4°C	>75 %					>50 %					>25 %			>10 %		
			RT	>75 %					>50 %					>25 %			>10 %		
	9	In chitosan	4°C	>75 %			>50 %				>25 %				>10 %	<10 %			
			RT	>75 %					>50 %					>10 %	<10 %				
	10	In PVA	4°C	>75 %	>50 %			>25 %							>10 %	<10 %			
			RT	>75 %		>50 %							>10 %	<10 %					
	11	In dextran	4°C	>75 %											>50 %	>25 %	>10 %		
			RT	>75 %		>50 %					>25 %				>10 %	<10 %			
	12	Ammonium alginate	4°C	>75 %	>25 %	<10 %													
			RT	>75 %			<10 %												
	13	In CMC	4°C	>75 %				>50 %	>25 %			>10 %				<10 %			
			RT	>75 %			>50 %					>25 %			>10 %	<10 %			

Table 2.8 (continued)

Layer-by-layer	14	Alginate—chitosan	4°C	>75 %			>50 %		>25 %		>10 %
			RT	>75 %		>50 %		>25 %		>10 %	<10 %
Covalent linkage	15	Alginate—polylysine	4°C	>75 %			>50 %		>25 %		>10 %
			RT	>75 %		>50 %		>25 %		>10 %	<10 %
	16	Alginate—PEI	4°C	>75 %			>50 %		>25 %		>10 %
			RT	>75 %		>50 %		>25 %		>10 %	<10 %
	17	HA—chitosan	4°C	>75 %			>50 %		>25 %		>10 %
			RT	>75 %		>50 %		>25 %		>10 %	<10 %
	18	Hyaluronic acid-PEI	4°C	>75 %			>50 %		>25 %		>10 %
			RT	>75 %		>50 %		>25 %		>10 %	<10 %
	19	PVS—chitosan	4°C	>75 %			>50 %		>25 %		>10 %
			RT	>75 %		>50 %		>25 %		>10 %	<10 %
	20	PAA—chitosan	4°C	>75 %			>50 %		>25 %		>10 %
			RT	>75 %		>50 %		>25 %		>10 %	<10 %
Encapsulation	21	Glutaraldehyde	4°C	>75 %			>50 %		>25 %		>10 %
			RT	>75 %		>50 %		>25 %		>10 %	<10 %
	22	Schiffbase II	4°C	>75 %			>50 %		>25 %		>10 %
			RT	>75 %		>50 %		>25 %		>10 %	<10 %
	23	EDC I	4°C	>75 %			>50 %		>25 %		>10 %
			RT	>75 %		>50 %		>25 %		>10 %	<10 %
	24	EDC with glycine	4°C	>75 %			>50 %		>25 %		>10 %
			RT	>75 %		>50 %		>25 %		>10 %	<10 %
	25	EDC/NHS II	4°C	>75 %			>50 %		>25 %		>10 %
			RT	>75 %		>50 %		>25 %		>10 %	<10 %
	26	Sodiumalginate II	4°C	>75 %			>50 %		>25 %		>10 %
			RT	>75 %		>50 %		>25 %		>10 %	<10 %
	27	Alginate—CMC	4°C	>75 %			>50 %		>25 %		>10 %
			RT	>75 %		>50 %		>25 %		>10 %	<10 %



method for enzyme immobilization, and also in this study it is difficult to cite one outstanding result.

For storage in 4 °C for periods up to 8 weeks simple adsorption in paper would probably be the choice. It shows rather low initial activity (~17 %) as compared with LbL sodium alginate-chitosan (highest initial activity of all the methods), but is extremely easy to prepare and does not require any other chemicals except the enzyme. All adsorption methods showed rather low initial activity (from 7 to 30 % as compared with LbL sodium alginate-chitosan method). BSA blocking method stands out, as it showed the longest storage stability regardless the temperature, it's easy to prepare and in resource limited settings powdered milk could be used instead of purified albumin.

In the case of entrapment methods very distinct results were observed for simple methods where enzyme was mixed with the polymer and LbL. For storage in lower temperatures entrapment in dextran would be the recommended method, it is simple, inexpensive and showed activity above 75 % of the initial value after 14 weeks (4 °C)—best results from all the methods tested.

Storage stability in room temperature was highest for entrapment in starch and chitosan (simple entrapment). Initial activity was even lower for the simple entrapment methods than for adsorption, probably because of the lesser accessibility of the enzyme when enclosed in polymer. Simple entrapment methods are extremely easy to prepare, on the contrary to LbL which require multiple addition steps and drying. Layer-by-layer methods, showed high initial activity, unfortunately deactivation progressed very fast. Highest initial activity from all the methods tested was observed for LbL sodium alginate-chitosan. This method retained more than 50 % of initial stability after 10 weeks for storage in 4 °C but only for 3 weeks when stored in room temperature. Longest stability was observed for LbL sodium alginate-PEI 60 % after 20 weeks (4 °C).

Covalent linkage on paper is extremely inconvenient, requires multistep preparation and it is almost impossible to wash out the chemicals after reaction. Chemical residues can cause interference in posterior applications or slowly deactivate the enzyme as it was seen in case of glutaraldehyde crosslinking. Some treatments (oxidation with periodate, prolonged submersion etc.) affect the physical properties of paper, making it easier to tear, or compromising its flexibility. If despite this covalent linkage would be the method of choice EDC/NHS presented best results in this group. It retained 50 % of activity after 8 weeks of storage at room temperature.

Capsules produced in our laboratory by the syringe method were rather big: sodium alginate ~ 1.5 mm; sodium alginate-CMC ~ 2–2.5 mm; sodium alginate-chitosan ~ 4 mm (Fig. 2.43). Size of those capsules could be diminished by using other encapsulation methods like spray drying, but specialized equipment would be necessary. Chitosan capsules produced by interphase polymerization were smaller 0.5–1 mm. Small capsules and silica beads did not hold to paper, and could be used to produce bioactive paper when mixed in pulp. After complete drying, capsules changed their form becoming flat and completely covered the surface of paper. Inconsistent results were found for encapsulation in alginate with much

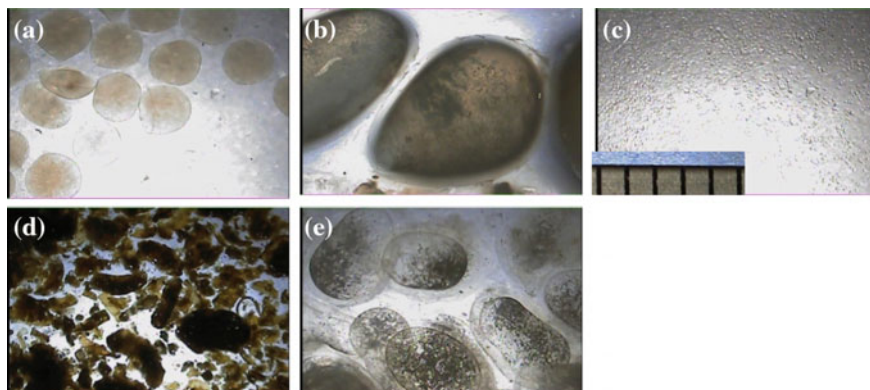


**Fig. 2.43** Microscopic images of capsules produced during this study. **a** Sodium alginate, **b** Sodium alginate-chitosan, **c** Covalent linkage to silica capsules, **d** Chitosan, **e** Sodium alginate-CMC; scale in mm for all images marked on **c**

higher initial activity for storage in room temperature, this can be explained by the incapability to relate the activity with quantity of enzyme present in each sample, high standard deviation was also observed in this case. Method of choice would be encapsulation in sodium alginate-CMC as it retained more than 50 % of activity after 8 weeks of storage in room temperature.

No methods showed satisfactory results after 24 weeks of storage. This study showed that protective agents such as sugars, that are widely used to prolong shelf life of enzymes stored in solution have no positive impact on storage stability of glucose oxidase on paper, blocking agents such as glycine or BSA should be used instead (Table 2.8).

### 2.3.3.5 Impact of Enzyme Immobilization on Flow in Paper Channel

In the colorimetric method the measurement error grows with time of the experiment, as the borders of the dye spot travelling through paper channel become more and more diffused (Fig. 2.44). Distance/time plot (not shown) demonstrates that the

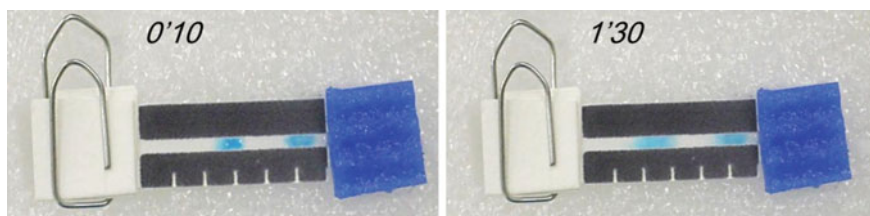
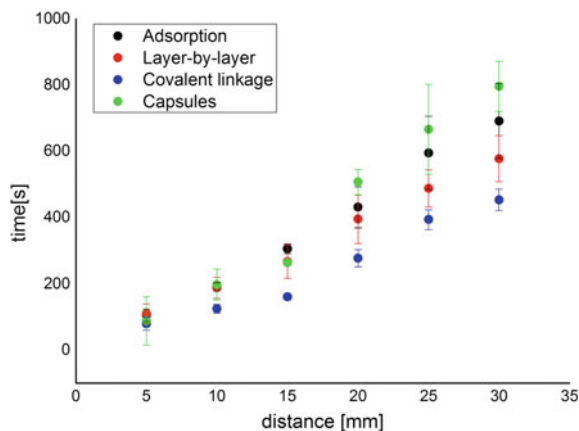


**Fig. 2.44** Photograph of the device after 10 and 90 s from application of the dye

**Fig. 2.45** Flow velocity in a bioactive paper-channel. Reprinted with permission from [128]



flow is most slowed down in case of covalent linkage. Other methods of immobilization result in similar velocity but adsorption showed the lowest reproducibility.

In the case of electrochemical method, on the contrary to the colorimetric attempt the fastest flow was observed for the covalent linkage. Unfortunately, the chemical residue present after immobilization resulted in much higher background signal (baseline  $\sim 25$  nA) in comparison with other immobilization methods ( $\sim 0.5$ – $2.5$  nA). This chemical residue could be the cause of slowness observed in the colorimetric attempt. The second fastest was Layer-by-layer method, which also presented the highest linearity. Flow velocity in a channel with adsorbed enzyme and microcapsules was similar (Single Factor Anova  $F < F_{\text{crit}}$ ). In some cases capsules upon drying partially clogged the channel. Adsorption was the least reproducible method in both measurements. Results of the electrochemical measurement are presented in Fig. 2.45.

### 2.3.3.6 Michaelis-Menten Kinetics

Table 2.9 summarizes the calculated values of  $V_{\text{max}}$  and  $K_m$  for free and immobilized GOx. Only methods considered most promising were tested in this study. All immobilization methods showed increase in the  $K_m$  value as compared with the free enzyme. It can be related to the lower accessibility of the active sites of immobilized GOx.

Lesser  $K_m$  value indicates higher affinity of enzyme and substrate, which results in faster response. The lowest increase was noted for EDC/NHS method (2.8 times higher) which could be explained by the fact that covalent linkage methods tend to specific orientation of the enzyme. Entrapment in starch and BSA blocking showed the highest increase of  $K_m$  (6.6 and 5.4 times respectively). Optimization of the

**Table 2.9** Kinetic parameters for free and immobilized GOx

	K <sub>m</sub> (mmol/L)	V <sub>max</sub> ((μmol/L)/min)
In solution	2.9	8.7
Adsorption	11.1	4.8
BSA blocking	15.8	3.8
Entrapment in PVA	10.6	4.9
Entrapment in starch	19.0	5.4
LbL sodium alginate-chitosan	12.6	4.5
LbL hyaluronic acid-PEI	9.0	5.1
Covalent linkage EDC/NHS	8.1	5.2

amount of BSA and the concentration of starch should be considered in those cases, as to retain their impact on stability but reduce the accessibility effects.

$V_{\max}$  describes the velocity with which the substrate occupies all active sites of all the enzyme molecules. Decrease of  $V_{\max}$  in all cases shows that no simple inhibition is taking place (competitive inhibition  $-V_{\max}$  remains constant, uncompetitive inhibition  $-V_{\max}$  decreases but  $K_m$  remains constant, competitive inhibition—both  $K_m$  and  $V_{\max}$  decrease), nevertheless mixed inhibition effects can still be present.

### 2.3.4 Electrochemical Detection

#### 2.3.4.1 Analysis of Glucose and Uric Acid

##### Optimization of Device's Architecture

In order to maximize the electrochemical response, several channel architectures were analyzed. Architectures were chosen in a way as to change the time of reaction of the analyte with enzyme deposited always in the middle of the channel, and the velocity with which hydrogen peroxide reaches the electrode. Results of computer modeling and chronoamperometric measurements are resumed in Fig. 2.46. Results of computer modeling demonstrate how water (blue) is substituted by another liquid of concentration 1 mol/L (red). Purpose of the visualization was to show the flow front (rounded or perpendicular), diffusion zone etc. and not velocity which was one of the input data (pressure difference).

In a straight channel (Fig. 2.46) straight flow front is observed, with constant velocity throughout the channel. Chronoamperometric analysis shows good separation of both compounds, with two broadened peaks and analysis time of 30 min. In architecture “Wide-narrow”, flow has a constant velocity till the enzymatic reaction zone, after which channel narrows therefore higher speed is obtained when reaching the electrode. Peaks are still broadened, but the time of analysis is slightly

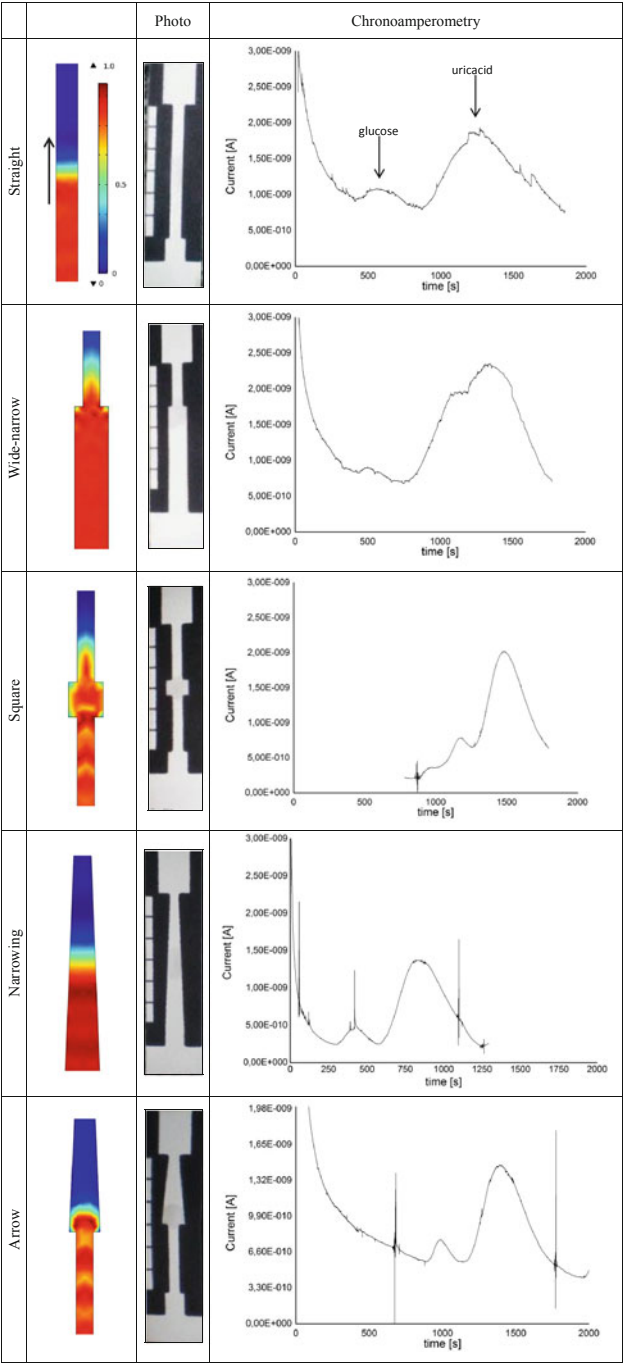


**Fig. 2.46** Results of computer modeling and chronoamperometric measurements for different channel architectures. Reprinted with permission from [128]

shorter. Interesting is also the wider diffusion zone observed in architecture “Wide-narrow” as compared with other types of channels. In architecture “Square”, flow is being slowed down inside a wider, square enzymatic reaction zone, and accelerates again after leaving it. Peaks are partially superimposed but the time of analysis drops to around 16 min. In architecture “Narrowing” flow gets gradually faster along the channel. Chronoamperometric measurements showed the shortest time necessary for both peaks to appear ( $\sim 15$  min). It is worth noting that architecture “Narrowing” conserves the straight, perpendicular flow front of a straight channel whereas other architectures do not. In architecture “Arrow” flow slows down entering the enzymatic reaction zone and later gradually accelerates. Peaks are well separated with around 18 min time of analysis.

Architectures “Narrowing” and “Arrow” were subjected to more detailed tests and due to greater reproducibility “Narrowing” channel was used in subsequent experiments.

The intensity of the signal was not commented because, as it will be seen later, on this stage it mainly depends on positioning on the electrode.

### Preliminary Test Destined to Construct a Calibration Curve

Repeatability of the obtained signal was too low to construct a calibration curve. Not only the intensity of peaks differed but also the relative position and time needed for analysis. It was noted that flow on each device is slightly different, especially during wetting of the enzymatic zone. During spotting, solution wicks differently each time depending on the arrangement of fibers. This characteristic is especially visible when numerous layers are being deposited.

### Uniformity of Enzyme Immobilization

When paper is dipped, fibers are covered uniformly with the solution. Thus this method was used to deposit enzyme on paper. Unfortunately in this case part of the channel has to be cut-out to perform the immobilization. When pieces simply overlap and are held by means of an adhesive tape (Fig. 2.11a) they tend to deflect upon wetting. In this way contact is not uniform over the entire width of the channel. Exerting more pressure by means of paper clips and a device holder (Fig. 2.11b), does not solve the problem if the channel remains loose. Flow is greatly enhanced in channels covered with a small piece of plastic, or stacked between two plastic slips, due to capillarity between paper and the cover and not only through the paper fibers. In this way time of reaction is too short to obtain satisfactory signal for glucose. Flow was even faster when pressure was exerted on top of the channel (Fig. 2.11d) as compared with pressure on the sides (Fig. 2.11c). Best results were obtained for the device in which small incisions were made in the middle of the channel and pieces were interwoven (Fig. 2.11e). In this case pressure

was exerted not only on the sides (adhesive tape) but also in the middle of the channel, allowing reproducible wetting.

Nevertheless, even after solving the problem of flow through the bioactive area, device continued to present large discrepancies between individual systems.

### Electrode Positioning

As it can be seen of Fig. 2.47 it is necessary to develop a more elaborate positioning method, to ensure repeatability of the results. Peaks obtained after repositioning of the electrode are 2–3 times lower than the ones registered before. Differences exist also between peaks obtained with the same position of the electrode, for example the first three peaks differ in height, peak width at  $\frac{1}{2}$  height and therefore area. But those differences could be diminished by more accurate spotting of the sample.

In the next step various manners of repeatable electrode positioning were proposed. In the case of sponge holders tested during the experiments it was not possible to obtain repeatable results, as paper was deflecting when becoming wet. When electrode was positioned on top, paper would deflect from the electrode resulting in lack of electrical contact, and too high pressure resulted in tears. Results were not repeatable even when the electrode area of the channel was supported on a slip of plastic placed in the sponge holder. This fact can be attributed to fibrous structure of paper, which results in electrode tip positioning on top or between the fibers. Similar problems (deflection, tears) were observed when the electrode was placed under the paper device (Fig. 2.12a).

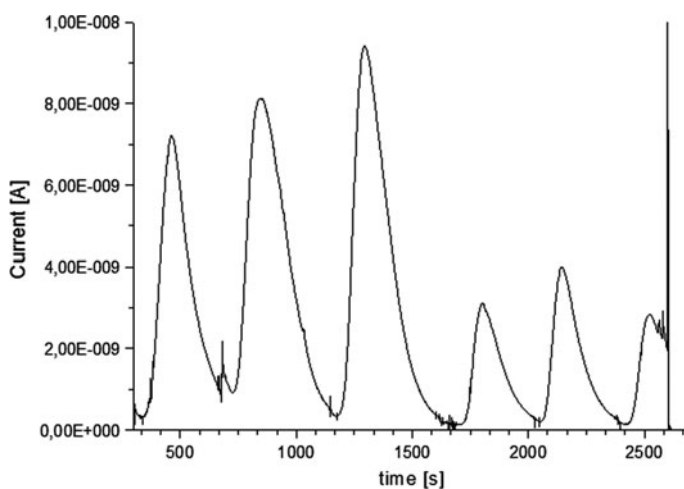


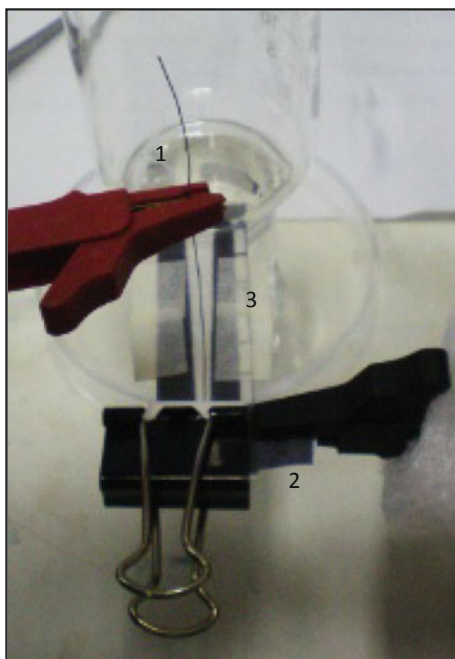
**Fig. 2.47** Signal repeatability for consecutive injections of 10 mmol/L uric acid solution. After three injections electrode was lifted and repositioned

A Pt wire was used instead of a capillary enclosed microelectrode, allowing new configurations. First the wire was stacked across the width of the channel (Fig. 2.12b), but again wet paper would twist and deflect from the electrode, resulting in lack of electrical contact, regardless if the wire was positioned on top or bottom side of the channel. When electrode was enclosed between two layers of plastic measurements became repeatable. Unfortunately, obtained signal was characterized by high background and noise. Next, a small orifice was made 3 mm from the end of the channel, and Pt wire was gently forced through (Fig. 2.12c). In this way paper surrounds the circumference of the electrode, resulting in repeatable contact. After promising results calibration curve was constructed.

### Calibration Curve

Glucose: After optimization of the device (Fig. 2.48) it was possible to construct a calibration curve, presenting good linearity ( $R^2 = 0.980$ ) in all examined range (2.0–10.0 mmol/L). Calibration curve (Fig. 2.49) is described by equation  $y = 2.22 (\pm 0.14) \cdot 10^{-6}x - 2.01 (\pm 0.83) \cdot 10^{-6}$ ,  $N = 3$ . Limit of detection, estimated as the concentration of the analyte giving a signal equal  $3 \times$  the standard deviation of the blank is equal 1.4 mmol/L.

**Fig. 2.48** Final device for the detection of glucose and uric acid. 1. Pt wire working electrode, 2. reference electrode drawn with a pencil, 3. bioactive channel





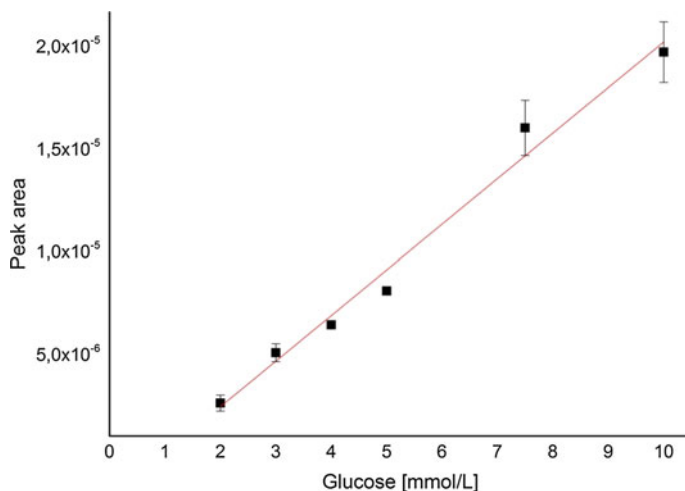


**Fig. 2.49** Calibration curve for glucose–electrochemical method, lateral flow assay, with bioactive channel, immobilization by means of layer-by-layer (potential 0.7 V, 1  $\mu$ L of sample). Reprinted with permission from [128]

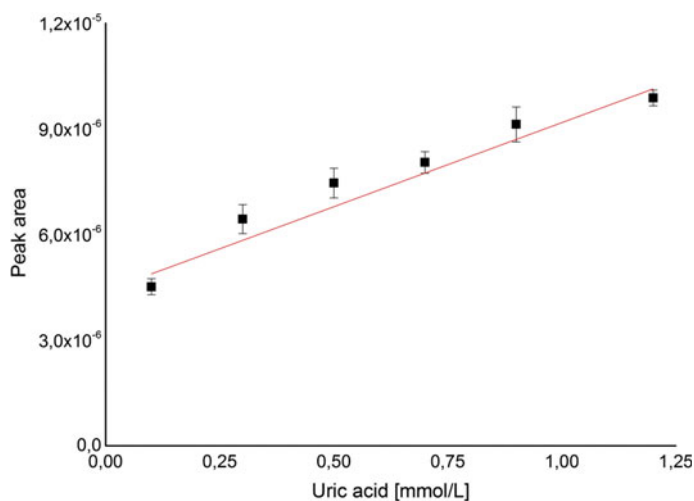


**Fig. 2.50** Calibration curve for uric acid–electrochemical method, lateral flow assay, with bioactive channel, immobilization by means of layer-by-layer (potential 0.7 V, 1  $\mu$ L of sample). Reprinted with permission from [128]

Uric acid: It was possible to construct a calibration curve, presenting good linearity ( $R^2 = 0.958$ ) in all examined range (0.1–1.2 mmol/L). Calibration curve (Fig. 2.50) is described by equation  $y = 4.78(\pm 0.44) \cdot 10^{-6}x + 4.40(\pm 0.34) \cdot 10^{-6}$ ,  $N = 3$ .

### 2.3.4.2 Analysis of Glucose, Cholesterol and Uric Acid

#### Architecture

Assembly of the devices shown in Fig. 2.13 proved difficult as the parts were small and delicate. Papers of different thickness were tested. Thickness of sample and detection pads did not impact the assembly but the bioactive channels were easier to set up when made from thicker paper (Whatman n°3).

Two assembly methods were proposed. In the case of threading incisions were made on both sides of the bioactive channels and each channel was forced through a small orifice in the sample and conjugation pads. This type of assembly proved to be more secure and would not dismantle upon usage. In the other device proposed, incisions were made only on one side of the channels, and sample and conjugation pads had fitting angular incisions. Device prepared in this way was easier to assembly, and channels would not tear or crumple so often but it was prone to dismantle upon usage. No inconsistencies were noted between devices of the same type upon wetting of the channels. More secure contact between pieces of paper of the threaded device allowed for faster wetting of consecutive parts. Threaded device was chosen for subsequent tests.

#### Conservation of Laminar Flow

As it can be seen on Fig. 2.51 regardless the architecture of the channel laminar flow is maintained after the junction. Diffusion is present on the boundary between two flowing solutions but apart from that flow is undisturbed till the end of the channel, which confirms the possibility of application of two electrode system.

#### Preliminary Tests and Optimization of the Architecture

After modification of the one electrode system and inclusion of two constrictions it was possible to obtain signal as seen in Fig. 2.52. Three maximums are visible in

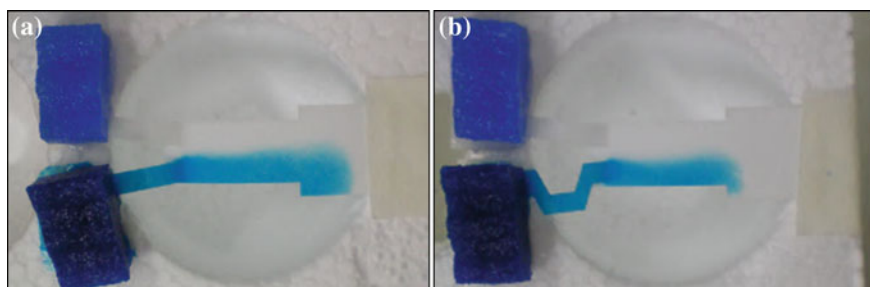


**Fig. 2.51** Visualization of laminar flow upon leaving of the channel

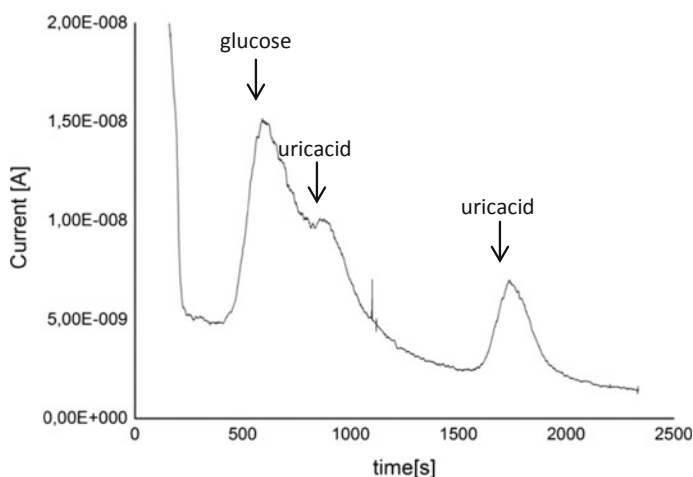


**Fig. 2.52** Response of one electrode system, mixed sample glucose and uric acid

the graph, associated with uric acid (two maximums) and glucose (one) which proves that use of a one electrode system with channels of different length would be a promising solution to detect all three compounds.

It was not possible to detect cholesterol in any of the experiments. Probably another carrier solution should be used to move cholesterol molecules across paper matrix (addition of surfactant, organic solvent etc.). Additional tests confirmed activity of cholesterol oxidase used in this study.

## 2.4 Partial Conclusions

Table 2.10 resumes parameters of calibration curves obtained for devices with both types of detection. Only as a reminder, normal levels of compounds of interests are: glucose 3.5–5.3 mmol/L (blood), 0.1–0.8 mmol/L (urine), cholesterol 5.2 mmol/L (blood), uric acid 0.1–0.4 mmol/L (blood), 1.5–4.4 mmol/L (urine). Therefore proposed devices with colorimetric detection at current stage of development could be applied for the quantification of all compounds in blood, but in the case of borderline high levels of cholesterol and glucose only providing qualitative response. Regardless this shortcoming this kind of sensor still can be applied as an initial point of care screening device quantifying normal levels of compounds of interest or indicating the need of more specialized assistance in case of higher concentrations. In order to increase the working range of this sensor other geometry, with greater surface area of the detection zone could be applied. Inversely to the test with blood in the case of urine, device would be able to quantify glucose in all range, even for higher than normal levels, but the working range for high concentrations of uric acid would have to be increased.

**Table 2.10** Analytical parameters of developed systems with colorimetric and electrochemical detection. Presented range in mmol/L

	Colorimetric detection			Electrochemical detection		
	Equation	R <sup>2</sup>	Range	Equation	R <sup>2</sup>	Range
Glucose	$y = 11.97 \pm 1.25x + 3.7 \pm 2.6$	0.938	0.2–5.0	$y = 2.22(\pm 0.14) \cdot 10^{-6}x - 2.01(\pm 0.83) \cdot 10^{-6}$	0.980	2.0–10.0
Cholesterol	$y = 17.08 \pm 0.74x + 0.33 \pm 0.49$	0.991	1.0–5.0	–	–	–
Uric acid	$y = 12.7 \pm 0.44x + 4.4 \pm 0.30$	0.993	0.1–2.5	$y = 4.78(\pm 0.44) \cdot 10^{-6}x + 4.40(\pm 0.34) \cdot 10^{-6}$	0.958	0.1–1.2

System with electrochemical detection could quantify both uric acid and glucose in blood but for test with urine would have to be optimized for lower concentrations of glucose (i.e. longer enzymatic reaction time) and higher concentrations of uric acid (i.e. other electrode material).

Sensitivity is not the only consideration when choosing the best detection method. Preliminary tests were performed with real samples (results not shown) in order to indicate future steps of development. Electrochemical detection can be affected by fouling of proteins on the electrode surface, resulting in higher background current and lower detection signal. It is also prone to interference related to detection of other electroactive compounds present in the sample. Furthermore other species present in the sample could react with hydrogen peroxide formed upon enzymatic reaction before it can be detected on the electrode. In the case of colorimetric detection the biggest concern is the color of the sample. Probably delicate coloration due to urine samples would not affect results obtained with proposed starch-iodide method, but intense color associated with red blood cells would surely have a negative impact on sensitivity. To overcome this obstacle sampling zone could be modified with agglutination antibodies, or fabricated from a plasma separation membrane.

One issue arises from the developments described above—device would have to work in flow conditions, therefore the problem of cholesterol retention on paper would have to be solved. In order to move cholesterol from the sampling layer, an organic solvent could be used or surfactant added to the running buffer. Cholesterol oxidase modified paper could be also in direct contact with the sampling pad, in this way enzyme could react with cholesterol in the sampling area and later only hydrogen peroxide would flow to the detection zone. This type of construction could result in interference observed in uric acid and glucose assays due to hydrogen peroxide originating from the cholesterol reaction, therefore another architecture would have to be proposed. Layers of the device could function as flaps, and in this way alternately be moved to contact specified areas of the device.

Apart from the device also the detection system should be considered. For resource limited setting one-component systems are preferred. With two components, namely a disposable test and a reader, it is highly possible that the system will not function due to lack of supplies (disposable tests) or malfunction of the equipment and absence of technical support. In the case of electrochemical systems efforts are being made to develop ever more affordable but not less reliable readers but still with this kind of detection some kind of specialized equipment will always be necessary. Detection system could be disposable together with the test but this kind of one-component integration of electrochemical devices is not always possible for a reasonable price. When thinking of colorimetric system, equipment free quantitative detection can be accomplished by appropriate design of the device (distance or time-based detection). Cell phone cameras and downloadable software could also be used for intensity-based quantification. In this way detector of this two-component system could be easily replaced by another telephone, by simply installing appropriate software.

Summarizing, for extremely low cost applications, in order to reach wider public and be applicable in real-life situations system should be self-contained and one component, use unprocessed sample, not require any specialized training and be easy to interpret. Based on the results obtained during this work, in the nearest future abovementioned requisites would be met easier with colorimetric systems.

## References

1. Galant a. L, Kaufman RC, Wilson JD (2015) Glucose: detection and analysis. *Food Chem* 188:149–160. doi:[10.1016/j.foodchem.2015.04.071](https://doi.org/10.1016/j.foodchem.2015.04.071)
2. WHO Diabetes WHO Fact sheet. <http://www.who.int/mediacentre/factsheets/fs312/en/>. Accessed 1 June 2015
3. Dungchai W, Chailapakul O, Henry CS (2009) Electrochemical detection for paper-based microfluidics. *Anal Chem* 81:5821–5826. doi:[10.1021/ac9007573](https://doi.org/10.1021/ac9007573)
4. Perez-Ruiz F, Dalbeth N, Bardin T (2014) A review of uric acid, crystal deposition disease, and gout. *Adv Ther* 32:31–41. doi:[10.1007/s12325-014-0175-z](https://doi.org/10.1007/s12325-014-0175-z)
5. Lakshmi D, Whitcombe MJ, Davis F et al (2011) Electrochemical detection of uric acid in mixed and clinical samples: a review. *Electroanalysis* 23:305–320. doi:[10.1002/elan.201000525](https://doi.org/10.1002/elan.201000525)
6. Dungchai W, Chailapakul O, Henry CS (2010) Use of multiple colorimetric indicators for paper-based microfluidic devices. *Anal Chim Acta* 674:227–233. doi:[10.1016/j.aca.2010.06.019](https://doi.org/10.1016/j.aca.2010.06.019)
7. Morzycki JW (2014) Recent advances in cholesterol chemistry. *Steroids* 83:62–79. doi:[10.1016/j.steroids.2014.02.001](https://doi.org/10.1016/j.steroids.2014.02.001)
8. Birtcher KK, Ballantyne CM (2004) Cardiology patient page. Measurement of cholesterol: a patient perspective. *Circulation* 110:e296–e297. doi:[10.1161/01.CIR.0000141564.89465.4E](https://doi.org/10.1161/01.CIR.0000141564.89465.4E)
9. Ding S-N, Shan D, Zhang T, Dou Y-Z (2011) Performance-enhanced cholesterol biosensor based on biocomposite system: Layered double hydroxides-chitosan. *J Electroanal Chem* 659:1–5. doi:[10.1016/j.jelechem.2011.04.003](https://doi.org/10.1016/j.jelechem.2011.04.003)
10. MacLachlan J, Wotherspoon a. TL, Ansell RO, Brooks CJW (2000) Cholesterol oxidase: sources, physical properties and analytical applications. *J Steroid Biochem Mol Biol* 72:169–195. doi:[10.1016/S0960-0760\(00\)00044-3](https://doi.org/10.1016/S0960-0760(00)00044-3)
11. Steiner M-S, Duerkop A, Wolfbeis OS (2011) Optical methods for sensing glucose. *Chem Soc Rev* 40:4805–4839. doi:[10.1039/c1cs15063d](https://doi.org/10.1039/c1cs15063d)
12. Newman JD, Turner APF (2005) Home blood glucose biosensors: a commercial perspective. *Biosens Bioelectron* 20:2435–2453. doi:[10.1016/j.bios.2004.11.012](https://doi.org/10.1016/j.bios.2004.11.012)
13. Heller A, Feldman B (2008) Electrochemical glucose sensors and their applications in diabetes management. *Chem Rev* 108:2482–2505
14. Information on EC 1.7.3.3—factor-independent urate hydroxylase. <http://www.brenda-enzymes.org/enzyme.php?ecno=1.7.3.3>. Accessed 3 June 2015
15. Kand'ar R, Drábková P, Hampel R (2011) The determination of ascorbic acid and uric acid in human seminal plasma using an HPLC with UV detection. *J Chromatogr B: Anal Technol Biomed Life Sci* 879:2834–2839. doi:[10.1016/j.jchromb.2011.08.007](https://doi.org/10.1016/j.jchromb.2011.08.007)
16. Steel E (1958) The determination of uric acid in biological materials. *Biochem J* 68:306–309
17. Piermarini S, Migliorelli D, Volpe G et al (2013) Uricase biosensor based on a screen-printed electrode modified with Prussian blue for detection of uric acid in human blood serum. *Sensors Actuators, B Chem* 179:170–174. doi:[10.1016/j.snb.2012.10.090](https://doi.org/10.1016/j.snb.2012.10.090)
18. Ca X, Kalchb K, Neuhold C, Owrevc B (1994) An improved voltammetric method for the determination of trace amounts of uric acid with electrochemically pretreated carbon paste electrodes. *Talanta* 3:407–413

19. Zen J-M, Hsu C-T (1998) A selective voltammetric method for uric acid detection at Nafion®-coated carbon paste electrodes. *Talanta* 46:1363–1369
20. Shankar SS, Swamy BEK, Chandrashekar BN, Gururaj KJ (2013) Sodium do-decyl benzene sulfate modified carbon paste electrode as an electrochemical sensor for the simultaneous analysis of dopamine, ascorbic acid and uric acid: a voltammetric study. *J Mol Liq* 177:32–39
21. Ramirez-Berriozabal M, Galicia L, Gutierrez-Granados S et al (2008) Selective electrochemical determination of uric acid in the presence of ascorbic acid using a carbon paste electrode modified with b-cyclodextrin. *Electroanalysis* 20:1678–1683
22. Amiri M, Bezaatpour A, Pakdel Z, Nekouei K (2012) Simultaneous voltammetric determination of uric acid and ascorbic acid using carbon paste/cobalt Schiff base composite electrode. *J Solid State Electrochem* 16:2187–2195
23. Burke RW, Diamondstone BI, Velapoldi R a, Menis O (1974) Mechanisms of the Liebermann Burchard and Zak color reactions for cholesterol. *Clin Chem* 20:794–801
24. Li X, Liu X (2014) Fabrication of three-dimensional microfluidic channels in a single layer of cellulose paper. *Microfluid Nanofluidics* 1:1–9. doi:[10.1007/s10404-014-1340-z](https://doi.org/10.1007/s10404-014-1340-z)
25. Fung KK, Chan CPY, Renneberg R (2009) Development of enzyme-based bar code-style lateral-flow assay for hydrogen peroxide determination. *Anal Chim Acta* 634:89–95. doi:[10.1016/j.aca.2008.11.064](https://doi.org/10.1016/j.aca.2008.11.064)
26. Allen MP, DeLizza A, Ramel U et al (1990) A noninstrumented quantitative test system and its application for determining cholesterol concentration in whole blood. *Clin Chem* 36:1591–1597
27. Allen MP (1995) Laminated assay device. United States Patent 5409664, 15:1–15
28. Chen X, Chen J, Wang F et al (2012) Determination of glucose and uric acid with bienzyme colorimetry on microfluidic paper-based analysis devices. *Biosens Bioelectron* 35:363–368. doi:[10.1016/j.bios.2012.03.018](https://doi.org/10.1016/j.bios.2012.03.018)
29. Kumar A, Hens A, Arun RK et al (2015) A paper based microfluidic device for easy detection of uric acid using positively charged gold nanoparticles. *Analyst* 140:1817–1821. doi:[10.1039/C4AN02333A](https://doi.org/10.1039/C4AN02333A)
30. Deng L, Chen C, Zhu C et al (2014) Multiplexed bioactive paper based on GO@SiO<sub>2</sub>@CeO<sub>2</sub> nanosheets for a low-cost diagnostics platform. *Biosens Bioelectron* 52:324–329. doi:[10.1016/j.bios.2013.09.005](https://doi.org/10.1016/j.bios.2013.09.005)
31. Zhu WJ, Feng DQ, Chen M et al (2014) Bienzyme colorimetric detection of glucose with self-calibration based on tree-shaped paper strip. *Sensors Actuators, B Chem* 190:414–418. doi:[10.1016/j.snb.2013.09.007](https://doi.org/10.1016/j.snb.2013.09.007)
32. Noh H, Phillips ST (2010) Fluidic timers for time-dependent, point-of-care assays on paper. *Anal Chem* 82:8071–8078. doi:[10.1021/ac1005537](https://doi.org/10.1021/ac1005537)
33. Demirel G, Babur E (2014) Vapor-phase deposition of polymers as a simple and versatile technique to generate paper-based microfluidic platforms for bioassay applications. *Analyst* 139:2326–2331. doi:[10.1039/c4an00022f](https://doi.org/10.1039/c4an00022f)
34. Garcia PDT, Cardoso TMG, Garcia CD et al (2014) A handheld stamping process to fabricate microfluidic paper-based analytical devices with chemically modified surface for clinical assays. *RSC Adv* 4:37637–37644. doi:[10.1039/C4RA07112C](https://doi.org/10.1039/C4RA07112C)
35. Carrilho E, Martinez AW, Whitesides GM (2009) Understanding wax printing a simple micropatterning process for paper based Microfluidics.pdf. 81:7091–7095
36. Cate DM, Dunchai W, Cunningham JC et al (2013) Simple, distance-based measurement for paper analytical devices. *Lab Chip* 13:2397–2404. doi:[10.1039/c3lc50072a](https://doi.org/10.1039/c3lc50072a)
37. Ornatka M, Sharpe E, Andreescu D, Andreescu S (2011) Paper bioassay based on ceria nanoparticles as colorimetric probes. *Anal Chem* 83:4273–4280. doi:[10.1021/ac200697y](https://doi.org/10.1021/ac200697y)
38. Carvalhal RF, Kfoury MS, Piazzetta MHDO et al (2010) Electrochemical detection in a paper-based separation device. *Anal Chem* 82:1162–1165. doi:[10.1021/ac902647r](https://doi.org/10.1021/ac902647r)
39. Liu H, Crooks RM (2012) A paper-based electrochemical sensing platform with integral battery and electrochromic read-out. *Anal Chem* 84:1–3. doi:[10.1021/ac203457h](https://doi.org/10.1021/ac203457h)

40. Labroo P, Cui Y (2014) Graphene nano-ink biosensor arrays on a microfluidic paper for multiplexed detection of metabolites. *Anal Chim Acta* 813:90–96. doi:[10.1016/j.aca.2014.01.024](https://doi.org/10.1016/j.aca.2014.01.024)
41. Ruecha N, Rangkupan R, Rodthongkum N, Chailapakul O (2014) Novel paper-based cholesterol biosensor using graphene/polyvinylpyrrolidone/polyaniline nanocomposite. *Biosens Bioelectron* 52:13–19. doi:[10.1016/j.bios.2013.08.018](https://doi.org/10.1016/j.bios.2013.08.018)
42. Zhao C, Thuo MM, Liu X (2013) A microfluidic paper-based electrochemical biosensor array for multiplexed detection of metabolic biomarkers. *Sci Technol Adv Mater* 14:054402. doi:[10.1088/1468-6996/14/5/054402](https://doi.org/10.1088/1468-6996/14/5/054402)
43. Nie Z, Deiss F, Liu X et al (2010) Integration of paper-based microfluidic devices with commercial electrochemical readers. *Lab Chip* 10:3163–3169. doi:[10.1039/c0lc00237b](https://doi.org/10.1039/c0lc00237b)
44. Yu J, Ge L, Huang J et al (2011) Microfluidic paper-based chemiluminescence biosensor for simultaneous determination of glucose and uric acid. *Lab Chip* 11:1286–1291. doi:[10.1039/c0lc00524j](https://doi.org/10.1039/c0lc00524j)
45. Awqatty B, Samaddar S, Cash KJ et al (2014) Fluorescent sensors for the basic metabolic panel enable measurement with a smart phone device over the physiological range. *Analyst* 139:5230–5238. doi:[10.1039/C4AN00999A](https://doi.org/10.1039/C4AN00999A)
46. Hortin GL, Sviridov D (2008) Analysis of molecular forms of albumin in urine. *Proteomics - Clin Appl* 2:950–955. doi:[10.1002/prca.200780145](https://doi.org/10.1002/prca.200780145)
47. Puglia MJ, Lott J, Proffitt J, Cast TK (1999) High-sensitivity dye binding assay for albumin in urine. *J Clin Lab Anal* 13:180–7
48. Polkinghorne KR (2006) Detection and measurement of urinary protein. *Curr Opin Nephrol Hypertens* 15:625–630. doi:[10.1097/01.mnh.0000247502.49044.10](https://doi.org/10.1097/01.mnh.0000247502.49044.10)
49. Busher JT (1990) Serum albumin and globulin. In: Walker H, Hall W, Hurst J (eds) *Clinical methods: the history, physical, and laboratory examinations*, 3rd edn. Butterworth Publishers, pp 497–499
50. Bradford MM (1976) A rapid and sensitive method for the quantitation of microgram quantities of protein utilizing the principle of protein-dye binding. *Anal Biochem* 72:248–254
51. Lowry OH, Rosebrough NJ, Farr L et al (1951) Protein measurement with the Folin phenol reagent. *J Biol Chem* 193:265–275. doi:[10.1007/s10982-008-9035-9](https://doi.org/10.1007/s10982-008-9035-9)
52. Martinez AW, Phillips ST, Butte MJ, Whitesides GM (2007) Patterned paper as a platform for inexpensive, low-volume, portable bioassays. *Angew Chemie - Int Ed* 46:1318–1320. doi:[10.1002/anie.200603817](https://doi.org/10.1002/anie.200603817)
53. Wang W, Wu W-YY, Zhu J-JJ et al (2010) Tree-shaped paper strip for semiquantitative colorimetric detection of protein with self-calibration. *J Chromatogr A* 1217:3896–3899. doi:[10.1016/j.chroma.2010.04.017](https://doi.org/10.1016/j.chroma.2010.04.017)
54. Sechi D, Greer BP, Johnson J, Hashemi N (2013) Three-dimensional paper-based microfluidic device for assays of protein and glucose in urine. *Anal Chem* 85:10733–10737
55. Luo L, Li X, Crooks RM (2014) Low-voltage origami-paper-based electrophoretic device for rapid protein separation. *Anal Chem* 86:12390–12397
56. Pozuelo M, Blondeau P, Novell M et al (2013) Paper-based chemiresistor for detection of ultralow concentrations of protein. *Biosens Bioelectron* 49:462–465. doi:[10.1016/j.bios.2013.06.007](https://doi.org/10.1016/j.bios.2013.06.007)
57. Szucs J, Gyurcsányi RE, Gyurcsányi E et al (2012) Towards protein assays on paper platforms with potentiometric detection. *Electroanalysis* 24:146–152. doi:[10.1002/elan.201100522](https://doi.org/10.1002/elan.201100522)
58. Wu L, Ma C, Zheng X et al (2015) Paper-based electrochemiluminescence origami device for protein detection using assembled cascade DNA–carbon dots nanotags based on rolling circle amplification. *Biosens Bioelectron* 68:413–420. doi:[10.1016/j.bios.2015.01.034](https://doi.org/10.1016/j.bios.2015.01.034)
59. Sheldon RA. (2007) Enzyme immobilization: the quest for optimum performance. *Adv Synth Catal* 349:1289–1307. doi:[10.1002/adsc.200700082](https://doi.org/10.1002/adsc.200700082)



60. Mateo C, Palomo JM, Fernandez-Lorente G et al (2007) Improvement of enzyme activity, stability and selectivity via immobilization techniques. *Enzyme Microb Technol* 40:1451–1463. doi:[10.1016/j.enzmictec.2007.01.018](https://doi.org/10.1016/j.enzmictec.2007.01.018)
61. Hanefeld U, Gardossi L, Magner E (2009) Understanding enzyme immobilisation. *Chem Soc Rev* 38:453–468. doi:[10.1039/b711564b](https://doi.org/10.1039/b711564b)
62. Cao L (2005) Immobilised enzymes: Science or art? *Curr Opin Chem Biol* 9:217–226. doi:[10.1016/j.cbpa.2005.02.014](https://doi.org/10.1016/j.cbpa.2005.02.014)
63. Pelton R (2009) Bioactive paper provides a low-cost platform for diagnostics. *TrAC Trends Anal Chem* 28:925–942. doi:[10.1016/j.trac.2009.05.005](https://doi.org/10.1016/j.trac.2009.05.005)
64. Brady D, Jordaan J (2009) Advances in enzyme immobilisation. *Biotechnol Lett* 31:1639–1650. doi:[10.1007/s10529-009-0076-4](https://doi.org/10.1007/s10529-009-0076-4)
65. Sheldon RA (2007) Enzyme immobilization: the quest for optimum performance. *Adv Synth Catal* 349:1289–1307. doi:[10.1002/adsc.200700082](https://doi.org/10.1002/adsc.200700082)
66. Guzik U, Hupert-Kocurek K, Wojcieszynska D (2014) Immobilization as a strategy for improving enzyme properties-application to oxidoreductases. *Molecules* 19:8995–9018. doi:[10.3390/molecules19078995](https://doi.org/10.3390/molecules19078995)
67. Ho C-M (2001) Fluidics- the link between micro and nano sciences and technologies. *IEEE MEMS* 2001:375–384
68. Whitesides GM (2006) The origins and the future of microfluidics. *Nature* 442:368–373. doi:[10.1038/nature05058](https://doi.org/10.1038/nature05058)
69. Stone H, Kim S (2001) Microfluidics: basic issues, applications, and challenges. *AIChE J* 47:1250–1254
70. Kleinstreuer C (2013) Theory. In: John Wiley & Sons I (ed) *Microfluid. Nanofluidics Theory Sel. Appl.* pp 1–8
71. Washburn EW (1921) The dynamics of capillary flow. *Phys Rev* 17:273–283. doi:[10.1103/PhysRev.17.273](https://doi.org/10.1103/PhysRev.17.273)
72. Fu E, Ramsey SA, Kauffman P et al (2011) Transport in two-dimensional paper networks. *Microfluid Nanofluidics* 10:29–35. doi:[10.1016/j.biotechadv.2011.08.021](https://doi.org/10.1016/j.biotechadv.2011.08.021). **Secreted**
73. Dickinson E, Ekstrom H, Fontes E (2014) COMSOL multiphysics: finite element software for electrochemical analysis. A mini-review. *Electroch* 40:71–74
74. Segal IA (2015) Finite element methods for the incompressible Navier-Stokes equations. Delft Institute of Applied Mathematics
75. Schilling E, Yager P (2009) Microfluidic tutorial-a highly biased primer. <http://faculty.washington.edu/yagerp/microfluidictutorial/tutorialhome.htm>. Accessed 10 June 2015
76. Erickson D (2005) Towards numerical prototyping of labs-on-chip: modeling for integrated microfluidic devices. *Microfluid Nanofluidics* 1:301–318. doi:[10.1007/s10404-005-0041-z](https://doi.org/10.1007/s10404-005-0041-z)
77. Kleinstreuer C (2013) Modeling and simulation aspects. In: *Microfluid. Nanofluidics Theory Sel. Appl.*, 1st edn. Wiley, pp 363–373
78. Whatman<sup>TM</sup> Cellulose chromatography paper. <https://www.fishersci.com>. Accessed 16 June 2015
79. Bracher PJ, Gupta M, Whitesides GM (2010) Patterned paper as a template for the delivery of reactants in the fabrication of planar materials. *Soft Matter* 6:4303–4309. doi:[10.1039/c0sm00031k](https://doi.org/10.1039/c0sm00031k)
80. Sayyah SM, El-salam HMA, Khaliel AB, Mohamed EH (2011) Graft polymerization of acrylonitrile onto paper and characterization of the grafted product. *J Appl Polym Sci* 120:1411–1419. doi:[10.1002/app](https://doi.org/10.1002/app)
81. Vesel A, Mozetic M, Hladnik A et al (2007) Modification of ink-jet paper by oxygen-plasma treatment. *J Phys D Appl Phys* 40:3689–3696. doi:[10.1088/0022-3727/40/12/022](https://doi.org/10.1088/0022-3727/40/12/022)
82. Hu L, Wu H, La Mantia F et al (2010) Thin, flexible secondary Li-ion paper batteries. *ACS Nano* 4:5843–5848. doi:[10.1021/nn1018158](https://doi.org/10.1021/nn1018158)
83. Papel Vegetal Schoellershammer. <http://www.microservice.com.br/>. Accessed 16 June 2015
84. Hanlon JF, Kelsey RJ, Forcinio H (1998) Paper and paperboard. In: *Handbook of package engineering*, 3rd edn. CRC Press, pp 44–49

85. Carrilho E, Martinez AW, Whitesides GM et al (2009) Understanding wax printing: a simple micropatterning process for paper-based microfluidics. *Anal Chem* 81:7091–7095. doi:[10.1021/ac901071p](https://doi.org/10.1021/ac901071p)
86. Tian K, Dasgupta PK (1999) Automated measurement of lipid hydroperoxides in oil and fat samples by flow injection photometry. *Anal Chem* 71:2053–2058. doi:[10.1021/ac9813181](https://doi.org/10.1021/ac9813181)
87. Matsui S, Echigo S, Shishida K (1998) Comparison among the methods for hydrogen peroxide measurements to evaluate advanced oxidation processes: application of a spectrophotometric method using copper (II) ion and 2,9-Dimethyl-1,10-phenanthroline. *Environ Sci Technol* 32:3821–3824
88. Repka V (1999) Improved histochemical test for in situ detection of hydrogen peroxide in cells undergoing oxidative burst or lignification. *Biol Plant* 42:599–607. doi:[10.1023/A:1002687603731](https://doi.org/10.1023/A:1002687603731)
89. Dhaouadi A, Monser L, Sadok S, Adhoum N (2006) Flow-injection methylene blue-based spectrophotometric method for the determination of peroxide values in edible oils. *Anal Chim Acta* 576:270–274. doi:[10.1016/j.aca.2006.06.026](https://doi.org/10.1016/j.aca.2006.06.026)
90. Salem I, El-Maazawi MS (2000) Kinetics and mechanism of color removal of methylene blue with hydrogen peroxide catalyzed by some supported alumina surfaces. *Chemosphere* 41:1173–1180. doi:[10.1016/S0045-6535\(00\)00009-6](https://doi.org/10.1016/S0045-6535(00)00009-6)
91. Wisitsoraat A, Karuwan C, Wong-ek K et al (2009) High sensitivity electrochemical cholesterol sensor utilizing a vertically aligned carbon nanotube electrode with electropolymerized enzyme immobilization. *Sensors* 9:8658–8668. doi:[10.3390/s91108658](https://doi.org/10.3390/s91108658)
92. Galanos DS, Vazis G MA, Kapoulas VM (1964) Serum glycerides, free cholesterol, and cholesterol. *J Lipid Res* 5:242–244
93. Sackett GE (1925) Modification of Bloor's Method for the determination of cholesterol in whole blood or blood serum. *J Biol Chem* 64:203–205
94. Martin SP, Lamb DJ, Lynch JM, Reddy SM (2003) Enzyme-based determination of cholesterol using the quartz crystal acoustic wave sensor. *Anal Chim Acta* 487:91–100. doi:[10.1016/S0003-2670\(03\)00504-X](https://doi.org/10.1016/S0003-2670(03)00504-X)
95. Moraes ML, de Souza NC, Hayasaka CO et al (2009) Immobilization of cholesterol oxidase in LbL films and detection of cholesterol using AC measurements. *Mater Sci Eng, C* 29:442–447. doi:[10.1016/j.msec.2008.08.040](https://doi.org/10.1016/j.msec.2008.08.040)
96. Babaei A, Zendehehd M, Khalilzadeh B, Taheri A (2008) Simultaneous determination of tryptophan, uric acid and ascorbic acid at iron(III) doped zeolite modified carbon paste electrode. *Colloids Surfaces B Biointerfaces* 66:226–232. doi:[10.1016/j.colsurfb.2008.06.017](https://doi.org/10.1016/j.colsurfb.2008.06.017)
97. Hasebe Y, Nawa K, Ujita S, Uchiyama S (1998) Highly sensitive flow detection of uric acid based on an intermediate regeneration of uricase. *Analyst* 123:1775–1780. doi:[10.1039/a802214c](https://doi.org/10.1039/a802214c)
98. Chen Y, Meng Y, Tang J et al (2010) Extraction of uricase from *Candida utilis* by applying polyethylene glycol (PEG)/ NH<sub>4</sub> SO<sub>4</sub> aqueous two-phase system. 9:4788–4795
99. Tiffany TO, Jansen JM, Burtis C et al (1972) Enzymatic kinetic rate and end-point analyses of substrate, by use of a GeMSAEC fast analyzer. *Clin Chem* 18:829–840
100. Chandra U (2011) Determination of dopamine in presence of uric acid at poly (Eriochrome Black t) film modified graphite pencil electrode. *Am J Anal Chem* 02:262–269. doi:[10.4236/ajac.2011.22032](https://doi.org/10.4236/ajac.2011.22032)
101. Hossain SMZ, Luckham RE, McFadden MJ, Brennan JD (2009) Reagentless bidirectional lateral flow bioactive paper sensors for detection of pesticides in beverage and food samples. *Anal Chem* 81:9055–9064. doi:[10.1021/ac901714h](https://doi.org/10.1021/ac901714h)
102. Cha R, Wang D, He Z, Ni Y (2012) Development of cellulose paper testing strips for quick measurement of glucose using chromogen agent. *Carbohydr Polym* 88:1414–1419. doi:[10.1016/j.carbpol.2012.02.028](https://doi.org/10.1016/j.carbpol.2012.02.028)
103. Mentele MM, Cunningham J, Koehler K et al (2012) Microfluidic paper-based analytical device for particulate metals. *Anal Chem* 84:4474–4480. doi:[10.1021/ac300309c](https://doi.org/10.1021/ac300309c)

104. Duly EB, Grimson S, Grimson P et al (2003) Measurement of serum albumin by capillary zone. *J Clin Pathol* 56:780–782
105. Grimsley GR, Pace CN, Pace NC (2003) Spectrophotometric determination of protein concentration. In: *Current protocols in protein science*. Wiley, p Supplement 33
106. Rendl M, Bönisch A, Mader A et al (2011) Simple one-step process for immobilization of biomolecules on polymer substrates based on surface-attached polymer networks. *Langmuir* 27:6116–6123. doi:[10.1021/la1050833](https://doi.org/10.1021/la1050833)
107. Zanon NCM, Oliveira ON, Caseli L (2011) Immobilization of uricase in Langmuir and Langmuir-Blodgett films of fatty acids and a possible uric acid colorimetric sensor. *J Colloid Interface Sci* 373:69–74. doi:[10.1016/j.jcis.2011.07.095](https://doi.org/10.1016/j.jcis.2011.07.095)
108. Olkkonen J, Lehtinen K, Erho T (2010) Flexographically printed fluidic structures in paper. *Anal Chem* 82:10246–10250. doi:[10.1021/ac1027066](https://doi.org/10.1021/ac1027066)
109. Pierre C (2004) The sol-gel encapsulation of enzymes. *Biocatal Biotransformation* 22:145–170. doi:[10.1080/10242420412331283314](https://doi.org/10.1080/10242420412331283314)
110. Schilling KM, Lepore AL, Kurian J a, Martinez AW (2012) Fully enclosed microfluidic paper-based analytical devices. *Anal Chem* 84:1579–85. doi:[10.1021/ac202837s](https://doi.org/10.1021/ac202837s)
111. Mulhbach J, McGeeney K, Ispas-Szabo P et al (2002) Modified high amylose starch for immobilization of uricase for therapeutic application. *Biotechnol Appl Biochem* 36:163–170. doi:[10.2147/IJN.S33835](https://doi.org/10.2147/IJN.S33835)
112. Liu Q, Michael A, Yu X (2007) Immobilization and bioactivity of glucose oxidase in hydrogel microspheres formulated by an emulsification—internal gelation—adsorption—polyelectrolyte coating method. *Int J Pharm* 339:148–156. doi:[10.1016/j.ijpharm.2007.02.027](https://doi.org/10.1016/j.ijpharm.2007.02.027)
113. Zhang Y, Zhi T, Zhang L et al (2009) Immobilization of carbonic anhydrase by embedding and covalent coupling into nanocomposite hydrogel containing hydrotalcite. *Polymer (Guildf)* 50:5693–5700. doi:[10.1016/j.polymer.2009.09.067](https://doi.org/10.1016/j.polymer.2009.09.067)
114. Wu XJ, Choi MMF (2004) Spongiform immobilization architecture of inotropy polymer hydrogel coentrapping alcohol oxidase and horseradish peroxidase with octadecylsilica for optical biosensing alcohol in organic solvent. *Anal Chem* 76:4279–4285. doi:[10.1021/ac049799d](https://doi.org/10.1021/ac049799d)
115. Alkasir RSJ, Ornatska M, Andreescu S (2012) Colorimetric paper bioassay for the detection of phenolic compounds. *Anal Chem* 84:9729–9737. doi:[10.1021/ac301110d](https://doi.org/10.1021/ac301110d)
116. Mertz D, Vogt C, Hemmerlé J et al (2011) Tailored design of mechanically sensitive biocatalytic assemblies based on polyelectrolyte multilayers. *J Mater Chem* 21:8324. doi:[10.1039/c0jm03496g](https://doi.org/10.1039/c0jm03496g)
117. Deng C, Chen J, Nie Z, Si S (2010) A sensitive and stable biosensor based on the direct electrochemistry of glucose oxidase assembled layer-by-layer at the multiwall carbon nanotube-modified electrode. *Biosens Bioelectron* 26:213–219. doi:[10.1016/j.bios.2010.06.013](https://doi.org/10.1016/j.bios.2010.06.013)
118. Lvov YM, Grozdits G, Us C (2010) Layer-by-layer nanocoating for paper fabrication. *US Pat* 1–10
119. Lu H, Rusling JF, Hu N (2007) Protecting peroxidase activity of multilayer enzyme-polyion films using outer catalase layers. *J Phys Chem B* 111:14378–14386. doi:[10.1021/jp076036w](https://doi.org/10.1021/jp076036w)
120. Hoshi T, Saiki H, Anzai J-I (2003) Amperometric uric acid sensors based on polyelectrolyte multilayer films. *Talanta* 61:363–368. doi:[10.1016/S0039-9140\(03\)00303-5](https://doi.org/10.1016/S0039-9140(03)00303-5)
121. Ma J, Cai P, Qi W et al (2013) The layer-by-layer assembly of polyelectrolyte functionalized graphene sheets: a potential tool for biosensing. *Colloids Surfaces A Physicochem Eng Asp* 426:6–11. doi:[10.1016/j.colsurfa.2013.02.039](https://doi.org/10.1016/j.colsurfa.2013.02.039)
122. Wang S, Li S, Yu Y (2004) Immobilization of cholesterol oxidase on cellulose acetate membrane for free cholesterol biosensor development. *Artif Cells Blood Substit Immobil Biotechnol* 32:413–425. doi:[10.1081/LABB-200027479](https://doi.org/10.1081/LABB-200027479)
123. Albayrak N, Yang S (2002) Immobilization of *Aspergillus oryzae* beta-galactosidase on tosylated cotton cloth. *Enzyme Microb Technol* 31:371–383

124. Isobe N, Lee D-S, Kwon Y-J et al (2011) Immobilization of protein on cellulose hydrogel. *Cellulose* 18:1251–1256. doi:[10.1007/s10570-011-9561-8](https://doi.org/10.1007/s10570-011-9561-8)
125. Saxena U, Goswami P (2010) Silk mat as bio-matrix for the immobilization of cholesterol oxidase. *Appl Biochem Biotechnol* 162:1122–1131. doi:[10.1007/s12010-010-8923-2](https://doi.org/10.1007/s12010-010-8923-2)
126. Blandino A, Macías M, Cantero D (2003) Calcium alginate gel as encapsulation matrix for coimmobilized enzyme systems. *Appl Biochem Biotechnol* 110:53–60
127. Alexakis T (1992) Microencapsulation of DNA within cross-linked chitosan membranes
128. Witkowska Nery E, Santhiago M, Kubota LT (2016) Flow in a paper-based bioactive channel—study on electrochemical detection of glucose and uric acid. *Electroanalysis* 28
129. Witkowska Nery E, Kubota LT (2015) Evaluation of enzyme immobilization methods for paper-based devices—a glucose oxidase study. *J Pharm Biomed Anal* 117:551–559

Analysis of Samples of Clinical and Alimentary Interest  
with Paper-based Devices

Witkowska Nery, E.

2016, XVII, 184 p. 83 illus., 80 illus. in color., Hardcover

ISBN: 978-3-319-28671-6